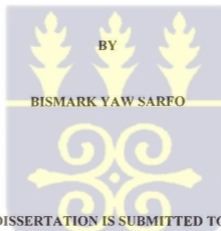


**CHEMOKINE MEDIATORS OF CEREBRAL
MALARIA: A COMPARATIVE STUDY OF
THE ROLE OF RANTES IN MURINE AND
HUMAN CEREBRAL MALARIA**



**THIS DISSERTATION IS SUBMITTED TO THE
UNIVERSITY OF GHANA, LEGON IN PARTIAL
FULFILMENT OF THE REQUIREMENTS FOR THE
AWARD OF PH.D. DEGREE IN BIOCHEMISTRY**

SEPTEMBER 2004

DECLARATION

I, Bismark Yaw Sarfo hereby declare that the experimental work described in this research work was conducted by me under the supervision of Prof. Jonathan K. Stiles, Prof. Fredrick N. Gyang and Prof. Michael D. Wilson, except for the references to the work of other researchers which were duly cited.



Bismark Yaw Sarfo

(Candidate)



Prof. Fredrick N. Gyang

(Supervisor)



Prof. Jonathan K. Stiles

(Supervisor)



Prof. Michael D. Wilson

(Co-Supervisor)

DEDICATION

To my family



ACKNOWLEDGEMENTS

I wish to express my sincere thanks and appreciation to Prof. Jonathan K. Stiles for giving me the opportunity to conduct this research work in his laboratory, and also for his immense guidance and advice during the entire period of my studies. I am also grateful to Prof. James Lillard Jr, for his guidance and contribution. I am indebted to the following people of Morehouse School of Medicine, Atlanta Georgia, USA; Prof. Gerald Sonnenfeld, Dr. Shailesh Singh, Ms. Ikovwa Irune, Ms. Yvonne Powers, Ms Ethel Mills, Dr. Ravichandra Palaniappan, Dr. Udai P. Singh and Dr. Jacqueline Hibbert, all of the Department of Microbiology, Biochemistry and Immunology, Prof. Winston Thompson, Dr Melissa Green and Ms. Alicia Branch of the Department of Obstetrics and Gynaecology, Prof. Joseph Whittaker and Mr. Tabari Baker of the Department of Anatomy and Neurobiology, Dr. Alexander Quarshie of the Clinical Research Center and Mr. Lawrence Brako of the Electron microscopy department.

Thank you, Dr. P. Jolly of the University of Alabama, at Birmingham, USA, for providing the human plasma samples for this study.

I am also thankful to the following people for their diverse role and support during my stay in the USA; Ms Agnes Aboah of Augusta Georgia, Messrs Rexford Asare of the University of Kentucky and Aboagye Dacosta of the Oklahoma State University.

My utmost gratitude goes to Prof. M.D. Wilson and Dr. Daniel Y. Boakye of the Noguchi Memorial Institute for Medical Research (NMIMR) for the confidence they have reposed in me. Their mentoring and fatherly guidance will forever remain in my memory. My

sincere thanks also go to all the members and staff of the Parasitology department of NMIMR.

I am grateful to Prof. F.N Gyang for his mentorship and contribution to this study. To Dr Yaa Osei-Difie, Dr. W.S.K Gbewonyo, Dr. Naa Adamafo, Mr. Sulemana Dramanu, Ms Christiana Netey and Ms. Hetty Antwi-Boasiako, all of the Department of Biochemistry, University of Ghana, thank you for all your support.

My appreciation also goes to the following people; Dr. R.K.Gyasi, Prof A.A Adjei and Dr. H Armah of the Pathology department, University of Ghana Medical School.

May the almighty God richly bless all of my family members, including Mr. Kwabena Donkor, Hon. Francis Osei-Sarfo, Mrs Rebecca Ampong, Mr. Richard Sarfo, Mr. Boakye Sarfo and Mr. Emmanuel Sarfo for their prayers and support.

I also wish to acknowledge the support and prayers of the following people; Mrs Salla Boakye and the family, Mr. Abdul-Inusah Nasiru and his wife Fatima Ibrahim as well as Mr. Kpebu K. Smith.

I am very thankful to the volunteers and members of families of deceased patients whose samples were used for some aspects of this study.

This study received financial support from UNDP/World Bank/WHO Special Program for Research and Training in Tropical Diseases.



TABLE OF CONTENTS

DECLARATION.....	i
DEDICATION.....	ii
ACKNOWLEDGEMENTS.....	iii
TABLE OF CONTENTS.....	v
LIST OF ILLUSTRATION.....	xiii
LIST OF TABLES.....	xiv
ABBREVIATIONS.....	xv
ABSTRACT.....	xix
CHAPTER ONE.....	1
INTRODUCTION.....	1
1.1 <i>Plasmodium</i> parasites and malaria.....	1
1.2 Rationale and justification of study.....	3
1.3 General hypothesis.....	4
1.4 Objectives.....	5
1.5 Approach of study.....	6
CHAPTER TWO.....	7
LITERATURE REVIEW.....	7
2.1 Life cycle of <i>Plasmodium</i> parasites, and the malaria disease.....	7
2.2 Global epidemiology of malaria, and economic development.....	11
2.3 Current strategies for malaria control.....	16



2.3.1	The use of anti-malarial drugs and their discovery.....	16
2.3.2	Vector control.....	18
2.3.2.1	Use of nets and insecticide treated bed nets.....	18
2.3.2.2	Larval control.....	19
2.4	Clinical manifestations and pathogenesis of malaria.....	19
2.4.1	Uncomplicated malaria.....	19
2.4.2	Complicated or severe malaria.....	20
2.4.2.1	Severe malaria anaemia.....	21
2.4.2.2	Cerebral malaria (CM).....	22
2.5	Immunity to malaria infection.....	25
2.6	Central nervous system (CNS) and malaria.....	29
2.7	Immune mediators of malaria in mouse models, human and primate.....	31
2.7.1	Immune mediators of malaria in mouse models.....	31
2.7.1.1	The role of adhesion molecules.....	31
2.7.1.2	The role of cytokines.....	33
2.7.1.3	The role of chemokines and receptors.....	34
2.7.2	Immune mediators of malaria in human and primate models.....	40
2.7.2.1	The role of adhesion molecules.....	40
2.7.2.2	The role of cytokines.....	45
2.7.2.3	The role of chemokines and receptors.....	45
2.8	RANTES as a proinflammatory chemokine.....	46
2.9	Current research strategies for understanding malaria pathogenesis.....	49
2.9.1	Murine malaria models and malaria research.....	49
2.9.2	Human post mortem tissue and peripheral blood samples.....	52



CHAPTER THREE.....	53
MATERIALS AND METHODS.....	53
A MATERIALS.....	53
3.1 Laboratory animals, reagents and supplies.....	53
3.1.1 <i>P.yoelii</i> 17X parasites.....	53
3.1.2 cDNA micro-array.....	53
3.1.3 TRIZOL ^R	54
3.1.4 ELISA.....	55
3.1.5 Antibodies.....	55
3.1.6 RT-PCR and PCR.....	55
3.1.8 SDS-PAGE/Western Blot.....	56
B METHODS.....	58
3.2 Mouse malaria studies-1.....	58
3.2.1 <i>P.yoelii</i> 17X murine malaria model.....	58
3.2.2 Preparation of infected mouse brain tissue samples.....	58
3.3 Transcriptional analysis of <i>P.yoelii</i> 17X induced immunomodulator mRNA expression.....	59
3.3.1 Total RNA isolation from <i>P.yoelii</i> 17X infected mouse brain.....	59
3.3.2 DNase treatment of total RNA samples.....	60
3.3.3 Testing of total RNA samples for possible DNA contamination.....	61
3.3.4 cDNA array-screening of <i>P.yoelii</i> 17X induced immunomodulators.....	62
3.3.4.1 Probe synthesis from total RNA.....	62
3.3.4.2 Column purification of synthesized probes.....	63

3.3.4.3	Hybridizing cDNA probes to the Atlas array.....	63
3.3.4.4	Washing of hybridized array membrane.....	64
3.3.4.5	Gene analysis.....	65
3.3.5	Reverse transcription of purified mouse brain RNA to cDNA for PCR analysis.....	66
3.3.5.1	Amplification by PCR and semi-quantitative analysis of <i>P.yoelii</i> 17X induced immunomodulators.....	66
3.4	Tissue and plasma protein analysis of <i>P.yoelii</i> 17X induced RANTES expression.....	68
3.4.1	SDS/Western Blot analysis of <i>P.yoelii</i> 17X induced RANTES protein expression in mouse brain.....	68
3.4.1.1	Protein isolation and assay from mouse brain.....	68
3.4.1.2	Preparing SDS-PAGE gel.....	69
3.4.1.3	Transfer of protein onto membrane.....	70
3.4.1.4	Western Blot analysis.....	71
3.4.2	Peripheral blood analysis of <i>P.yoelii</i> 17X induced RANTES expression.....	73
3.5	Ultrastructural and immunohistological analysis of <i>P.yoelii</i> 17X infected brain samples.....	74
3.5.1	Ultrastructural analysis of <i>P.yoelii</i> 17X infected brain samples.....	74
3.5.2	Immunohistological analysis of GFAP expression in <i>P.yoelii</i> 17X infected mouse brain.....	75
3.6	Human malaria studies.....	76
3.6.1	Human cerebral malaria (CM) and non-malaria (NM) brain samples.....	76

3.6.2	Transcriptional analysis of RANTES, CCR1, CCR3 and CCR5 in cerebrum, cerebellum, brain stem and hippocampus of CM and NM samples.....	77
3.6.2.1	RNA isolation and DNase treatment, from CM and NM samples.....	77
3.6.2.2	Reverse transcription of purified human brain RNA to cDNA for PCR analysis.....	78
3.6.2.3	PCR amplification and semi-quantitative analysis of CM induced RANTES, CCR1, CCR3, and CCR5.....	78
3.6.3	Tissue and plasma protein analysis of malaria induced RANTES, CCR1, CCR3 and CCR5 expression.....	79
3.6.3.1	Protein isolation and analysis from CM and NM samples.....	79
3.6.3.2	Preparing SDS-PAGE gel for protein analysis.....	79
3.6.3.3	Transfer of protein onto membrane.....	80
3.6.3.4	Western Blot analysis.....	80
3.7	Determination of <i>P.falciparum</i> antigen and malaria induced plasma RANTES expression by ELISA.....	81
3.7.1	Determination of <i>P.falciparum</i> antigen.....	81
3.7.2	<i>P.falciparum</i> induced plasma RANTES expression.....	82
3.8	Statistical analysis.....	83
3.9	Mouse malaria studies-2.....	83
3.9.1	Role of RANTES in severity and mortality of murine malaria.....	83
CHAPTER FOUR.....		86
RESULTS.....		86

4.1	Mouse malaria studies-1	86
4.1.1	<i>P.yoelii</i> 17X murine malaria model	87
4.2	Transcriptional analysis of <i>P.yoelii</i> 17X induced immunomodulator expression	89
4.2.1	cDNA array gene statement and analyses of <i>P.yoelii</i> 17X induced immunomodulators	89
4.2.2	Semi-quantitative RT-PCR validation and analysis of immunomodulator gene expression during <i>P.yoelii</i> 17X infection	92
4.2.2.1	Adhesion molecule-PECAM-1, ICAM-1, VCAM-1 mRNA expression	92
4.2.2.2	Cytokine-INF- γ , TNF- α , IL-12 and iNOS mRNA expression	96
4.2.2.3	Chemokine- MIP-2alpha, MCP-1, RANTES mRNA expression	101
4.2.2.4	Chemokine receptor-CCR1, CCR3 and CCR5 mRNA expression	105
4.3	Tissue and plasma protein expression of <i>P.yoelii</i> 17X induced RANTES	109
4.3.1	<i>P.yoelii</i> 17X induced RANTES protein expression	109
4.3.2	<i>P.yoelii</i> 17X infection induce plasma RANTES expression	111
4.4	Ultrastructural and immunohistological analysis of <i>P.yoelii</i> 17X infected brain samples	113
4.4.1	Ultrastructural analysis of <i>P.yoelii</i> 17X infected brain samples	113
4.4.2	Immunohistological analysis of GFAP expression in <i>P.yoelii</i> 17X infected mouse brain	115
4.5	Human malaria studies	117
4.5.1	Post-mortem CM and NM brain samples	117

4.5.2	Transcriptional analysis of RANTES, CCR1, CCR3 and CCR5 in cerebellum, cerebrum, brain stem and hippocampus of CM and NM brain samples.....	118
4.5.3	Western Blot and plasma analyses of RANTES, CCR1, CCR3 and CCR5.....	123
4.5.3.1	Western Blot analysis of RANTES, CCR1, CCR3 and CCR5 protein in cerebellum, cerebrum, brain stem and hippocampus of CM and NM samples.....	123
4.5.4	<i>P. falciparum</i> induce RANTES expression in plasma.....	126
4.5.5	Correlation of RANTES expression with malaria infection.....	128
4.6	Murine malaria studies-2.....	130
4.6.1	Role of RANTES in severity and survival during <i>P. yoelii</i> 17X malaria in mice.....	130
CHAPTER FIVE.....		135
DISCUSSION.....		135
5.1	<i>P. yoelii</i> 17X murine malaria studies-1.....	135
5.2	Murine malaria studies-2.....	146
5.3	Human malaria studies.....	147
5.4	Conclusions.....	152
SUGGESTIONS FOR FUTURE STUDIES.....		155
REFERENCES.....		156
APPENDICES.....		172

LIST OF ILLUSTRATIONS

Figure 1: Approach of study.....	6
Figure 2: Life cycle of human malaria parasite.....	9
Figure 3: Global distribution of malaria.....	12
Figure 4: Classification of chemokines and receptors.....	38
Figure 5: Sequestration of <i>P.falciparum</i> IRBC in brain microvessel.....	43
Figure 6: Schematic illustration of cellular adhesion in <i>P.falciparum</i> malaria.....	44
Figure 7: RANTES recruits inflammatory cells into site of inflammation.....	48
Figure 8: Murine malaria model.....	86
Figure 9: <i>P.yoelii</i> 17X infection induces spleno-hepatomegaly in SW mice.....	88
Figure 10: Autoradiograph of cDNA microarray analysis of mRNA expression in mouse brain.....	90
Figure 11: <i>P. yoelii</i> 17X upregulates PECAM-1 mRNA expression in mouse brain.....	93
Figure 12: <i>P. yoelii</i> 17X upregulates ICAM-1 mRNA expression in mouse brain.....	94
Figure 13: <i>P. yoelii</i> 17X upregulates VCAM-1 mRNA expression in mouse brain.....	95
Figure 14: <i>P. yoelii</i> 17X upregulates INF-gamma mRNA expression in mouse brain....	97
Figure 15: <i>P. yoelii</i> 17X upregulates TNF-alpha mRNA expression in mouse brain.....	98
Figure 16: <i>P. yoelii</i> 17X upregulates IL-12 mRNA expression in mouse brain.....	99
Figure 17: <i>P. yoelii</i> 17X induced iNOS mRNA expression in mouse brain.....	100
Figure 18: <i>P. yoelii</i> 17X upregulates MIP-2alpha mRNA expression in mouse brain...102	
Figure 19: <i>P. yoelii</i> 17X upregulates MCP-1 mRNA expression in mouse brain.....	103
Figure 20: <i>P. yoelii</i> 17X upregulates RANTES mRNA expression in mouse brain...104	
Figure 21: <i>P. yoelii</i> 17X upregulates CCR1 mRNA expression in mouse brain.....	106

Figure 22: <i>P. yoelii</i> 17X upregulates CCR3 mRNA expression in mouse brain.....	107
Figure 23: <i>P. yoelii</i> 17X upregulates CCR5 mRNA expression in mouse brain.....	108
Figure 24: <i>P. yoelii</i> 17X upregulates RANTES protein expression in mouse brain...	110
Figure 25: <i>P. yoelii</i> 17X upregulates RANTES protein expression in mouse plasma.	112
Figure 26: <i>P. yoelii</i> 17X induces ultra structural changes in mouse cerebellum.....	114
Figure 27: <i>P. yoelii</i> 17X induces morphological changes in astrocytes in mouse brain.....	116
Figure 28: CM upregulates RANTES, CCR3 and CCR5 mRNA expression in cerebellum.....	119
Figure 29: CM upregulates RANTES, CCR3 and CCR5 mRNA expression in cerebrum.....	120
Figure 30: CM upregulates RANTES mRNA expression in brain stem.....	121
Figure 31: CM upregulates RANTES mRNA expression in hippocampus.....	122
Figure 32: CM upregulates RANTES and CCR protein expression in cerebellum...	124
Figure 33: CM upregulates RANTES and CCR protein expression in cerebrum.....	125
Figure 34: <i>P. falciparum</i> upregulates RANTES expression in plasma.....	127
Figure 35: Plasma RANTES expression correlated positively with malaria antigens.	129
Figure 36: Course of <i>P. yoelii</i> 17X infection in mock and anti-RANTES antibody treated mice.....	132
Figure 37: Survival of mock and anti-RANTES antibody treated mice, infected with <i>P. yoelii</i> 17X parasites.....	133
Figure 38: <i>P. yoelii</i> 17X infection upregulates RANTES expression in plasma of mock antibody treated mice.....	134
Figure 39: Proposed model for RANTES-mediated brain pathogenesis during CM....	154

LIST OF TABLES

Table 1: Loss from the economic growth penalty of malaria endemicity in 31 African countries.....	15
Table 2: Chemokine nomenclature.....	35
Table 3: Examples of animal models used for malaria brain immunopathological studies.....	51
Table 4: <i>Plasmodium yoelii</i> 17X infection alters immunomodulator gene expression in mouse brain at peak parasitemia (day 8 post infection).....	91

ABBREVIATIONS

BBB, blood brain barrier
BCA-1, B-cell-attracting chemokine 1
bp, base pair
BT, <i>Bacillus thuringiensis</i>
CCL, c-c chemokine ligand
CCL2, c-c chemokine ligand 2
CCL5, c-c chemokine ligand 5
CCR1, c-c chemokine receptor 1
CCR3, c-c chemokine receptor 3
CCR5, c-c chemokine receptor 5
CD 36, cellular differentiation antigen
cDNA, complementary DNA
CSF, cerebrospinal fluid
CM, cerebral malaria
CNS, central nervous system
CTACK, cutaneous T-cell-attracting chemokine
CTL, cytotoxic T lymphocytes
DARC, duffy antigen receptor for chemokines
dATP, deoxyadenosine triphosphate
DC-CK1, dendritic cell-derived CC chemokine 1
dCTP, deoxycytidine triphosphate
dGTP, deoxyguanosine triphosphate
DDT, Dichloro-Diphenyl-Trichloroethane

dTTP, deoxythymidine triphosphate
DNA, deoxyribonucleic acid
DNase, deoxyribonuclease
ECM, experimental cerebral malaria
ELAM 1, Endothelial leukocyte adhesion molecule 1
ELC, EBL-1-ligand chemokine
ELISA, enzyme-linked immunosorbent assay
ENA-78, epithelial-cell-derived neutrophil attractant 78
eV, electron volts
FACS, fluorescence activated cell sorting
GAPDH, glyceraldehydes-3-phosphate dehydrogenase
GCP, granulocyte chemotactic protein
GRO, growth-related oncogene
HCC, haemofiltrate CC chemokine
HIV, human immunodeficiency virus
HIVE, HIV encephalitis
HRP, Histidin rich protein
ICAM-1, intercellular adhesion molecule-1
IL, interleukin
IL-12, interleukin-12
iNOS, inducible nitric oxide synthase
IP-10, interferon-inducible protein 10
iRBC, infected red blood cell
I-TAC, interferon-inducible T-cell alpha



knr, knockdown resistance

LARC, liver- and activation-regulated chemokine

LEC, liver-expressed chemokine

Lkn-1, leukotactin

LSA-1, liver stage antigen-1

MCP, monocyte chemoattractant protein

MDC, macrophage-derived chemokine

MEC, mammary-enriched chemokine

MHC-I, major histocompatibility complex class I

MIG, monokine induced by interferon γ

MIP, macrophage inflammatory protein

mM, millimolar

mRNA, messenger ribonucleic acid

MPIF, myeloid progenitor inhibitory factor

NAP, neutrophil-activating peptide

NM, non-malaria

NCM, non-cerebral malaria

PCR, polymerase chain reaction

PECAM-1, platelet endothelial cell adhesion molecule-1

PF4, platelet factor 4

PF4-KO, pore forming protein- knock out

PfEMP, *Plasmodium falciparum* erythrocyte membrane protein

RANTES, regulated on activation, normal T-cell expressed and secreted

RBC, red blood cell

RNA, ribonucleic acid

RT-PCR, reverse transcriptase-polymerase chain reaction

SCM-1 α/β , single C motif-1 α/β

SDF, stromal-cell-derived factor

SDS-PAGE, sodium dodecyl sulphate polyacrylamide gel electrophoresis

SLC, secondary lymphoid tissue chemokine

SW, swiss webster

TARC, thymus- and activation-regulated chemokine

Taq, *thermus aquaticus*

TECK, thymus-expressed chemokine

TEMED, N,N, N,-tetramethyl ethylene-diamine

Th1, T helper 1

TNF- α , tumour necrosis factor-alpha

TSP, Thrombospondin

μ M, micromolar

VCAM-1, vascular cell adhesion molecule-1

v/v, volume/volume

w/v, weight/volume

ABSTRACT

Although the involvement of cytokines and adhesion molecules in malaria-induced brain inflammation has been established, the role of chemokines and chemokine receptors remain unclear. This unexplained component of cerebral malaria (CM) pathology may be responsible for the heterogeneity in the observed features of CM and the difficulty in its characterization. RANTES (regulated on activation normal T cell expressed and secreted), a chemokine involved in the generation of inflammatory infiltrates plays a special role in the modulation of inflammation. Trafficking of inflammatory T helper 1 (Th1) cells into the brain is mediated partly by RANTES interactions with C-C chemokine receptor 5 (CCR5) receptor.

The main hypotheses of this study are: (a) RANTES, and corresponding receptors mediate malaria induced brain immunopathogenesis (b) Blocking RANTES which is upregulated during malaria infection will abrogate or minimize the outcome of the disease.

Studies were directed at i) Characterizing and analyzing the expression of RANTES and corresponding receptors CCR1, CCR3 and CCR5 in a mouse model of CM (SW mice/*P. yoelii* 17X) using cDNA microarray, RT-PCR and Western Blot analyses ii) Evaluating effect of *P.yoelii* 17X infection on mouse brain by electron microscopy and immunohistological analyses iii) Evaluating expression of RANTES and receptors in cerebellum, cerebrum, brain stem and hippocampus of post-mortem CM and non-malaria (NM) tissue samples using RT-PCR and Western Blot analyses

- iv) Comparing and contrasting levels of RANTES in plasma of rodent malaria model and malaria-positive human subjects using ELISA
- v) Determine the functional role of RANTES by anti-RANTES antibody blocking experiment using *P. yoelii* 17X infected mice.

Transcriptional analyses results indicate significant upregulation of chemokines; macrophage inflammatory protein-2 α (MIP-2 α), monocyte chemoattractant protein-1 (MCP-1) and RANTES, chemokine receptors; CCR1, CCR3, and CCR5, adhesion molecules; platelet endothelial cell adhesion molecule-1 (PECAM-1), intercellular adhesion molecule-1 (ICAM-1), vascular cell adhesion molecule-1 (VCAM-1) and cytokines; interferon-gamma (INF- γ), tumour necrosis factor-alpha (TNF- α) and interleukin-12 (IL-12) at peak parasitemia during *P.yoelii* 17X infection. Western Blot analysis revealed upregulation of RANTES protein in *P.yoelii* 17X infected mouse brain.

Ultrastructural analysis showed that *P. yoelii* 17X infection induces perivascular oedema in cerebellum in mouse brain at peak parasitemia. Immunohistological analysis demonstrates high immunoreactivity of glial fibrillary acidic protein (GFAP) in *P. yoelii* 17X infected mouse brain.

RANTES, CCR3 and CCR5 but not CCR1 mRNA are significantly upregulated in the cerebellum and cerebrum ($P < 0.0001$) in CM than NM samples.

There were no changes in the expression of CCR1, CCR3 and CCR5 mRNA in brain stem and hippocampus of CM and NM. RANTES mRNA expression in cerebellum and

cerebrum is highly significant ($P < 0.0001$) compared with the brain stem ($P = 0.0018$) and hippocampus ($P = 0.0027$) in CM group.

CCR5 and RANTES proteins were significantly upregulated in cerebellum ($P < 0.0013$ for CCR5, $P < 0.0001$ for RANTES) and cerebrum ($P < 0.0124$ for CCR5, $P < 0.0001$ for RANTES) but not brain stem and hippocampus of CM than in NM. Western Blot analysis could not detect CCR3 protein

RANTES was significantly upregulated in plasma of murine malaria model and malaria positive subjects compared with controls. RANTES concentration in plasma correlated with *P. falciparum* infection.

At day of sacrifice, level of parasitemia ($4.2 \times 10^6/\text{ml} \pm 0.2$) in mock antibody treated mice was higher ($P < 0.05$) than in mice in which RANTES was blocked with anti-RANTES antibody ($1.2 \times 10^6/\text{ml} \pm 0.2$). Anti-RANTES antibody treated mice survived longer (14 days) than mock antibody treated mice (10 days).

This is the first temporal study of murine malaria associated RANTES and receptors CCR1, CCR3 and CCR5 expression. *P. yoelii* 17X murine malaria model is useful in characterizing differentially expressed genes associated with human clinical malaria.

There is an association of RANTES expression in malaria-induced brain immunopathogenesis and endothelial lesions in infected mice.

Cerebellum and cerebrum in humans were the focal points for increased malaria-induced RANTES and CCR5 expression. Active sequestration of infected red blood cells (IRBCs) and platelets in addition to leukocytes in these regions of the brain could exacerbate CM immunopathology.

Blocking of RANTES decreased parasitemia and mortality associated with *P. yoelii* 17X infection.

CHAPTER ONE

INTRODUCTION

1.1 *Plasmodium* parasites and malaria

Malaria is caused by infection with *Plasmodium*, a genus of protozoan parasites. The four species of *Plasmodia* known to be causative agents of human malaria are *Plasmodium vivax*, *Plasmodium ovale*, *Plasmodium malariae* and *Plasmodium falciparum*, the latter being the most lethal (WHO, 1996).

P.vivax has the widest geographical distribution. It is prevalent in tropic and subtropical regions and also found in some temperate zones. Relapses may occur up to eight years after initial infection. It causes benign tertian malaria and is the second most harmful of all malaria species.

P.ovale is the rarest of the four species of *Plasmodium* and also causes benign tertian malaria. It is tied with *P.malariae* as being less dangerous and is common on the West Coast of Africa. *P.malariae* infection is difficult to diagnose because of its similarity with *P.vivax*. *P. ovale* on the contrary is quite easy to diagnose with its distinctive morphology. *P. ovale* infected cells are oval shaped and slightly larger than uninfected red blood cells. Both *P.ovale* and *P.vivax* have a dormant hypnozoite stage in the liver that can last for weeks or months before the development of erythrocytic schizogony.

P. malariae is patchily distributed over tropical Africa, Eastern Asia, Oceania and the Amazon area (WHO, 1996). It causes quartan malaria and accounts for 7% of malaria cases and can have relapses 53 years after initial infection. The classic symptoms of malaria- fever, malaise with intermittent paroxysms are typical of *P. vivax*, *P. ovale*, and *P. malariae*.

P. falciparum malaria infection is the commonest and widespread of human malaria and is generally more severe and fatal in non-immune individuals and young children aged 0-9 years if untreated. It is responsible for more than 50% of all malaria cases in the world and characterized by febrile illness which may be expressed as periodic paroxysms occurring every 48 hours with afebrile and relatively asymptomatic intervals (Campbell, 1997). Other major symptoms of *P. falciparum* malaria are chills, vomiting, convulsion, headache, drowsiness and skeletal muscle pain.

Malaria is a significant cause of abortion, stillbirth, child mortality, low birth weight, death in pregnant women, impaired growth in children and loss of productivity in adults. *Falciparum* malaria annually infects 300 million people causing at least 100 million cases of acute illness leading to approximately 2 million global deaths per year (Campbell, 1997). Increasing tourism, failure in vector control and increasing resistance of malaria parasite to current antimalarials has increased the threat of this disease. Approximately 15% of fatal malaria cases are due to cerebral malaria (CM) (Greenwood, 1999), resulting in brain inflammation, coma, convulsions, neurological complications, acidosis, hypoglycemia, and sudden death particularly among children and immunocompromised adults (WHO, 2000). Increasing migration, failure in vector control and increasing

resistance of malaria parasite to current antimalarials has increased the threat of malaria infection. Recent studies in Africa and South East Asia show that acute or chronic inflammation associated with malaria is deleterious to brain development of survivors and reportedly impairs cognitive function even after treatment (Fernando *et al.*, 2003, Boivin, 2002). Malaria-induced brain inflammation is reportedly mediated by complex cellular and immunomodulator interactions of co-regulators including cytokines and adhesion molecules. However the involvement of chemokines in brain immunopathogenesis of this disease is still unclear. In this study, RANTES expression was upregulated in plasma during malaria infection, implicating these molecules in immunopathogenesis of the disease.

1.2 Rationale and justification of study

Adhesion molecules, cytokines and chemokines are involved in suppression of erythropoiesis, and blood brain barrier (BBB) inflammation during parasite infections.

Although adhesion molecules and cytokines play a role in immunopathogenesis of CM, the mechanisms by which leukocytes, platelets and infected red blood cells are sequestered have not been elucidated at the molecular level. Since chemokines directly influence leukocytes migration, it is plausible that they will influence sequestration of leukocytes, platelets and IRBCs. Recent findings indicate that sequestration of leukocytes occur in CM.



Studies using rodent CM models have been criticized as not reproducing the brain pathology associated with CM in humans. In the *P.berghei* model, the presence of platelets and mononuclear cells in brain venules finds a parallel in pediatric CM; platelet activation during parasite infection may entrap leukocytes which are recruited to distal brain microvessels where IRBCs are sequestered. In other studies upregulation of ICAM-1 and VCAM-1 adhesion molecules in *Plasmodium yoelii* and *P.berghei* ANKA suggests another parallel between human and rodent malaria pathogenesis. Recent data also indicates that experimental CM is induced in perforin-deficient (PFP-KO) mice after adoptive transfer of cytotoxic CD8⁺ T cells from infected mice, which were directed, to the brain of PFP-KO mice. This specific recruitment of T cells might involve chemokine-chemokine receptor interaction. Other studies also indicate that susceptibility to ECM is delayed in CCR5-knockout mice.

Furthermore, trafficking of inflammatory T helper 1 (Th1), but not Th2, cells into the brain is mediated in large part by RANTES interactions with CCR5 receptor. Sequestration of platelets and leukocytes in brain microvasculature are also associated with CM immunopathology. Malaria enhances expression of CCR5 on placenta in pregnant women. Chemokines and their corresponding receptors mediate malaria and CM conditions hence understanding the role of these immune markers could enable a new strategy for preventing or minimizing the outcome of CM and other severe forms of the disease.

1.3 General hypothesis

It is hypothesized that the chemokine RANTES and its corresponding receptors CCR1, CCR3 and CCR5 play a role in malaria brain pathology and that blocking RANTES which is up-regulated in the brain during CM could prevent or minimize the outcome of the disease.

1.4 Objectives

- i) Determine malaria-induced global alterations in immunomodulator gene expression in brain at peak parasitemia in *Plasmodium yoelii* 17X mouse model
- ii) Evaluate temporal expression of the chemokine RANTES and its corresponding receptors CCR1, CCR3, and CCR5 in brain and RANTES in plasma during *P.yoelii* 17X malaria infection
- iii) Evaluate effect of *P.yoelii* 17X infection on mouse brain
- iv) Evaluate retrospectively, expression of RANTES and receptors CCR1, CCR3, and CCR5 in post-mortem human cerebral malaria tissue samples
- v) Localize expression of human brain RANTES, CCR1, CCR3 and CCR5 during CM
- vi) Evaluate RANTES expression in plasma of murine malaria model and malaria-positive human subjects
- vii) Determine the functional role of RANTES by anti-RANTES blocking experiment using *P. yoelii* 17X infected mice

Understanding of the role of RANTES and its receptors CCR1, CCR3 and CCR5 in immunopathogenesis of CM in particular and malaria in general will emerge after the completion of this study.

1.5 Approach of study

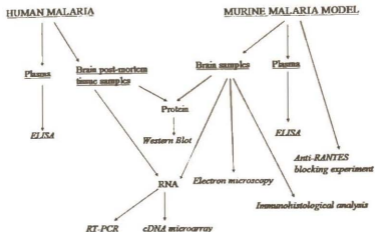


Figure 1: Approach of study; Utilize, cDNA micro-array, RT-PCR, Western Blot and ELISA to characterize and localize expressions of selected immunomodulators including RANTES and receptors CCR1, CCR3 and CCR5 in brain and plasma of murine malaria model and human post-mortem CM tissue samples. Electron microscopy and immunohistology were used to evaluate the effect of *P.yoelii* 17X infection on mouse brain. Anti-RANTES experiment was performed to analyze the function of RANTES in murine malaria model.

CHAPTER TWO

LITERATURE REVIEW

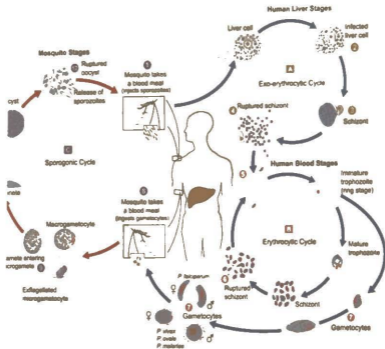
2.1 Life cycle of *Plasmodium* parasites, and the malaria disease

Plasmodium infected female *Anopheles* mosquitoes inject sporozoites into the bloodstream of the host during feeding. The sporozoites invade the hepatocytes where they undergo maturation and multiplication called exo-erythrocytic schizogony. Some of the sporozoites enter into a dormant phase called hypnozoite in *P. vivax* and *P. ovale* and can reactivate and undergo schizogony at a later time resulting in a relapse, a phenomenon referred to as recrudescence.

In *P. falciparum*, infected hepatocytes become enlarged, rupture and release schizonts (merozoites) into the bloodstream (Figure 2A). The merozoites invade erythrocytes (Figure 2B) and undergo an asexual replication to form the trophozoites. The parasite breaks down the hemoglobin of infected erythrocytes releasing hemozoin as a by-product. Hemozoin has been identified as a distinctive feature of blood-stage parasites. The end of erythrocytic stage is marked with nuclear division (Figure 2B). Infected erythrocytes rupture and release more merozoites. These merozoites invade new erythrocytes and initiate another asexual replication.

A percentage of schizonts (merozoites) differentiate into micro (male) and macro (female) gametocytes which when ingested by feeding female *Anopheles* mosquitoes

develop into micro-and macro-gametes respectively (Figure 2C). The microgamete fuses with the macrogamete forming a zygote which develops into an ookinete. The ookinete migrates across the mosquito midgut wall and matures into oocyst within the body cavity. The oocyst undergoes asexual replication called sporogony which results in the production of lots of sporozoites. The oocyst ruptures and releases the sporozoites which migrate to the salivary gland of the mosquito ready to be transmitted during the next feeding cycle of the vector (Figure 2C).



Source: www.dpd.cdc.gov/dpdx/M-R/Malaria/body_Malaria_page1.htm

Figure 2: Life cycle of human malaria parasite



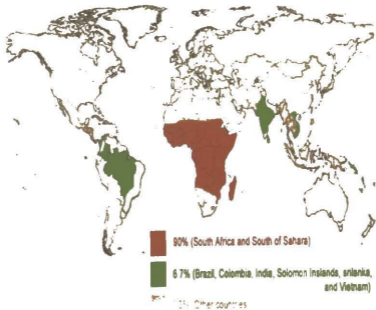
The clinical symptoms of malaria infection including chills, vomiting, convulsion, headache and drowsiness has been associated with the rupturing of infected red blood cells (RBC) during the erythrocytic stage of the life cycle. The simultaneous rupturing of parasitized RBCs and the release of parasite antigens and waste products is associated with the intermittent fever paroxysms commonly seen in malaria episodes. The rupturing of infected RBC is synchronous with the incidence of the disease. The typical pattern of fever with febrile episodes every 48 or 72 hours of *Plasmodium* infection is associated with the cyclic maturation of asexual stage; nausea and vomiting with fever spikes coincide with rupture of infected RBCs.

Each stage of the life cycle of the parasite is associated with species-specific proteins expressed on the surface membrane of the parasite, which appear to be targets of the host immune response. These species-specific proteins tend to be antigenically variable and highly polymorphic (McCutchan *et al.*, 1988). Notable among the malaria induced proteins on RBCs surface membrane is the *Plasmodium falciparum* erythrocyte membrane proteins (PfEMP) which have been implicated in adherence of infected RBCs to endothelial cells as well as non-infected RBCs leading to erythrocyte rosettes (Baruch *et al.*, 1996). Internal antigens released from infected RBCs during rupturing triggers the cytokine cascade of the immune system leading to much of the symptoms and immunopathogenesis associated with the parasites (Taverne *et al.*, 1990).

2.2 Global epidemiology of malaria, and economic development

At present, at least *falciparum* malaria annually infects 300 to 500 million people and causes over 2 million global deaths (WHO, 2000). Malaria is Africa's leading cause of under-five mortality (20%) and constitutes 20-50% of the continent's overall disease burden. It accounts for 40% of public health expenditure, 30-50% of inpatient admissions, and up to 50% of outpatient visits in areas with high transmission (Roll Back Malaria, 2002).

Malaria is generally endemic in the tropics, with extensions into the subtropics. Distribution varies greatly from country to country. More than 90% of all malaria cases occur in Africa. Approximately 10% of malaria is concentrated in other countries such as, India, Brazil, Sri-Lanka, Afghanistan, Vietnam, Cambodia, Thailand, Indonesia, and China. The disease is endemic in 91 countries worldwide (Figure 3) (WHO, 1996).



Source: <http://www.pon.nic.in/fil-free/vcre/malaria3.html>

Figure 3: Global distribution of malaria

Malaria affects the health and wealth of nations that are endemic to this disease. The disease is responsible for 44 million disability adjusted life years (DALYs) in Africa (WHO, 1996). It is estimated that malaria accounts for a reduction of 1.3% in the annual economic growth rate of endemic countries, and that the long-term impact in these countries is a reduction of gross national product (GNP) of more than half (Sachs & Malaney, 2002). In Africa, malaria accounts for up to one-third of all hospital admissions and up to one-fourth of all deaths of children under the age of 5 (Greenwood, 1999). Malaria is a significant cause of poverty in developing countries especially Africa, and has a measurable direct and indirect cost. It is also responsible for a major constraint to economic development (Table 1). The direct costs of malaria include expenses incurred on individuals and public expenditures on both prevention and treatment of the disease. The cost of malaria treatment ranges from US\$0.80 to US\$5.30 depending on local drug resistance. In countries with a heavy malaria burden, the disease may account for as much as 40% of public health expenditure, 30-50% of inpatient admissions, and up to 50% of outpatient visits (www.who.int/inf-fs/en/InformationSheet10.pdf).

The indirect costs of malaria include loss of productivity or income associated with illness. A bout of malaria is estimated to cost 10 working days, adding to the economic burden.

Annual economic growth in countries with high malaria transmission has been estimated to be lower than countries without malaria. Regression analysis using cross-country data between 1965 and 1990 confirmed the relationship between malaria and economic growth. Depending on a country's poverty, economic policy, tropical location, and life

expectancy among other factors, countries with intensive malaria incidence recorded an economic growth of 1.3% less per person per year, while a 10% reduction in malaria was associated with 0.3% increase in growth (Gallup & Sachs, 2001). Sachs and Malaney (2002) demonstrated the link between malaria in a country and that country's per capita gross domestic product (GDP) and argued that there is an inverse relationship between the two and that malaria causes underdevelopment. The total cost of malaria in terms of health care, treatment, and loss of productivity in Africa is estimated to be US\$2billion per year (WHO, 2000). Malaria may also impede the flow of trade, foreign investment and commerce, thereby affecting a country's economic growth.

Table 1. Loss from the economic growth penalty of malaria endemicity in 31 African countries, 1980-1995

<u>Country</u>	<u>Aggregate loss (millions of PPP- adjusted 1987 \$)</u>	<u>Per person loss (PPP-adjusted 1987\$)</u>	<u>As a fraction of actual 1995 income</u>
Benin	1172	214	18%
Botswana	503	347	5%
Burkina Faso	1684	162	18%
Burundi	730	117	18%
Cameroon	4227	318	18%
Central African Republic	884	270	18%
Chad	995	154	17%
Congo	759	288	18%
Congo, Dem. Rep.	7125	162	18%
Cote d'Ivoire	4107	294	18%
Gabon	1389	1290	17%
Gambia	251	226	18%
Gambia	251	226	18%
Ghana	5355	314	18%
Guinea Bissau	152	142	14%
Kenya	5272	198	18%
Lesotho	0	0	0%
Madagascar	2280	167	18%
Malawi	1072	110	18%
Mali	1222	125	17%
Mauritania	611	269	15%
Mauritius	0	0	0%
Namibia	832	539	10%
Niger	1457	161	17%
Nigeria	17315	156	18%
Rwanda	656	102	18%
Senegal	2426	286	18%
Sierra Leone	366	87	17%
South Africa	4056	98	1%
Togo	1166	285	18%
Zambia	1359	151	18%
Zimbabwe	4214	383	18%
Total	73 638	185	10%

Source: Malaria Foundation International. Based on results in Gallup J. and Sachs J., "The Economic Burden of Malaria" in Economics of Malaria. Figures are reported in purchasing power parity (PPP) adjusted dollars held constant at 1987 prices.

2.3 Current strategies for malaria control

2.3.1 The use of anti-malarial drugs and their discovery

Anti-malarial drugs prevent symptomatic blood stage asexual infection of malaria and are used for non-immune people who stay for a short time in malaria endemic area, pregnant women who are more susceptible to the disease and blood schizontocides in infected individuals.

Therapeutic use of drugs against malaria prevents development of asexual blood stage of the parasite. The discovery of drugs for malaria treatment has been through several approaches:

a) Consider natural compounds such as quinine and artemesia

Quinine, derived from a plant- the bark of the cinchona tree has been widely used for treating malaria since the 17th and 18th centuries. Artemisinin is also a drug against malaria derived from plant in China and has also been effective against the malaria parasite. Though the mechanism of action of these compounds is not very clear, they are believed to be responsible for inhibiting haem polymerization in the parasites. Haem is a by-product of haemoglobin degradation and is toxic to the malaria parasite if it is not polymerized. Quinine and artemisinin are believed to inhibit this process thereby leaving the toxic haemoglobin degraded product to kill the parasite.

b) Screening large numbers of potential compounds

Screening of large numbers of compounds led to the discovery of chloroquine, one of the cheapest and effective drugs against malaria for years. Mechanism of action of chloroquine is unclear but it is also believed to interfere with haem polymerization.

c) Looking at chemically related compounds

By looking for chemically related compounds, other quinoline compounds were discovered including mefloquine (Lariam) and amodiaquine which are used primarily as prophylaxis against malaria parasite.

d) By studying the metabolic pathways in the parasite

i) Folate pathway inhibitors

Some of the antimalarial drugs inhibit folate metabolism. Inhibition of two key enzymes in the folate metabolic pathway typically inhibits the parasite's growth at concentrations that have no detectable effects on host cells. Pyrimethamine (Daraprim) and Proguanil (Paludrine) are anti-malarial drugs which inhibit dihydrofolate reductase while sulphonamides and sulfones (Dapsone) as well as Fansidar (Pyrimethamine-sulfadoxine) inhibit dihydropteroate synthase enzyme in the folate metabolic pathway.

ii) Inhibitors of pyrimidine synthase-dehydroorotate dehydrogenase

Inhibitors of dihydroorotate dehydrogenase including 8-aminoquinolines such as Primaquine which is used for cure of relapsing *P. vivax*-tissue schizonts and also as gametocytocidal against *P. falciparum* and Atovaquone are effective drugs for controlling malaria.



iii) Protein inhibitors

Since degraded haemoglobin products provide amino acids for malaria parasite, inhibitors of haemoglobin degrading enzymes like Plasmeprin I and II (aspartic proteinase) and Falcipain (cysteine proteinase) are used to control malaria infection.

iv) Phospholipid metabolism inhibitors

Phospholipid metabolism inhibitors which target blockage of choline transporter are also used for malaria parasite control.

2.3.2 Vector control

2.3.2.1 Use of nets and insecticide treated bed nets

The objective of the malaria vector control strategy is to reduce malaria mortality and morbidity by reducing transmission of the disease. Vector control strategies include the use of insecticide impregnated bednets, indoor spraying of insecticides, personal protection measures, larval and environmental control. Dichloro-diphenyl-trichloroethane (DDT) was previously used in the 1960s as an insecticide for malaria vector control but because of vector resistance and its residual effect in the environment, its usage has been discontinued.

Currently pyrethroids including deltamethrin and lambda-cyhalothrin are the insecticides of choice and are effective at far lower doses with very minimal or no residual effect compared with DDT. A popular application of pyrethroids is in the impregnation of bednets (Curtis, 1997) so as to add a chemical barrier to the imperfect physical barrier presented by the net.

2.3.2.2 Larval control

Some of the strategies for mosquito larval control include:

1. Preventing mosquito breeding in stagnant waters
2. Stocking the breeding sites of mosquitoes with larvivorous fish such as Guppies
3. The use of bacterial toxin from *Bacillus thuringiensis* (BT) at the breeding sites as a highly specific agent against mosquito larvae
4. Situations where irrigations are carried out in carefully regulated intermittent schedules, such that fields are dried once a week to prevent the complete larval cycle.

2.4 Clinical manifestations and pathogenesis of malaria

2.4.1 Uncomplicated malaria

Presentation of uncomplicated *P. falciparum* malaria is very variable and may resemble that of many other diseases. Non-immune patients with uncomplicated malaria are prone to the development of severe life threatening malaria complications. Although fever is very common in uncomplicated malaria, it is absent in some cases. The fever is initially persistent rather than tertian. In addition symptoms such as rigors, headache, sweating, tiredness, loss of appetite and nausea may arise.

2.4.2 Complicated or severe malaria

If *P. falciparum* malaria is not promptly diagnosed and treated, the clinical picture may deteriorate rapidly, often with serious and severe consequences. Severe malaria is defined as parasitaemia of higher than 5%, a haemoglobin of less than 6g/dl, spontaneous hypoglycaemia or major organ dysfunction - particularly cerebral malaria. Most people who have *P. falciparum* parasites in their blood usually suffer from uncomplicated malaria associated with headaches, fever, chills, and weakness with muscle pains. However in a small minority of cases, severe and life threatening complications such as enlargement of spleen and liver (spleno-hepatomegaly), acidosis (acidic blood), hypoglycaemia (low blood sugar), kidney failure, severe anemia and cerebral malaria may occur.

Spleno-hepatomegaly, results from lysis of hepatocytes during schizogony in the liver in addition to massive immune response to the malaria parasites. One of the outcomes of hepatomegaly is jaundice. Cytoadherence of parasitized RBCs coupled with deposition of malaria parasite pigments and induction of proinflammatory cytokines in the spleen have been implicated in splenomegaly (Mashaal, 1986).

Malaria acidosis also referred to, as hyperpnea is associated with respiratory disturbances. The source of this complication is unknown but it is known to be responsible for most childhood malaria deaths (English *et al.*, 1997).

In areas of low transmission, hypoglycemia, anemia and convulsion are common in children. Hypoglycemia is the outcome of low blood sugar in *P.falciparum* infected person. Though direct parasite products and human immune response have been implicated in this condition, the mechanism involved is still not clear. About 38% of infected children die of hypoglycemia related complications (Chogle, 1998).

In most cases, cytoadherence of parasitized RBC's in glomerular capillary walls of infected adult results in kidney damage and renal failure (Mehta *et al.*, 2001). Acute renal failure occurs as a complication of *P.falciparum* in less than 1% of cases but mortality rate associated with this complication is estimated to be 45% (Saroj *et al.*, 2002).

Though the incidence of fever and chills have been associated with the lysis of infected RBC's during the erythrocytic stage of the parasite's life cycle, it is still unclear why only some episodes of malaria infection in non-immune and semi-immune individuals results in complications.

2.4.2.1 Severe malaria anaemia

Severe malaria anaemia is a result of hemolysis of parasitized RBC's. This complication is common in children between 1-2 years old. This complication is one of the principal manifestations in areas of high stable transmission. Non-parasitized RBC's exhibit deformability which causes more to be taken out by phagocytes in the spleen. This in addition to suppression of bone marrow and erythropoiesis results in anaemic conditions in patients.

2.4.2.2 Cerebral malaria (CM)

Cerebral malaria (CM) is defined according to established World Health Organization guidelines as Glasgow Coma score of 11 or less in adult or Blantyre coma score of 5 or less in children during the episode of severe malaria (WHO, 2000), other causes of unconsciousness such as hypoglycemia, meningitis or other encephalopathy having been excluded by clinical, biochemical, and cerebrospinal fluid (CSF) examination. Glasgow or Blantyre coma score is a scoring system used in quantifying level of consciousness following traumatic brain injury or during *P.falciparum* infection.

It consists of three parameters: best eye response, best verbal response and best motor response given as:

<u>Best Eye Response (E)</u>	<u>Score</u>
No eye opening	1
Eye opening to pain	2
Eye opening to verbal command	3
Eye opening spontaneously	4
<u>Best Verbal Response (V)</u>	<u>Score</u>
No verbal response	1
Incomprehensible sounds	2
Inappropriate words	3
Confused	4
Orientated	5
<u>Best Motor Response (M)</u>	<u>Score</u>
No Motor Response	1
Extension to pain	2
Flexion to pain	3
Withdrawal from pain	4



Localization	5
Obeys commands	6
Total score =E+V+M	

A total score of 13 to 15 indicates mild coma. A score between 9 and 12 indicates moderate coma, and a score of 8 or less indicates severe coma for Glasgow score (Jennett *et al.*, 1976 & 1978). The Blantyre Coma Scale, a related diagnostic tool, is used for children. A coma score of less than 3 indicates cerebral malaria infection.

Cerebral malaria (CM) complications are associated with seizures, convulsion, severe headache, drowsiness, behavioral changes and ultimately coma. This complication is common in areas of intermittent malaria transmission. Children below the age of 5 and non-immune individuals usually suffer from CM incidence. About 15% of CM patients die of the disease (Mturi *et al.*, 2003). It has been hypothesized that the neurological manifestations of CM are due to either sequestration of parasitized RBCs to the microvascular endothelial cells or induction of proinflammatory molecules.

Sequestration refers to the cytoadherence of trophozoite and schizont parasitized erythrocytes to endothelial cells. This leads to mechanical blockage (cerebral ischaemia) in the distal microvessels in the brain and subsequently limits the supply of oxygen, a condition referred to as hypoxia. The parasite can also induce localized metabolic effects such as hypoglycemia. The hypoxia and metabolic effects would then cause coma and other neurological complications and death. Cytoadherence involves receptor ligand interactions. *Plasmodium falciparum* erythrocyte membrane protein-1 (PfEMP-1)

expressed as an induced protein on parasitized erythrocytes have been implicated as a ligand, which binds to parasite's induced host endothelial receptors such as ICAM-1, VCAM-1 and CD 36 (Udomsangpetch *et al.*, 1997). *PfEMP-1* is a member of a highly variable (var) gene family with 40-50 different genes. This antigenic variation associated with *PfEMP-1* allows the parasite to evade the immune system and may also be responsible for differences in disease outcomes.

Others have suggested that coma which is associated with CM is mediated by short-lived molecules such as TNF- α and nitric oxide that affect cerebral functions. In this hypothesis, malaria antigens stimulate TNF- α production, which induces nitric oxide. These proinflammatory molecules partly induce the pathological effects associated with CM. Nitric oxide is known to affect neuronal function and, may lead to intracranial hypertension through its vasodilator activity. It has been postulated that, the sequestration and the proinflammatory molecules hypotheses are not mutually exclusive and that both phenomenon mediate CM pathogenesis. Thus antigens released by rupture of parasitized erythrocytes stimulate leukocytes such as macrophages which secrete TNF- α which in turn upregulates expression of ICAM-1 on brain endothelial cells (Porta *et al.*, 1993). This eventually leads to increase in binding of infected erythrocytes and increase in effects whether they are due to vascular blockage, soluble mediators or metabolic effects.

2.5 Immunity to malaria infection

In malaria stable endemic regions, *P.falciparum* parasitemia and its associated clinical disease is most common in children and non-immune adults. In The Gambia for instance, where *P.falciparum* transmission is highly seasonal but relatively stable from year to year, parasite rates do not begin to decline until the age of 10 to 12, whereas the incidence of clinical disease, that is fever which is associated with malaria parasitemia peaks at age 6 (Riley *et al.*,1990).

Not all people infected with the malaria parasite in endemic areas exhibit clinical symptoms. Healthy individuals are found with parasites in their blood without clinical symptoms. The incidence of parasitemia declines gradually with age. This phenomenon is interpreted as a steady acquisition of specific immunity to malaria (Barragan *et al.*, 1998). Immunity to malaria is the ability of the individual to control parasite multiplication, which can occur at either the pre-erythrocytic (hepatic) stage or during the erythrocytic stage or minimize clinical disease outcome. Antibodies directed against the major surface protein of the sporozoite called the circumsporozoite protein, (CSP) can inhibit their entry into liver cells (Hollingdale *et al.*, 1984). The precise pattern of immunity to malaria depends on local patterns of malaria transmission and also the degree of endemicity. It is suggested that multiple infections seem to be necessary to achieve effective anti-parasite immunity. Though resistance to infection with malaria increases with age in individuals living in endemic regions, it can take several decades to reach optimal protection, which may sometime never attain. Because immunity to malaria has been found to depend on both parasite transmissions and age, it has been

hypothesized that the malaria antigens that induce protective immune response might be poorly immunogenic.

The malaria antigens reportedly exhibit polymorphism; variation between different strains of the parasites as well as variability (changing within strains in line) (Felger *et al.*, 1997). Therefore immunity to the parasite requires accumulation of immunological memory to a large number of different antigenic epitopes before substantial protection is achieved. Currently the slow development of immunity to malaria is explained by two main hypotheses;

- a) Antimalarial immunity is essentially strain specific, and effective immunity is not achieved until the individual has been exposed to all the major antigenic variants circulating within the community (Day & Marsh, 1991) and
- b) Acute malaria is associated with immunosuppression, which hinders the development of protective immune response (Cohen *et al.*, 1961)

Antibody-dependent and antibody-independent immune effector mechanisms have been implicated in naturally acquired protective immunity to malaria. The ability of antibodies to confer immunity against malaria parasites in both *P. falciparum* and *P. vivax* is apparent from the protection afforded to neonates and infants by maternally derived antibodies (Edozien *et al.*, 1962, Logie *et al.*, 1973) and from clinical treatment trials with immune serum or purified immunoglobulins (Cohen *et al.*, 1961, McGregor *et al.*, 1962). Also,

research conducted using rodent malaria models with the transfer of whole immune serum or purified immunoglobulin to naïve animals indicates substantial modification of the course of blood stage infections, reduced peak parasitemia, and spontaneous resolution of infection (Holder, 1988).

Unlike antibody-dependent or humoral immunity, less is known about cellular immune response to malarial infection. Studies using murine models indicate that T-cell dependent immune mechanisms are crucial to the development of effective antimalarial immunity. For example, immunity against *Plasmodium yoelii* depends on the cooperation of immune T and B lymphocytes (Mogil *et al.*, 1987) while immunity to *Plasmodium chabaudi adami* appears to be antibody independent (Grun *et al.*, 1981). Direct killing of infected hepatocytes by cytotoxic T lymphocytes (CTL) appears to be mediated by major histocompatibility complex class I (MHC-I)-restricted recognition of sporozoite or liver stage antigens presented on the surface of infected liver cells in experimental murine systems (Kumar *et al.*, 1988). Sporozoite and liver stage antigen-1 (LSA-1) specific CTL activity has been demonstrated *in vitro* using peripheral blood lymphocytes from people with prior exposure to malaria (Malik *et al.*, 1991, Hill, *et al.*, 1991) but, at present, it is not known whether such mechanisms contribute to protective immunity in humans.

Since mature erythrocytes do not express MHC antigens, T cells are believed to fulfill two major functions in immunity to erythrocytic parasites, by providing help for antibody production and producing cytokines which activate macrophages to phagocytose infected erythrocytes and kill malaria parasites. Following activation by

interferon gamma (INF- γ), phagocytosis occurs via much more efficient Fc receptor-mediated parasite binding (Brown *et al.*, 1986).

Though macrophage-produced tumor necrosis factor-alpha (TNF- α) reportedly plays a role in the pathogenesis of acute malaria, it is also believed to mediate parasite killing (Clark & Cowden 1992). A potential mechanism for TNF-mediated parasite killing may be via induction of nitric oxide, (Rockett *et al.*, 1992) which has been implicated in murine immunity to *Plasmodium berghei* (Nussler *et al.*, 1993).

Whether T cell-mediated immunity to blood stage malaria predominates over antibody-mediated or vice versa is still unclear. Though several merozoite-specific antigens have been identified, the best characterized are the major *Plasmodium falciparum* merozoite surface proteins (PfMSP1) (Pf195) (Holder, 1988) and PfMSP2 (Pf48-53) (Smythe *et al.*, 1990) and the ring-infected erythrocyte surface antigen (RESA; Pf155) which is deposited into the erythrocyte membrane during invasion (Cowman *et al.*, 1984). Antibody-mediated immunity to these antigens and a number of other defined antigens appear to correlate with population level of acquired immunity, but this association does not always prove true at the individual level. Levels of antibody to parts of PfMSP1 in Ghanaian children reportedly did not correlate with protection from clinical malaria (Dodoo *et al.*, 1999). However cellular proliferation and INF- γ responses to PfMSP1 appear to be associated with resistance to clinical disease and high parasitemia (Riley *et al.*, 1992).

2.6 Central nervous system (CNS) and malaria

The brain is the control center of the body. Different areas of the brain control functions in different parts of the body. Infectious pathogens modulate these functions depending on the part of brain they infect (Shrestha *et al.*, 2003, Bifrare *et al.*, 2003). For instance, the brain is one of the most prominent targets of human immunodeficiency virus (HIV) infection, where it leads to HIV encephalitis (HIVE) and HIV-associated dementia (Price *et al.*, 1990).

Knowledge of the distribution, physiology, and pathology of immune mediators in the brain is fundamental for understanding the pathogenesis of the interaction between disease causing pathogens and the CNS.

Malaria infection of the CNS by *Plasmodium* parasites (CM) is associated with at least 2.3 million deaths annually, from an estimated 400 million cases each year worldwide and is the leading cause of hospitalization, mortality, and morbidity of children under five years in sub-Saharan Africa (Turner, 1997). The neuropathology of CM is characterized by neurological abnormalities precipitated by oedema in the brain. The cause of these complications is not very clear but it is known to be associated with the malaria parasites blocking cerebral capillaries and obstructing microcirculation causing necrosis in the brain (Grote *et al.*, 1997); as well as induction of proinflammatory molecules by the parasite. Although the mechanism of action for the pathogenesis of CM suggests global and possibly diffuse CNS involvement, it is diffuse and difficult to precisely characterize. Studies of CM cases from Vietnam show differential rates of sequestration within

different areas of the brain (Sein *et al.*, 1993), while axonal injury reportedly occurred in the cerebral cortices and cerebellum compared to the mid-brain structures or the brain stem (Medana *et al.*, 2002).

Different regions of the brain such as cerebrum, cerebellum and brain stem have been implicated in neurological associated disorders. Analysis of postmortem samples of victims of malaria revealed higher sequestration of infected RBC's in the cerebellum than the cerebrum (Sein *et al.*, 1993). This explains varied neurologic manifestations that result from brain dysfunction in human cerebral malaria. However, it is not clear why certain regions of the brain are more susceptible to malaria infection than others. The mechanism involved in CM neuropathology is also unclear.

CM factors predictive of neurological sequelae are prolonged coma, protracted convulsions, severe anemia and a two phase clinical course in which a patient recovers consciousness only to be followed by recurring convulsions and coma (Brester *et al.*, 1993). Looking at the seriousness and life-threatening nature of CM including intensive neuropathological cerebrovascular effects, it is assumed that the incidence of the disease during a critical period of brain development and organization as it occurs predominantly in children, will impact those brain systems which are most vulnerable to cerebrovascular damage. These vulnerable regions may support attention capacity, memory and cognitive functions and that any neuropsychological sequelae for CM will involve these abilities to a varying degree.

2.7 Immune mediators of malaria in mouse models, human and primate

2.7.1 Immune mediators of malaria in mouse models

2.7.1.1 The role of adhesion molecules

Adhesion molecules are a diverse family of extracellular and cell surface glycoproteins involved in cell-cell and cell-extracellular matrix adhesion, recognition, activation, and migration. Some of these molecules are calcium dependent while others are not.

Calcium dependent adhesion molecules also called cadherins are involved in cell to cell adhesion. Almost all vertebrates express cadherins. Cadherins connect cells together at specialized junctions.

Cell to cell surface carbohydrate binding proteins also called selectins bind to specific oligosaccharides on another cell in the presence of calcium. P-selectin is an example of a selectin which allows white blood cells to bind to endothelial cells.

Integrins are another class of adhesion molecules which mediate cell to cell binding. Integrins are transmembrane binding glycoproteins and they also bind cells to cellular matrix and are calcium dependent. Integrins on white blood cells allow tighter binding to endothelial cells before they migrate out of the blood stream to tissue. Leukocyte factor associated antigen (LFA-1) on white blood cells is an example of this class of molecule.

Non-calcium dependent cell to cell binding molecules belong to the immunoglobulin (Ig) superfamily. Neuronal cell adhesion molecules (NCAM's) and intercellular adhesion molecules (ICAMs) are examples of non-calcium dependent adhesion molecules.

Murine cerebral malaria studies have shown that cytoadherence of parasitized RBC via adhesion molecules including intercellular adhesion molecule 1 (ICAM1), vascular cell adhesion molecule 1 (VCAM1), and cluster of differentiation 31 (CD31) plays an important role in the pathogenesis of the disease. Immunostaining for ICAM-1 for instance revealed an increase in expression of this protein in the small venules and capillaries of the brains of *P.yoelii* infected mice (Shear *et al.*, 1998).

Although ICAM-1 and VCAM-1 for example, have previously been implicated in sequestration during ECM, recent experimental murine microcirculatory evidence indicates involvement of ICAM-1, but not VCAM-1, in the sequestration of IRBCs (Kaul *et al.*, 1998).

Recent findings also indicate that inhibition of P-selectin (platelet adhesion molecule) to the brain microvasculature protects against development of experimental malaria brain pathogenesis (Sun *et al.*, 2003).

2.7.1.2 The role of cytokines

Cytokines are non-antibody proteins secreted by inflammatory leukocytes and some non-leukocytic cells that act as intercellular mediators. They differ from classical hormones in that they are produced by a number of tissue or cell types rather than by specialized glands. They generally act locally in a paracrine or autocrine rather than endocrine manner. Cytokines made by lymphocytes are called lymphokine, while those made by monocytes are referred to as monokine. Cytokines with chemotactic activities are collectively referred to as chemokine and those made by one leukocyte and acting on other leukocytes are called interleukins.

The potential of cytokines as pathogenic elements of malaria can contribute directly or indirectly to many pathological processes associated with the disease. Rodent malaria models have provided further evidence of the important role of inflammatory processes in the development of CM (Brian & Riley, 2002). Cytokines such as interferon gamma (INF- γ), interleukin 12 (IL-12) and tumor necrosis factor alpha (TNF- α) have been implicated in the pathogenesis of CM. Studies with knockout mice infected with *Plasmodium berghei* ANKA have revealed an essential requirements of INF- γ , and IL-12 in the development of CM (Rudin *et al.*, 1997, Yanez *et al.*, 1996).

In malaria models in which INF- γ and IL-12 display a dominant pathological role, a protective effect has been demonstrated by IL-10 (Tran *et al.*, 2000). Neutralization of anti-inflammatory cytokine (IL-10) *in vivo* has been shown to increase the percentage of mice with CM in a CM-resistant strain (Kossodo *et al.*, 1997). In the case of TNF- α ,

although it reportedly plays an important role in CM pathogenesis, there was contradicting findings with TNF- α knockout mice infected with *P.yoelii* parasites. These animals have slightly higher levels of infected erythrocytes, but their susceptibility to death from this infection was not observed (Shear *et al.*, 1998). It was therefore concluded that though TNF- α may play a role in CM pathogenesis, it is not absolutely required for death.

2.7.1.3 The role of chemokines and receptors

Chemokines constitute a superfamily of small (8-16 kDa), soluble, pro-inflammatory proteins produced and secreted by a wide variety of cell types during the initial phase of host response to injury, allergens, antigens, or invading microorganisms. They are involved in a variety of immune and inflammatory responses, acting primarily as chemoattractants and activators of specific types of leukocytes and other cell types.

The chemokines have been classified into alpha (C-X-C), beta (C-C), gamma (C) and delta (C-X₃-C) based on the relative position of their first N-terminal cysteine residues (Figure 4). The alpha chemokines (C-X-C) have a single amino acid inserted between the first and second of their four cysteine residue, whereas these cysteines are not separated in the beta group (C-C). The gamma (C) chemokines have only one pair of cyteine while in the delta chemokines C-X₃-C, the first two cysteines are separated by three amino acids. The systematic name of chemokines is designated as CXCL, CCL, XCL, and CX₃CL based on each class (Table 2).

Table 2: Chemokine nomenclature

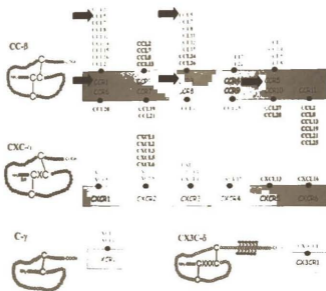
<u>SYSTEMATIC NAME</u>	<u>ORIGINAL NAME</u>	<u>RECEPTORS</u>
<u>CXC</u>	<u>Chemokines</u>	
CXCL1	GR0 α	CXCR2, CXCR
CXCL2	GRO β	CXCR2
CXCL3	GRO γ	CXCR2
CXCL4	PF4	Unknown
CXCL5	ENA-78	CXCR2
CXCL6	GCP-2	CXCR1, CXCR2
CXCL7	NAP-2	CXCR2
CXCL8	IL-8	CXCR1, CXCR2
CXCL9	Mig	CXCR3
CXCL10	P-10	CXCR3
CXCL11	I-TAC	CXCR3
CXCL12	SDF-1 α/β	CXCR4
CXCL13	BCA-1	CXCR5
CXCL14	BRAK	Unknown
CXCL15	Unknown	Unknown
CXCL16 -	Unknown	CXCR6
<u>C</u>	<u>Chemokines</u>	
XCL1	Lymphotactin/SCM-1 α	XCR1
XCL2	SCM-1 β	XCR1
<u>CX3C</u>	<u>Chemokines</u>	
CX3CL1	Fractalkine	CX3CR1
<u>CC</u>	<u>Chemokines</u>	
CCL1	i-309	CCR8
CCL2	MCP-1	CCR2
CCL3	MIP-1 α	CCR1, CCR5
CCL3L1	LD78 β	CCR1, CCR5
CCL4	MIP-1 β	CCR5
CCL5	RANTES	CCR1, CCR3, CCR5
CCL6	Unknown	Unknown
CCL7	MCP3	CCR1, CCR2, CCR3
CCL8	MCP-2	CCR3, CCR5
CCL9/CCL10	Unknown	CCR1
CCL11	Eotaxin	CCR3
CCL12	Unknown	CCR2
CCL13	MCP-4	CCR2, CCR3
CCL14	HCC-1	CCR1, CCR5
CCL15	HCC-2/Lkn-1/MIP-1 δ	CCR1, CCR
CCL16	HCC-4/LEC/LCC-1	CCR1, CCR2
CCL17	TARC	CCR4
CCL18	DC-CK1	Unknown

CCL19	MIP-3 β /ELC	CCR7
CCL20	MIP-3 α /LARC	CCR6
CCL21	6Ckine/SLC	CCR7
CCL22	MDC	CCR4
CCL23	MIPF-1/CKb8	CCR1
CCL24	Eotaxin-2	CCR3
CCL25	TECK	CCR9
CCL26	Eotaxin-3	CCR3
CCL27	CTACK	CCR10
CCL28	MEC	CCR3/CCR10

Source: <http://www.expertreviews.org>



The mechanism of chemokine action involves initial binding to specific seven transmembrane spanning G protein-linked receptors on target cells. Several of these receptors have been discovered for the different class of chemokines as CXCR, CCR, XCR, and CX₂CR (Figure 4). Chemokine ligands (CCL, Figure 4) can interact with more than one receptor and vice versa. For instance, regulated on activation normal T cell expressed and secreted (RANTES, CCL5), a beta chemokine, can bind to receptors CCR1, CCR3 and CCR5.



Source: Bajetto *et al.*, 2001

Figure 4: Classification of chemokines and receptors-based on the structural characteristics of their relative ligands. The list of chemokines signaling through each receptor is indicated.

Chemokines control immune cell trafficking and recirculation of leukocyte population between the blood vessels, lymph, lymphoid organs and tissues, a process significant in host immune surveillance, and acute and chronic inflammatory responses. In addition to their expressions during injury and infection, chemokines also play fundamental role in homeostasis, angiogenesis and angiostatic process, tumor and metastasis progression, and in the CNS (Bajetto *et al.*, 2001, Belperio *et al.*, 2000, Rossi & Zlonik 2000).

A comparative study using *Plasmodium berghei* ANKA infected C57BL/6 and BALB/c mice indicate that both strains of mice expressed CXCL10 (interferon-induced protein 10, IP-10) and CCL2 (monocyte chemoattractant protein -1, MCP-1) genes as early as 24 hours post-infection (Hanum *et al.*, 2003).

Other CM model studies show that experimental cerebral malaria (ECM) is induced in perforin-deficient mice (PFP-KO) after adoptive transfer of cytotoxic CD8⁺ T cells from infected C57BL/6 mice, which were directed to the brain of PFP-KO mice. The recruitment of cytotoxic CD8⁺ T cells into brains of PFP-KO mice might involve chemokine and their receptors, and this suggests that lymphocyte cytotoxicity and cell trafficking could be key players in ECM (Niteche *et al.*, 2003).

The use of rodent murine malaria models has demonstrated the involvement of leukocyte trafficking during CM pathogenesis. The *P.berghei* ANKA model suggests that sequestration of infected RBCs and platelets mediate CM. Thus, activated platelets may entrap leukocytes recruited to distal brain microvessels where infected RBCs are also

sequestered. In this model substantial number of CD8⁺ T cells in brain-sequestered-leukocytes (BSL) of CM infected mice were CCR5⁺ (Belnoue *et al.*, 2003). Also treatment of mice with monoclonal antibody (mAb) to leukocyte factor-associated antigen-1 (LFA-1) selectively abrogated the cerebral sequestration of platelets that correlated with prevention of ECM (Grau *et al.*, 1986).

While chemokine receptor CCR2 was observed to be non-essential for development of experimental cerebral malaria (Belnoue *et al.*, 2003a), CCR5 deficiency in mice reportedly decreases susceptibility to ECM (Belnoue *et al.*, 2003b). Though brain-sequestered CD8⁺ T cells which express certain chemokines and receptors are known to be responsible for ECM pathology, it is still unknown which class of chemokines and chemokine receptors expressed on these cells mediate ECM pathology.

2.7.2 Immune mediators of malaria in human and primate models

2.7.2.1 The role of adhesion molecules

The factors that determine whether CM develops or not are not clearly defined. However, one important determinant may be the role of endothelial receptors in cytoadherence of parasitized RBCs (Figure 6). Many of these receptors such as ICAM-1, VCAM-1, E-selectin, platelet cell adhesion molecule-1 (PECAM-1) and cluster of differentiation 36 (CD36) have been identified and characterized (Silamut *et al.*, 1999, Turner *et al.*, 1994).

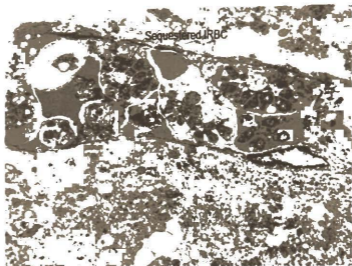
The molecules or knobs expressed on the surface of infected erythrocytes mediating cytoadherence to adhesion molecules on endothelia cells belong to a large family of the clonally variable antigens (*Plasmodium falciparum* erythrocyte membrane protein 1

(*PfEMP1*) (Craig & Scherf, 2001) encoded by the *var* genes. The knobs adhere to receptors on endothelial cells of cerebral vessels, followed by rosette formation and agglutination of the non-parasitized erythrocytes (Ringwald *et al.*, 1993) resulting in occlusion of cerebral vessels. Upregulation of ICAM-1 expression increased the binding of *PfEMP1* to brain capillaries and contributed to complications associated with cerebral malaria. Additionally, ICAM-1 expression is upregulated by cytokines such as TNF- α , and IL-1 (Rudin *et al.*, 1997, Jakobson *et al.*, 1995).

Furthermore, adhesion of infected erythrocytes to molecules such as chondroitin 4-sulphate and hyaluronic acid has been associated with placental malaria (Rogerson *et al.*, 1995). Following cytoadherence, there is sequestration of parasitized erythrocytes to endothelial cells (Macpherson *et al.*, 1985) leading to endothelial cell damage and associated complications.

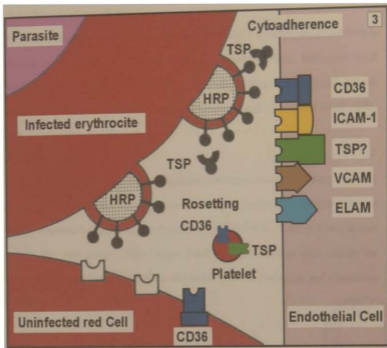
Macrophage activation and stimulation of the respiratory burst also results after binding of infected erythrocytes to CD36 (Ockenhouse *et al.*, 1989). Interestingly many of these receptors also act as endothelial receptors for leukocytes during inflammatory responses and immune surveillance. In most cases sequestration is mediated by parasite induced ligands on infected erythrocytes notably *PfEMP-1* which have been discovered to be responsible for antigenic variation in *P.falciparum*. *PfEMP-1* expressed on the surface of parasitized red blood cells (pRBC), specifically binds to CD36 and thrombospondin.

Excessive binding of *Plasmodium falciparum*-infected red blood cells (pRBCs) to adhesion molecules on the vascular endothelium (cytoadherence) and to uninfected erythrocytes (rosetting) (Figure 4) leads to occlusion of the microvasculature and thereby contribute directly to the acute pathology of severe human malaria.



Courtesy of EMSrii Pongporant)

Figure 5: Sequestration of *P.falciparum* infected erythrocytes in the distal microvasculature of the brain of cerebral malaria infected deceased patient.



Source: Manson's Tropical Diseases text book, 20th edition, pp 1098.

Figure 6: Schematic illustration of cellular adhesion in *P.falciparum* malaria. For cytoadherence (red cell to vascular endothelium) more than five potential receptors for the adhesive variant surface protein PfEMP1 have been identified. The molecules on the red cell surface involved in rosetting (infected red cell to uninfected red cell) appear to be different to those causing cytoadherence.

2.7.2.2 The role of cytokines

The increase in number and activity of macrophages and T lymphocytes during malaria infection cause the release of soluble cytokines including TNF- α , INF- γ and IL-1 β (Macpherson *et al.*, 1985, Maneeret *et al.*, 1999) which induce cytoadherence, vascular damage, activation of clotting and severe metabolic changes (Ringwald *et al.*, 1993, Rockett *et al.*, 1994, Nicolas *et al.*, 1994).

Apart from the possible direct effect of malaria parasites on brain endothelium and other organs such as the liver and kidney in infected hosts, the parasite also stimulates the host immune response, leading to overproduction of cytokines INF- γ , TNF- α , GM-CSF and IL-3 by Th1 cells (Grau, 1992). These T-cell derived cytokines then amplify the activation and recruitment of platelets and leukocytes via chemokine and chemokine receptors.



2.7.2.3 The role of chemokines and receptors

The potential roles of chemokines during malaria infection include host defense functions, such as leukocyte recruitment, participation in cell-mediated immunity and anti-protozoal activity. Though chemokines and chemokine receptors reportedly mediate pathogenesis of several parasitic diseases such as *toxoplasmosis*, *trypanosomiasis*, *leishmaniasis*, *amoebiasis* and *trichomoniasis* (Denny *et al.*, 1999, Liu *et al.*, 1999, Badolato *et al.*, 1996, Yu *et al.*, 1997, Shaio *et al.*, 1995) their involvement in malaria, especially CM is still unclear.

Observations made in a time-course studies of macrophage inflammatory protein-1alpha (MIP-1 α) and interleukin-8 (IL-8) secretion in patients with *P. falciparum* malaria indicate that IL-8 concentration correlated positively with parasite count and severity of the disease (Burgmann *et al.*, 1995). Recent studies also indicate that placentas of malaria-infected women have higher levels of CCR5 chemokine receptor expression than placentas of women without malaria (Tkachuk *et al.*, 2001) and that both fetal and maternal cells secrete inflammatory and immunoregulatory cells including beta-chemokines such as MCP-1, MIP-1alpha and IP-10 in response to *P. falciparum* (Suguitan *et al.*, 2003). This is further evidence that malaria infection induces the expression of chemokines, which may contribute to the immunopathology of the disease.

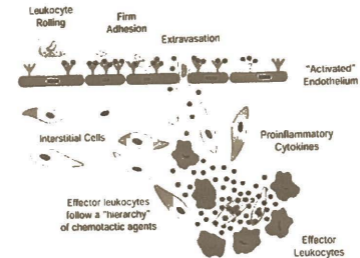
2.8 RANTES as a proinflammatory chemokine

RANTES is a chemokine that is involved in the generation of inflammatory infiltrates. It was identified as part of a screen for genes expressed 3-5 days after T cell activation. RANTES binds a variety of receptors including CCR1, CCR3 and CCR5, expressed by monocytes/macrophages, memory T cells, eosinophils, basophils and mast cells (Baggiolini & Dahinden., 1994).

Elevated levels of RANTES have been found in bronchoalveolar lavage (BAL) from asthmatics within 4 hr of allergen challenge (Holgate *et al.*, 1997) and in nasal lavage fluids from patients with allergic rhinitis (Rajakulasingam *et al.*, 1997). Thus, RANTES is implicated in the pathogenesis of allergic-type reactions with the potential to contribute to pathological changes observed in allergic inflammation. Immunoneutralization of

RANTES in CCR5 knock out murine model of chronic fungal asthma induced by *Aspergillus fumigatus* significantly reduced the peribronchial inflammation and airway hyperresponsiveness in asthmatic mice which demonstrate that functional RANTES and receptor CCR5 play a role in the persistence of chronic fungal asthma in mice (Schuh *et al.*, 2002).

RANTES binds to endothelial surfaces, where it acts as a signpost for immune cells. The interaction of immune cells in the bloodstream with selectins leads to their slow rolling along the vascular endothelium (Figure 6). RANTES does not only attract immune and other cells, but also upregulates both integrins such as lymphocytes function-associated antigen (LFA-1) involved in adhesion. Activated T lymphocytes, platelets and endothelial cells release large amount of RANTES 3-5 days after activation, giving this chemokine a special role in the maintenance and prolongation of an immune response (Kameyoshi *et al.*, 1992). Recently, the function of RANTES as a pro-inflammatory chemokine reportedly increased the likelihood of HIV infection (McDermott *et al.*, 2000). Though an association between malaria and HIV co-infection has been established (Xiao *et al.*, 1998), the involvement of RANTES as a pro-inflammatory chemokine vis-à-vis malaria immunopathology is still unclear.



Courtesy Alan M. Krensky

Figure 7. RANTES recruits inflammatory cells from bloodstream into site of inflammation. *The bloodstream acts as a reservoir for inflammatory cells. Upon infection resident macrophages release IL-1 and TNF-alpha, which in turn promote the release of chemokines. A soluble gradient of these chemokines is established within the tissue, recruiting various cell types that express receptors for different chemokines. RANTES binds to glycosaminoglycans on the endothelial cell surface, where it acts as a signpost for immune cells.*

2.9 Current research strategies for understanding malaria pathogenesis

2.9.1 Murine malaria models and malaria research

To understand the pathogenesis of CM, several animal models have been established with various types of *Plasmodium* parasites. Although these animal models do not exactly reproduce the human disease, they nevertheless exhibit some similarities to human CM, including clinical signs of the nervous system dysfunction and cerebral pathology. Recently, sequestration of platelets and leukocytes in brain microvasculature which was reported to be partly responsible for ECM has been identified to play an important role in human CM (Grau *et al.*, 2003). Also the similarities between defined malaria antigens in rodent and human parasites and between immune response pathways in mice and humans (Kaul *et al.*, 1994, Belnoue, *et al.*, 2003b, Grau, 1992) justify the use of models.

Although the histopathology of experimental CM varies according to parasite-host combinations, there are advantages and disadvantages in each of these models depending on the parameters of interest. Whereas parasitized RBC sequestration is common in *P.yoelii* 17X models, leukocyte sequestration is usually associated with CM in C57BL/6 and CBA/CA mice infected with *P.berghei* ANKA (Belnoue, *et al.*, 2003b).

The *P. yoelii* model has an advantage over the *P.berghei* ANKA model including IRBC sequestration which correlates with CM in humans and the tendency to allow models to survive over long periods of time so that immunological parameters can be measured during the infection. *P.berghei* ANKA (PbA) also has its own advantage including clinical relevance expression to human and the availability of susceptible and resistant strains. The susceptibility and resistance of these strains enable studies to be conducted to

ascertain why only some percentage of human population infected with malaria develops CM. The genetic variation associated with this phenomenon in PbA models may be compared with that of humans to ascertain the differences in CM susceptibility and resistance.

Differences in pathological changes in animal models have been found to be related to different malaria parasites. CBA mice exhibit a brain vascular pathology when infected with PbA but not with *P.yoelii* (Grau, *et al.*, 1987, Fujioka *et al.*, 1994). Pathological changes induced by a given parasite may vary among different mouse strains. For instance PbA-infected CBA develop fatal cerebral malaria (Rest, 1983), while DBA/2 mice develop a non-fatal cerebral syndrome (Neill *et al.*, 1993) but BALB/c mice do not develop any cerebral pathology (Grau, *et al.*, 1987).

Experimental CM cannot exactly mimic the brain pathological complications in human due to genetic variations, but the common features of this pathology which is shared by both human and murine model (Table 3) justify their use in research to understand disease conditions in human.

Table 3: Examples of animal models used for malaria brain immunopathological studies

Malaria parasite	Animal	Characteristics	Reference (s)
<i>P. yoelii</i> 17X	Swiss mice	IRBC sequestration	Kaul <i>et al.</i> , 1994,
<i>P. berghei</i> ANKA	C57BL/6	Leukocyte sequestration	Belnoue, <i>et al.</i> , 2003b
	CBA/Ca	Leukocyte sequestration	Grau <i>et al.</i> , 1986
	DBA/2	Non fatal CM	Neil <i>et al.</i> , 1993
	Hamster		Rest 1983
	BALB/c		Hanum <i>et al.</i> , 2003
<i>P. berghei</i> NK65	CBA/Ca		Waki <i>et al.</i> , 1992
<i>P. chabaudi</i>	C57BL/6		Garnica <i>et al.</i> , 2003
<i>P. knowlesi</i>	Rhesus monkey		Tatke <i>et al.</i> , 1989
<i>P. coatneyi</i>	Rhesus monkey	IRBC sequestration	Smith <i>et al.</i> , 1996
<i>P. fragile</i>	Rhesus monkey	IRBC sequestration	Fujioka <i>et al.</i> , 1994

2.9.2 Human post mortem tissue and peripheral blood samples

Post-mortem tissue and peripheral blood samples provide access to human samples infected with *Plasmodium*. Though cell degradation occurs after death, post-mortem samples taken shortly after death and preserved in the appropriate storage reagents are viable for research purposes and may serve as an adequate system for understanding malaria pathology and pathogenesis at the cellular and molecular level.

For the purpose of malaria research, it is important that patients from whom tissues are obtained be diagnosed before death for *Plasmodium* parasites in peripheral blood using standard methods such as microscopy. Cerebral malaria is diagnosed according to the Glasgow or Blantyre coma score during a malaria episode.

A peripheral blood sample from patients with malaria also provides a means by which research can be performed to understand systemic malaria pathogenesis during *Plasmodium* infection. While serum samples contain both peripheral and cellular material, plasma samples contain only secreted protein products. For instance, plasma samples instead of serum have been found to be ideal for determining secreted RANTES in peripheral blood because of the excessive release of RANTES during platelet and leukocyte lysis in serum.

CHAPTER THREE

MATERIALS AND METHODS

A MATERIALS

3.1 Laboratory animals, reagents and supplies

All animal experiments were conducted according to the principles set up by the *National Institutes of Health Guide for the Care and Use of Laboratory Animals* and approved by the Animal Care and Use Committee of Morehouse School of Medicine, Atlanta, Georgia, USA. Female SW mice (6-8 weeks) obtained from Jackson Laboratory (Bar Harbour, Maine, USA) were maintained on a 12hr light/dark cycle with access to food and water *ad libitum*, and maintained in laminar flow racks under pathogen-free conditions.

3.1.1 *P.yoelii* 17X parasites

Stocks of *P. yoelii* 17X parasitized blood were generously provided by Dr. Hannah Shear, (Division of Hematology, Montefiore Medical Center, Bronx, New York, U.S.A.). *P. yoelii* 17X rodent malaria strain causes a syndrome in female SW mice that resembles human malaria characterized by, fever (ruffled fur) and spleno-hepatomegaly by day 8 post infection (peak parasitemia).

3.1.2 cDNA micro-array

The commercial system used to investigate cDNA micro-array gene expression (Atlas™ 1.0; CLONTECH, Palo Alto, CA, USA) consists of two identical nylon membranes spotted with 588 different mouse genes grouped in functional blocks, including immune

mediators, growth factors, neurotrophins, neurotransmitters and pro- and anti- apoptotic genes. An approximate estimate of the abundance level of a target cDNA in RNA population can be made by comparing its signal to the signals obtained with housekeeping genes of known abundance (eg GAPDH). A complete list of the cDNA samples and controls on each array, as well as their corresponding GenBank accession numbers, may be found at CLONTECH's Atlas web site (www.atlas.clontech.com). [α - 32 P] dATP (Amersham Biosciences, Piscataway, NJ, USA) was used to label mRNA. Expression profiles of different mouse brain mRNA populations (from infected and uninfected mice) at day 8 post-infection were compared and analyzed by autoradiography and quantified by CLONTECH gene analysis software.

3.1.3 TRIZOL^R

TRIZOL^R reagent (GIBCO BRL, Life Technologies, Gaithersburg, MD, USA) was used to isolate total RNA from tissue samples (*P.yoelii* 17X infected, human CM and control samples). TRIZOL^R is a mono-phasic solution of phenol and guanidine isothiocyanate and allows for the maintenance of RNA integrity while disrupting cells and dissolving cell components. It has the added advantage of allowing for simultaneous isolation of DNA, RNA and protein for gene analysis. TRIZOL^R was stored at 4 °C until used.



3.1.4 ELISA

Enzyme-Linked Immunosorbent Assay (ELISA) kits for quantifying amount of peripheral blood chemokine (RANTES) expression were purchased from BioSource International (Camarillo, CA, USA). *Plasmodium falciparum* specific antigens present in malaria-positive subjects were detected using a *P. falciparum* specific ELISA kit purchased from CeLLabs PTY Ltd, Brookvale NSW, Australia. All assay components including primary and secondary antibodies, blocking reagents, and washing buffer were all supplied and used according to manufacturer's instructions.

3.1.5 Antibodies

Commercially available antibodies against RANTES (R&D Systems, Inc. MN), CCR3 (Alexis Biochemicals, CA, USA), CCR5 (ProSci Incorporated, CA, USA), α -tubulin (Sigma-Aldrich, MO, USA) and mouse anti-GFAP (Santa Cruz, CA, USA) were used to determine their protein products.

3.1.6 RT-PCR and PCR

DNase Treatment. Total RNA samples were treated with DNase I (GIBCO BRL, Life Technologies, Gaithersburg, MD, USA) to remove possible genomic DNA contamination.

cDNA Synthesis. Reverse Transcription of RNA to cDNA was performed using reverse transcriptase (RT) kit (Maxim Biotech, Inc., San Francisco, CA, USA).

PCR Kit. Amplification of cDNA by PCR was performed using Taq DNA polymerase, 10X Buffer and dNTPs (Qiagen, Santa Clarita, CA, USA).

Agarose. Molecular biology grade agarose (Fisher Scientific Suwanee, GA, USA)

was used for gel separation of DNA < 1000bp whiles agarose-LE, (Ambion Inc. Austin TX, USA) was used for RNA analysis.

3-N-morpholino propanesulfonic (MOPS) buffer. Agarose-LE for RNA electrophoresis analysis were prepared in 1X MOPS buffer for formaldehyde denaturing gel (Ambion Inc. Austin, TX, USA).

RNase ZAP. RNase ZAP (Ambion Inc. Austin, TX, USA) was used to remove possible RNase contamination from glass and plastic surfaces.

RNAlater . Tissue samples were stored in RNAlater (Ambion™ Inc. TX, USA) to prevent degradation of cell products

Loading Dye. 1X final concentration of Blue/Orange loading dye (0.03% bromophenol blue, 0.03% xylene cyanol FF, 0.4% orange G, 15% Ficoll^R 400, 10mM Tris-HCl (pH 7.5) and 50mM EDTA (pH 8.0) (Promega Madison, WI, USA) was used to monitor migration of DNA products samples on agarose gel.

3.1.8 SDS-PAGE/Western Blot

Lysis Buffer. Tissue samples were homogenized with lysis buffer (0.5% Triton X-100, 0.15M NaCl, 2mM EDTA, 1mM PMSF, Aprotinin, 1X PBS).

Sample Buffer. Protein samples were suspended in sample buffer (1.24M Tris, pH 6.8, 20% (w/v) SDS, 23% (w/v) glycerol, 0.05% Bromophenol blue before loading on gel.

Separating Gel. The composition of the SDS-PAGE separation gel were 30% Acrylamide, 1.5M Tris pH 8.8, 10% SDS, 10% Ammonium Persulphate, and TEMED (Sigma-Aldrich, MO, USA).

Stacking Gel. SDS-PAGE stacking gel was prepared with 30% Acrylamide,

1.0M Tris, pH 6.8, 10% SDS, 10% Ammonium Persulphate and TEMED (Sigma-Aldrich, MO, USA).

Running Buffer. SDS-PAGE running buffer consisted of 25mM Tris, 192mM Glycine, 0.1% (w/v), SDS pH 8.3.

Transfer Buffer. Transfer buffer ingredients were 25mM Tris base, 192mM Glycine, 20% Methanol.

Nitrocellulose Membrane. Protein samples were transferred onto nitrocellulose membrane (BioRAD, Hercules CA, USA).

Blocking Agent (Milk). Nitrocellulose membrane was blocked with 5% (w/v) evaporated milk.

Membrane Washing Buffer. Membrane was washed with buffer made from TBS + 0.1% Tween 20.

Protein Detection Kit. Chemiluminescent detection kit , Luminol (Enhancer) and peroxide buffer (PIERCE Biotech Inc, Rockford, IL, USA) was used to detect protein bands.

X-Ray Film. Bands of protein were developed and detected on high performance chemiluminescence film (Fisher Scientific Suwanee, GA, USA).

B METHODS

3.2 Mouse malaria studies-1

3.2.1 *P.yoelii* 17X murine malaria model

Female Swiss Webster (SW) mice were injected intra-peritoneally with 10^6 (100 μ l) *P. yoelii* 17X parasitized blood kindly provided by Dr. Hannah Shear, Division of Hematology, Montefiore Medical Center, Bronx, New York, USA. Uninfected control mice were injected with 100 μ l of uninfected blood. Parasitemia was determined by counting the number of parasitized red blood cells (RBC's) in a total count of 300 to 500 RBCs on Wright-Giemsa-stained tail-snip-thin blood smears.

Parasitemia was monitored 2, 4, 6, and 8 days post-infection. This rodent malaria strain causes a syndrome in female SW mice that resembles human malaria (Kaul *et al.*, 1994) characterized by fever (ruffled fur) and spleno-hepatomegaly by day 8 post infection.

3.2.2 Preparation of infected mouse brain tissue samples

All mice were sedated with halothane (2-Bromo-2-chloro-1, 1, 1-trifluoroethane, 0.01% Thymol, Halocarbon Labs. River Edge, NJ, USA) prior to dissection. Groups of ten (10) female mice were sacrificed after day 2, 4, 6 and 8 post infections. Uninfected control mice (10) were also sacrificed on each of the time point. For each time point, 5 brains from infected mice were collected and stored in RNAlater (AmbionTM Inc. U.S.A) at -80°C for RNA isolation, 3 brains were cryoprotected in 4% paraformaldehyde at 4°C for immunohistology and the rest (2) were stored at -80°C for protein analysis. Similarly, 5 brains from uninfected mice were stored for RNA isolation, 3 for immunohistology and 2 for protein analysis.

3.3 Transcriptional analysis of *P.yoelii* 17X induced immunomodulator expression

3.3.1 Total RNA isolation from *P.yoelii* 17X infected mouse brain

Each of the mouse brain stored in RNAlater was homogenized and total RNA was isolated using TRIZOL[®] reagent (GIBCO BRL Life Technologies, Rockville, MD, USA). Six hundred microliters (600 μ l) of chloroform (200 μ l of chloroform/1ml of TRIZOL[®]) was added to homogenized brain samples in TRIZOL[®], vortexed for 15 seconds followed by incubation at room temperature for 3 minutes.

The samples were centrifuged at 12,000g/4^oC for 15 minutes and the supernatant (aqueous phase) was pipetted into new microfuge tubes. Five hundred microliters (500 μ l) isopropanol (95%) was added to the supernatant, mixed by vortexing and incubated at room temperature for 10 minutes. Following centrifugation at 12,000g/4^oC for 15minutes, the RNA pellets were washed in 70% ethanol by centrifugation at 7,500g/4^oC for 5 minutes. RNA pellets were dried briefly and dissolved in 50 μ l of nuclease free water.

Concentration of RNA was determined by measuring absorbance at 260nm/280nm. A 260nm/280nm ratio of 1.5-2.0 was considered to be good quality RNA sample. The integrity of RNA sample was determined on 1% formaldehyde-agarose gel using ethidium bromide stain.

3.3.2 DNase treatment of total RNA samples

Total mouse brain RNA samples were treated with RNase-free DNase I (GIBCO BRL, Life Technologies, Rockville, MD U.S.A) to remove possible genomic DNA contamination. A hundred microliter (100 μ l) reaction mix containing mouse brain total RNA (12 μ g), 10 μ l of 10X DNase I buffer, 5 μ l of 1unit/ μ l DNase I (Life Technologies, Rockville, MD U.S.A) and nuclease free water was prepared and incubated at 37 $^{\circ}$ C for 30 minutes.

Ten microliters (10 μ l) of 10X Termination mix (0.1M EDTA, pH 8.0, 1mg/ml glycogen) was added to the reaction mixture to terminate DNase I activity. The reaction mix was divided into two 1.5ml microfuge tubes after which 55 μ l of phenol:chloroform:isoamyl alcohol (25:24:1; pH 4.5, Fisher Scientific, Suwanne, GA, USA) was added to each and subjected to vortex mixing followed by 10 minutes centrifugation at 12,000g/4 $^{\circ}$ C to separate phases. The purpose of this step was to remove DNase I enzyme protein from the reaction mixture, which might inhibit downstream PCR reaction.

The top aqueous layer was pipetted into a new microfuge tube and chloroform (55 μ l) was added to the tube, mixed by vortexing and centrifuged at 12,000g/4 $^{\circ}$ C for 10 minutes. The top aqueous layer obtained after this process contained the RNA and was transferred into a fresh microfuge tube and precipitated in 5 μ l of sodium acetate (2M NaOAc pH 4.5) with 150 μ l of 95% ethanol. The reaction mix was kept on ice for 10 minutes followed by centrifugation at 12,000g/4 $^{\circ}$ C for 15 minutes. RNA pellets were washed with

80% ethanol (50 μ l) at 12,000g/4 $^{\circ}$ C for 5 minutes, air-dried briefly and resuspended in 50 μ l of nuclease free water.

3.3.3 Testing of total RNA samples for possible DNA contamination

After DNase treatment, RNA samples were tested by PCR analysis using the mouse GAPDH PCR primer pair to ensure that there was no DNA contamination after DNase treatment. Hundred nanograms (100ng) of DNase-treated total RNA samples were used as template in a standard PCR reaction mixture consisting of 10 mM KCl, 10 mM (NH₄)₂SO₄, 20 mM Tris-HCl (pH 8.8), 2 mM MgSO₄, 0.1% Triton X-100, 200 μ M each of four deoxynucleotides, (dATP, dCTP, dTTP dGTP) and 1 unit of AmpliTaq Gold DNA polymerase (Perkin-Elmer, Boston, MA, USA), in a reaction volume of 100 μ l. Amplification was performed for 30 cycles in a thermocycler (Perkin Elmer Gene Amp PCR System 2400TM, Fisher Scientific, Pittsburgh, PA, USA), each cycle being for 2 min at 94 $^{\circ}$ C, 1 min at 55 $^{\circ}$ C and then 1 min at 72 $^{\circ}$ C, with a final incubation of 10 min at 72 $^{\circ}$ C. The presence or absence of PCR products was determined on 2%-agarose/ethidium-bromide stained gel.

3.3.4 cDNA array-screening of *P.yoelii* 17X induced immunomodulators

3.3.4.1 Probe synthesis from total RNA

Global alterations in *P.yoelii* 17X induced immunomodulator gene expressions in mouse brain at peak parasitemia were determined by cDNA microarray (CLONTECH, CA, USA). Five micrograms (5 μ g) of *P.yoelii* 17X infected (day 8 post infection) and uninfected DNase-treated, pool mouse brain RNA was reverse transcribed in the presence of 10 μ Ci/ μ l of (α -³²P) dATP, for micro-array analysis.

The following reagents were combined in a 0.5ml microcentrifuge tube at room temperature; 2 μ l of 5X reaction buffer, 1 μ l of 10X dNTP mix, 3.5 μ l of 10 μ Ci/ μ l of (α -³²P) dATP to provide a total volume of 6.5 μ l. The reaction mix was preheated at 70 $^{\circ}$ C.

In a separate 0.5ml microfuge tube, 5 μ g of total RNA and 1 μ l of cDNA synthesis primer mix (CLONTECH, CA) were combined, vortexed briefly and incubated at 70 $^{\circ}$ C for 2 minutes. The reaction was further incubated for 2 minutes at 50 $^{\circ}$ C. During this incubation, 1 μ l of reverse transcriptase (CLONTECH, CA, USA) was added and the reaction was kept at room temperature.

After the 2-minute incubation at 50 $^{\circ}$ C, the radiolabeled 6.5 μ l master mix probe was added to each tube, mixed briefly and incubated for further 25 minutes at 50 $^{\circ}$ C. The reaction process was stopped by adding 1 μ l of termination mix (0.1M EDTA in 1mg/ml glycogen).

3.3.4.2 Column purification of synthesized probes

To purify the labeled cDNA from unincorporated ^{32}P nucleotides and small (<0.1kb) cDNA fragments, probe synthesis reaction was diluted to 200 μl total volume with buffer NT2 (CLONTECH, CA, USA). The reaction mix was transferred into a Nucleospin Extraction Spin Column (CLONTECH, CA, USA) placed into a 2-ml collection tube and centrifuged at 14,000 rpm for 1 minute. The collection tube was discarded into appropriate radioactive waste container. Four hundred microliters (400 μl) of buffer NT3 (CLONTECH, CA, USA) was added onto the NucleoSpin column, which have been inserted into a fresh 2-ml collection tube, and centrifuged at 14,000 rpm for 1min. The collection tube and its contents were again discarded into the radioactive container. This step was repeated twice. The NucleoSpin column was finally transferred into a clean 1.5-ml microfuge tubes and soaked with 100 μl of buffer NE (CLONTECH, CA, USA) for 2 minutes. The purified cDNA probes were finally eluted from the column by centrifugation at 14,000 rpm for 1 minute.

3.3.4.3 Hybridizing cDNA probes to the Atlas array

ExpressHyb (CLONTECH, CA, USA) was prewarmed at 70 $^{\circ}\text{C}$ while 0.5mg of sheared salmon testes DNA was denatured by heating at 100 $^{\circ}\text{C}$ for 5 minutes and quickly chilled on ice. Heat-denatured sheared salmon testes DNA was mixed with prewarmed ExpressHyb (CLONTECH, CA, USA) and kept at 70 $^{\circ}\text{C}$ until used.

The Atlas array membrane was pre-wet in a hybridization bottle so that it adhered to the inside walls of the bottle without creating air pockets. Five milliliters (5ml) of the

denatured sheared salmon DNA and the ExpressHyb solution was added to the bottle, such that the solution is evenly distributed over the membrane. This step was prepared quickly to prevent the array from drying. The membrane was prehybridized with continuous agitation at 15rpm at 70°C for 30 minutes in a hybridization incubator.

Hundred microliters (100µl) of the labeled probe was added to 11µl of 10X denaturing solution (1M NaOH, 10mM EDTA) and incubated at 70°C for 10 minutes. The labeled probe reaction mix was added directly to the array membrane and the prehybridization solution, and hybridized overnight at 70°C (16hrs).

3.3.4.4 Washing of hybridized array membrane

After the overnight hybridization, the hybridization solution was carefully removed from the bottle and discarded into the radioactive waste container and replaced with 200ml of prewarmed (70°C) wash solution 1 (8.765g NaCl, 4.41g Na₃Citrate.2H₂O, pH 7.0, 10g of SDS) with continuous agitation at 15 rpm for 30 minutes. This step was repeated three more times after which the membrane was again washed with 200µl of wash solution 2 (0.44g NaCl, 0.22g Na₃Citrate.2H₂O, pH 7.0, 0.5g of SDS) at 70°C.

The Atlas array membrane was carefully removed from the bottle with forceps. Excess wash solution was removed from the membrane by shaking. The damp membrane was immediately marked with a notch at one corner for easy identification and covered with a plastic wrap. The membrane was exposed to Kodak BioMax Ms x-ray film at 80°C with



an intensifying screen, overnight. The film was developed by Kodak X-Omat 2000A X-ray autoradiographer.

3.3.4.5 Gene analysis

The positions of hybridization signals on the x-ray film were identified and analyzed using Atlas™ Image 1.0 software (CLONTECH, CA, USA). This software provides orientation grid such that scanning the signals on the x-ray film and precisely aligning it to the grid diagram, it provides the enclosed array gene list on the membrane. The differential gene expression in *P.yoelii* 17X infected and control mouse brain were then analyzed and normalized to those of glyceraldehydes-3-phosphate dehydrogenase (GAPDH), which was used as the housekeeping gene. The resulting data were expressed as the ratio of the relative change in mRNA levels in the infected brain samples and uninfected controls.

Due to sequence-dependent hybridization characteristics and variation inherent in any hybridization reaction, it is important that cDNA array results are corroborated with RT-PCR analysis. RT-PCR analysis was therefore conducted to confirm expression of selected genes of interest.

3.3.5 Reverse transcription of purified mouse brain RNA to cDNA for PCR analysis

To synthesize the first -strand cDNA for PCR amplification, 10µg of DNase-treated mouse brain RNA and 4µl (50µM) of random hexamer (50µM; Maxim Biotech, Inc., San Francisco, CA, USA) (used as a primer) were combined in a total volume of 14.5µl with nuclease free water and incubated at 70°C for 5 minutes. The reaction mix was quickly chilled on ice and 0.5µl of RNase inhibitor (130 Units/µl) (Maxim Biotech, Inc., San Francisco, CA, USA), 10µl of 5X RT buffer, 20µl of 10mM mixed dinucleoside triphosphate and 1µl of reverse transcriptase (250 Units/µl) (Moloney Murine Leukemia Virus Reverse Transcriptase - Maxim Biotech, Inc., San Francisco, CA, USA) were added and incubated at 37°C for 60 minutes. The reaction was terminated by incubation at 95°C for 20 minutes and quickly chilled on ice. Fifty microliters (50µl) of nuclease free water was added to dilute the RT mixture to a volume of 100µl. A volume of 2µl cDNA was used in each PCR reaction.



3.3.5.1 Amplification by PCR and semi-quantitative analysis of *P.yoelii* 17X induced immunomodulators

Gene sequences with accession numbers for adhesion molecules; PECAM-1 (NM_008816) ICAM-1 (BE_630415), and VCAM-1 (NM_011693); cytokines, INF-γ (K_00083), TNF-α (NM_013693), IL-12 (M_86671), and iNOS (NM_008712); chemokines, MIP-2 (NM_009140), MCP-1 (NM_011333) and RANTES (AF_252285); chemokine receptors CCR1 (NM_009912), CCR3 (NM_009914) and CCR5 (D_83648) and glyceraldehyde-3-phosphate dehydrogenase (GAPDH, XM_357288) were obtained

from the National Center for Biotechnology Information (NCBI) database. Sense and antisense primers, optimized for PCR amplification which generated amplicons of 100, 106, 102, 98, 100, 102, 101, 94, 100, 97, 103, 96, 100 and 120 base pairs in size for PECAM-1, ICAM-1, VCAM-1, INF- γ , TNF- α , IL-12, INOS, MIP-2, MCP-1, RANTES, CCR1, CCR3, CCR5 and GAPDH respectively were then designed (Appendix) using Primer 3 software program from Whitehead Institute at the Massachusetts Institute of Technology (MIT, Boston, MA, USA). Thermodynamic analysis of the primers was conducted using computer programs: Primer Premier™ (Integrated DNA Technologies, Coralville, IA, USA), and MIT Primer III (Boston, MA, USA). The resulting primer sets were compared against the entire mouse genome using the national center for biotechnology and information (NCBI) to confirm specificity and insure that the primers flanked mRNA splicing regions.

PCR was conducted on *P. yoelii* 17X infected mouse brain RNA samples using these primers. Complementary DNA sequences were amplified in a 50 μ l reaction mixture prepared by adding the following components; 35 μ l of nuclease free water, 5 μ l of 10x PCR buffer, 20ng each of specific primer pair/ μ l, 2 μ l of dinucleoside triphosphate (10mM), 0.5ul (5 Units/ μ l) of *Taq* polymerase and 2 μ l of diluted RT product (cDNA; used as template). Conditions for DNA amplifications were set as follows: heating at 94°C for 5 minutes, followed by 25 cycles of DNA denaturation at 94°C for 1 minute, an annealing step at X°C (see appendix vii (table 3)) for respective temperature values) for 1 minute, strand extension at 72°C for 1 minute and a final extension step at 72°C for 10 minutes in a thermocycler. Primers specific for GAPDH (housekeeping gene) was used

as internal control. Negative controls, from which template mRNA was omitted, were included in each amplification experiment.

The number of cycles required to attain products in the linear range of the PCR was determined before the final assays were run. Working within this range, it was possible to determine expression differences after 25-30 cycles.

PCR products were analyzed on 2%-agarose/ethidium-bromide gels and quantified using Gelexpert software (NucleoTech, San Mateo, CA, USA). Band intensities in each experiment were normalized to the mean intensity of GAPDH. Data were expressed as the relative change in mRNA level in infected and uninfected controls.

3.4 Tissue and plasma protein analysis of *P.yoelii* 17X induced RANTES expression

3.4.1 SDS/Western Blot analysis of *P.yoelii* 17X induced RANTES protein expression in mouse brain

3.4.1.1 Protein isolation and assay from mouse brain

Protein was isolated from *P.yoelii* 17X infected and uninfected mice brains using lysis buffer (0.5% Triton X-100, 0.15M NaCl, 2mM ethylenediamine tetra-acetic acid (EDTA), 1mM phenyl methyl sulfonyl fluoride (PMSF), 22µg aprotinin/µl, 1X phosphate buffered saline (PBS)). Brain tissue samples were homogenized in 5ml of lysis buffer, and centrifuged at 13000 rpm for 20 minutes. Supernatant containing the protein was pipetted and stored at -80 °C until used. Protein concentration was determined by Lowry method (BioRad, Hercules, CA, USA) using Bovine Serum Albumen (BSA) as standard.

Stock concentration of 1.4mg/ml of BSA standard was diluted with lysis buffer to prepare serial concentration as; 0.2, 0.4, 0.6, 0.8, 1.0, 1.2, 1.4mg/ml. Duplicates of ten microliters (10 μ l) of standards and protein samples were pipetted into a 96 well plate. Twenty five microliters (25 μ l) of *reagent A* (BioRad, Hercules, CA, USA) was added to each well followed by 200 μ l of *reagent B* (BioRad, Hercules, CA, USA). Optical density of samples was read at 750nm using Micro-Titer plate reader (Molecular Devices SpectraMax 250™ Sunnyvale, CA, USA). Concentration of samples was extrapolated from BSA standard curve.

3.4.1.2 Preparing SDS-PAGE gel

Glass plates and spacers were assembled in sodium dodecyl sulphate polyacrylamide gel electrophoresis (SDS-PAGE) mini-vertical gel unit (HOEFER Scientific Instruments San Francisco, CA, USA) before gel was cast. Separating gel (15%) was prepared as follows; 8ml of 30% acrylamide, and 5ml of 1.5M Tris, pH 8.8, (BioRad, Hercules, CA, USA) were added to 6.6ml distilled water and stirred in a baker briefly, after which 200 μ l of 10% ammonium persulphate was added followed by addition of 40 μ l of N,N,N',N'-Tetramethylethylenediamine:N,N,N',N'-Di-(dimethylamino) ethane (TEMED) (Sigma-Aldrich, MO, USA) with brief mixing. Gel was poured immediately and overlaid with 70% ethanol to create smooth surface, followed by incubation at room temperature for 1 hour.

After 1hr incubation, the ethanol was poured off and the separating gel was rinsed twice with distilled water and overlaid with 5% stacking gel prepared from the following recipes: 1.8ml, 30% acrylamide, 1.3ml, 1.0M Tris, pH 6.8 and 100 μ l of 10% SDS with

6.8ml distilled water and degassed for 3 minutes. Hundred microliters (100 μ l) of 10% ammonium persulphate was added, with 40 μ l of TEMED (Sigma-Aldrich, MO, USA) mixed briefly and poured immediately on top of the separating gel before casting comb.

Gel was incubated for 1 hour at room temperature. Equal amounts of protein (25 μ g) samples were precipitated in cold acetone and resuspended in loading buffer (1.24M Tris, pH 6.8, 20% (w/v) SDS, 23% (w/v) glycerol and 0.05% bromophenol blue) before running on SDS-PAGE. Twice the volume of cold acetone (100%) was added to samples, vortexed briefly and incubated on ice for 10 minutes to precipitate protein. Samples were then centrifuged at 14000 rpm for 10 minutes and the supernatant was poured off. The pellet was resuspended in 15 μ l of 1X loading buffer before loading. SDS-PAGE was run for 3 hours at 100v and 110mA.

3.4.1.3 Transfer of protein onto membrane

Gel was removed from electrophoretic unit, and kept in transfer buffer (25mM Tris, pH 8.3, 192 mM glycine, 20% methanol) until used. Nitrocellulose membrane (BioRad, Hercules, CA, USA) was cut according to the dimension of the gel and soaked in transfer buffer. Filter papers cut to the size of membrane/gel and sponges were soaked in transfer buffer in different container before the transfer unit (IDEA Scientific Company, Minneapolis, MN, USA) was assembled. The transfer sandwich unit containing some amount of transfer buffer was assembled in the following order starting from the cathode; white plastic grid, sponge, filter paper, gel nitrocellulose membrane (without moving membrane or gel, an object with smooth surface, (4ml pipette) was rolled over set up to remove any trapped bubbles), filter paper, sponge and white plastic grid.



The transblot sandwich was slowly slide into the transfer tank after more transfer buffer had been added to the unit. Running condition for transfer was set at maximum voltage and 350mA for 9 hours. After transfer, nitrocellulose membrane was removed from transblot sandwich; rinsed briefly with deionized water before western blot was performed.

3.4.1.4 Western Blot analysis

Nitrocellulose membranes were incubated on orbital shaker (400rpm) in 5% (w/v) evaporated milk for 1 hour to block non-specific spots on membrane. Membranes were then washed with tris-buffered saline (TBS)-0.1 % Tween 20 (washing buffer), 3 times (changing buffer at 10 minutes interval). After the third wash, membranes were screened with primary antibodies according to manufacturer's recommendation: 1:1000 biotinylated anti-mouse recombinant RANTES (R&D Systems, Inc. MN, USA) and 1:2000 anti-mouse α -tubulin (Sigma-Aldrich, MO, USA). Membranes were incubated with horizontal shaking (Bellco Biotech, Vineland, NJ, USA) set at 300rpm at 4 °C overnight.

Membranes were washed twice on a shaker (Bellco Biotech, Vineland, NJ, USA) set at 400rpm with wash buffer (5 minutes each) and incubated with the appropriate secondary antibodies. Membrane probed with biotinylated anti-mouse recombinant RANTES (R&D Systems, Inc. MN, USA) was incubated with 1:4000 streptavidin-horse-radish peroxidase (HRP) secondary antibody for 1 hour at room temperature while membrane probed with

α -tubulin was incubated with 1:5000 anti-mouse IgG secondary antibody at the same conditions.

After secondary antibody incubation, membranes were washed again for 30 minutes, changing wash buffer at every 10 minutes interval. Membranes were then developed with a chemiluminescent (PIERCE Biotech Inc. IL, USA) detection kit. Five hundred microliters (500 μ l) each of luminol (enhancer solution A, PIERCE Biotech Inc. IL, USA) and peroxidase buffer (solution B, PIERCE Biotech Inc. IL, USA) were mixed on transparent spread wraps. Membranes were removed from wash buffer. Excess buffer was blotted out with filter paper and incubated at room temperature on detection reagents on wraps for 5 minutes, with protein surface on membrane facing down. Membranes were wrapped in transparent wraps after detection reagents have been blotted out and put in autoradiography cassette (Fisher Scientific Suwanee, GA, USA).

Bands of protein were developed and detected on high performance chemiluminescence film (Fisher Scientific Suwanee, GA, USA) using Kodak X-Omat 2000A (Eastman Kodak Company, Rochester NY, USA) autoradiographer. Bands of protein corresponding to RANTES (7.8 kDa) and α -tubulin (55.0kDa) were quantified for *P.yoelii* 17X infected and uninfected control cases using Versa Doc Imaging System (BioRad, CA, USA). RANTES protein expression was normalized to that of α -tubulin.

3.4.2 Peripheral blood analysis of *P.yoelii* 17X induced RANTES expression

To determine if expression of RANTES is localized or systemic, peripheral blood plasma RANTES expression from *P.yoelii* 17X infected (day 2, 4, 6, and 8 post infection) and control mice was determined using RANTES specific ELISA kit (Biosource International Camarillo, CA, USA). Since RANTES can be released by platelets during serum collection, the use of serum samples to determine peripheral RANTES expression was avoided. Instead, blood was collected in 50 μ l of heparin (1 Units/ μ l) (Elkins-Sinn, Inc, Cherry Hill, NJ, USA), centrifuged at 13,000rpm for 10 minutes to obtain plasma samples, which were stored at - 80 $^{\circ}$ C until used. Duplicates of standards (39.0, 78.1, 156, 312, 625, 1250, 2500 pg/ml concentration range), controls, and samples (1:20 diluted) were aliquoted (100 μ l) into RANTES coated microtiter wells and incubated for 2 hours at 37 $^{\circ}$ C. The solution was aspirated after incubation and wells were washed with 400 μ l (4 times) wash buffer (Biosource International Camarillo, CA, USA). Biotinylated anti-RANTES conjugated antibody (100 μ l) (Biosource International Camarillo, CA, USA) was added to the wells and incubated at 37 $^{\circ}$ C for 1 hour. Wells were washed again. Hundred microliters (100 μ l) of Streptavidin-Horse Radish Peroxidase (Streptavidin-HRP) was then added to each well, incubated at room temperature for 30 minutes and washed again as before. Hundred microliters (100 μ l) of stabilized chromogen (Tetramethylbenzidine) was added to each well and kept in the dark at room temperature for 30 minutes. The reaction was stopped by adding 100 μ l of stop solution (0.3M H₂SO₄).

Concentrations of test samples were determined at 450nm in a micro-titer plate reader (Molecular Devices SpectraMax 250™ Sunnyvale, CA, USA). The minimum detectable dose of mouse RANTES using this kit have been found to be <20 pg/ml.

3.5 Ultrastructural and immunohistological analysis of *P.yoelii* 17X infected brain samples

3.5.1 Ultrastructural analysis of *P.yoelii* 17X infected brain samples

To evaluate effects of *P.yoelii* 17X infection on mouse brain microvessels at peak parasitemia, whole infected and uninfected brains were dissected, cut into smaller cubes (2 mm³), washed twice with phosphate buffered saline (PBS), and fixed for 60 minutes in 100 mM potassium phosphate buffer pH 7.2, containing 0.1 % glutaraldehyde and 2% formaldehyde, freshly prepared from paraformaldehyde. After fixation, the brains were dehydrated in methanol (95%) and embedded in Lowicryl K4M at -20 °C. Thin sections were collected on 300-mesh nickel grids and examined by transmission electron microscopy at 60 eV.

3.5.2 Immunohistological analysis of GFAP expression in *P.yoelii* 17X infected brain

P.yoelii 17X infected and uninfected mice brains harvested at peak parasitemia were perfused in 4% paraformaldehyde in 0.02M KPBS (Potassium Phosphate Buffered Saline) until completely saturated, and then transferred into 10% sucrose for 4 hours at room temperature.

Parasagittal sections of 20 μ m thickness brain tissues obtained using a cryostat were serially placed into 0.02M KPBS solution in a 12-well microplate for free floating processing.

Tissues were incubated for 10 minutes in a 0.2% sodium borohydride (prepared with 0.02M KPBS) on a rocker set at 400rpm to minimize auto-fluorescence. Tissues were washed 3 times (10 minutes each) in 0.02M KPBS. Tissue samples were blocked for 1 hour in 0.02M KPBS solution containing 0.1% triton X-100 and 10% normal goat serum.

Samples were incubated with 1:200 rabbit anti-GFAP (glial fibrillary acidic protein) primary antibody for 2 hours at room temperature on a rocker. Tissues were washed 3 times (10 minutes each) after primary antibody incubation and then incubated again at room temperature on a rocker for an hour, in 1:1000 dilution of goat-anti-rabbit secondary antibody prepared in 0.02M KPBS. Tissues were washed 3X (10 minutes each) in 0.02M KPBS after secondary antibody incubation, and mounted on slides in anti-fade medium and visualized and photographed, on an Olympus BH70 microscope with an attached laser confocal-imaging system.

3.6 Human malaria studies

3.6.1 Human cerebral malaria (CM) and non-malaria (NM) brain samples

Autopsy samples were obtained with informed parental consent of children below the age of 9 who died from CM (n=12 cases) and NM (n=6 cases) while on admission at the Children's Ward of Korle-Bu Teaching Hospital, University of Ghana Medical School,

Accra, Ghana. Inclusion criteria for sample collection were WHO Blantyre coma score of 3 or less and the presence of malaria parasites. The presence of *P.falciparum* parasites in the peripheral blood was detected by routine parasitological examination in all patients' while on admission. Exclusion criteria were determined as absence of unconsciousness due to hypoglycemia, absence of encephalopathy, no history of neurological illness and absence of malaria parasites.

To determine which region of the brain expresses high levels of RANTES and receptors CCR1, CCR3 and CCR5, brain sections taken from four regions of the brain, (namely, cerebellum, cerebrum, brain stem and hippocampus) of confirmed human CM and NM post-mortem brain tissue samples were used in this study. CM was defined according to established World Health Organization guidelines (WHO, 2000); a Blantyre Coma score of 5 or less during the episode of severe malaria, excluding other causes of unconsciousness such as hypoglycemia, meningitis or other encephalopathy.

Non-malaria controls were cases in which no history of neurological illness was recorded. Brain tissue samples were stored in RNAlater (Ambion™ Inc. TX, USA) to preserve RNA during transportation and subsequently processed for total RNA and protein isolation. Consent of parents/guardians/relatives of deceased subjects and approval by the Institutional Review Boards (IRB) of the University of Ghana Medical School, Accra, Ghana and Morehouse School of Medicine, Atlanta, USA, were obtained prior to commencement of this study.

3.6.2 Transcriptional analysis of RANTES, CCR1, CCR3 and CCR5 in cerebrum, cerebellum, brain stem and hippocampus of CM and NM samples

3.6.2.1 RNA isolation and DNase treatment, from CM and NM samples

Total RNA was isolated from four regions of the brain (namely, cerebellum, cerebrum, brain stem and hippocampus) of confirmed human CM and NM post-mortem brain tissue samples using TRIZOL Reagent (GIBCO BRL, Life Technologies Inc., Rockville, MD, USA) and procedure as provided in 3.3.1. Potential genomic DNA contamination was removed from these samples by treatment with RNase-free DNase (Invotrogen, San Diego, CA, USA) for 30 minutes at 37 °C. RNA was then precipitated and resuspended in nuclease free water and tested for traces of DNA contamination.

3.6.2.2 Reverse transcription of purified human brain RNA to cDNA for PCR analysis

Synthesis of purified human brain RNA to cDNA for PCR analysis was performed as described in 3.3.5.

3.6.2.3 PCR amplification and semi-quantitative analysis of CM induced RANTES, CCR1, CCR3, and CCR5

Human mRNA sequence of RANTES, CCR1, CCR3, CCR5 and glyceraldehyde-3-phosphate dehydrogenase (GAPDH) obtained from the National Institute of Health-National Center for Biotechnology Information (NIH-NCBI) gene bank database accession numbers NM_002985, NM_001295, NM_001837, NM_000579 and M_33197,

respectively were used to design primers for PCR analysis. PCR amplification generated amplicons of 154, 130, 193, 101, and 226 base pairs in size for RANTES, CCR1, CCR3, CCR5 and GAPDH mRNA respectively.

Primers were designed using the Primer 3 software program from Whitehead Institute at the Massachusetts Institute of Technology (MIT, Boston, MA, USA) as before and compared against the entire human genome using NCBI to confirm specificity and insure that the primers flanked mRNA splicing regions. Complementary DNA (cDNA) was generated, as before, and amplified with specific cDNA primers using *Taq* polymerase and polymerase chain reaction (PCR) reagents (Qiagen Inc. Valencia, CA, USA).

Conditions for DNA amplifications were set as follows: heating at 94°C for 4 minutes, followed by 25 cycles of DNA denaturation at 94°C for 1 minute, an annealing step at X°C (appendix) for 1 minute, strand extension at 72°C for 1 minute and a final extension step at 72°C for 10 minutes in a thermocycler (Perkin-Elmer, Norwalk, CT, USA). Primers specific for GAPDH (housekeeping gene) was used as internal control. The required number of cycles needed to attain products in the linear range was determined as before. Negative controls were included in each amplification experiment. PCR products were analyzed on 2%-agarose/ethidium-bromide gels and quantified using Gelexpert software (NucleoTech, San Mateo, CA, USA). Band intensities in each experiment were normalized to the mean intensity of GAPDH.

3.6.3 Tissue and plasma protein analysis of malaria induced RANTES, CCR1, CCR3 and CCR5 expression

3.6.3.1 Protein isolation and analysis from CM and NM samples

To localize portion of brain where RANTES, CCR3 and CCR5 expression occur, protein was isolated from cerebrum, cerebellum, brain stem and hippocampus of CM (n=12) and NM (n=6) post-mortem brain tissue samples using lysis buffer and procedure as described in 3.4.1.1.

3.6.3.2 Preparing SDS-PAGE gel for protein analysis

Fifteen percent (15%) of SDS-PAGE gel was prepared with the same running conditions as described in 3.4.1.2

3.6.3.3 Transfer of protein onto membrane

The same procedure described in 3.4.1.3 was used to transfer CM and NM tissue proteins onto membranes. Running condition for transfer was set at maximum voltage and 350mA for 9 and 22 hours for RANTES (7.8kDa), and CCR3 (41kDa), CCR5 (40kDa) and α -tubulin respectively.

3.6.3.4 Western Blot analysis

Membranes were washed as before and screened with primary antibodies according to manufacturer's recommendation: 1:1000 biotinylated anti-human recombinant RANTES (R&D Systems, Inc. MN, USA), 1:1000 polyclonal anti-human CCR3 (Alexis Biochemicals, CA, USA), 1:2000 polyclonal anti-human CCR5 (ProSci Incorporated,



Poway CA, USA) and 1:2000 anti-human α -tubulin (Sigma-Aldrich, MO, USA). Membrane probed with biotinylated anti-human recombinant RANTES (R&D Systems, Inc. MN, USA) was incubated with 1:4000 streptavidin-horse-radish peroxidase (HRP) secondary antibody for 1 hour at room temperature while membranes probed with anti-human CCR3, CCR5 and α -tubulin were incubated with 1:5000 anti-human IgG secondary antibodies at the same conditions.

Bands of protein were developed and detected on high performance chemiluminescence film (Fisher Scientific Suwanee, GA, USA) using the Kodak X-Omat 2000A (Eastman Kodak Company, Rochester NY, USA) autoradiographer as before. Bands of protein corresponding to RANTES (7.8 kDa), CCR5 (40.0kDa) and α -tubulin (55.0kDa) were quantified for all CM and NM cases using the Versa Doc Imaging System (BioRad, CA, USA). RANTES and CCR5 protein expressions were normalized to that of α -tubulin.

3.7 Determination of *P.falciparum* antigen and malaria induced plasma RANTES expression by ELISA

3.7.1 Determination of *P.falciparum* antigen

Plasmodium falciparum specific antigens present in plasma, collected from 64 malaria positive male and female adult volunteers with informed consent in Ejura, a peri-urban community in the Ashanti region of Ghana, were detected using a *P. falciparum* specific antigen ELISA kit (CeLLabs PTY Ltd, Brookvale NSW, Australia) which is specific for the histidine rich protein secreted by *P.falciparum* at the merozoite stage of the infection. Blood plasma of malaria antigens in the 64 adult Ghanaian subjects (NCM) and 19 non-

exposed malaria naïve male and female African- American adult volunteers in Atlanta, a city in the Georgia State of USA, as controls were determined. Two hundred microliter (200µl) duplicates of negative and positive controls as well as sample diluent were dispensed into microplates coated with purified recombinant proteins specific for the histidine rich protein. Ten microliters (10µl) of sample was added in each sample well and incubated for 45 minutes at 37 °C. Microplate was washed five times by delivering and aspirating 300µl wash buffer (CeLLabs PTY Ltd, Brookvale NSW, Australia) per well. Hundred microliters (100µl) of diluted enzyme conjugate was pipetted into each well of microplate, sealed and incubated for 45 minutes at 37 °C. Microwells were washed again as before after which 100µl of chromogen (tetramethylbenzidine /substrate .hydrogen peroxide) (CeLLabs PTY Ltd, Brookvale NSW, Australia) mixture was added and incubated at room temperature for 15 minutes. Hundred microliters (100µl) of stop solution (0.3M H₂SO₄) was added to each well before optical density was read at 450nm. The sensitivity as well as specificity of the test has been shown to be > 98% with a reported false positive rates of <2%.

3.7.2 *P.falciparum* induced plasma RANTES expression

Plasma samples obtained from malaria positive subjects was used to determine peripheral RANTES expression during parasite infection. Blood was collected in EDTA, centrifuged at 13,000 rpm for 10 minutes to obtain plasma samples, which were stored at -20° C until used. Peripheral blood plasma RANTES levels in the 64 adult Ghanaian malaria positive subjects (NCM) in Ejura and the 19 non-exposed malaria naïve African- American adult volunteers in Atlanta as controls, was determined using a RANTES

specific ELISA (Biosource Int. CA, USA). Hundred microliter (100 μ l) duplicates of standards (50 pg/ml to 5000 pg/ml concentration range), controls and test samples (1:51 diluted) were added to anti-RANTES antibody coated wells. Fifty microliters (50 μ l) of anti-RANTES horse-radish peroxidase conjugate was added to each well and incubated for 2 hours at room temperature on a horizontal shaker (Bellco Biotech Vineland NJ, USA) set at 700 rpm. Wells were subsequently washed with 400 μ l of wash buffer (Biosource Int. CA, USA). Two hundred microliters (200 μ l) of freshly prepared chromogenic solution (Tetramethylbenzidine) containing hydrogen peroxide was added to each well and incubated for 30 minutes at room temperature on a horizontal shaker at 700 rpm. Fifty microliters (50 μ l) of stop solution (0.3M H₂SO₄) was added to each well to terminate the reaction. Samples optical densities were read at 450 nm with Micro-Titer plate reader (Molecular Devices SpectraMax 250TM Sunnyvale, CA, USA).

Concentrations of test samples were read from a standard curve and multiplied by 51 to correct for the 1:51 dilution. The minimum detectable concentration for this kit is estimated to be 2pg/ml. The strength of association between RANTES expression and *P. falciparum* antigens in malaria subjects were assessed using correlation analysis.

3.8 Statistical analysis

A two-tailed student's t-test software (Intercooled Stata 8.0, STATA Corporation, TX, USA) was used for statistical analysis. Average of densitometric measurements from agarose gel electrophoretic and Western Blot analyses for CM and NM samples were log-transformed to normalize the distribution for CM (n=12) and NM (n=6) and also to

correct for small sample size for parametric statistical analysis. Data were expressed as the mean \pm SEM. Data from CM (n=12) and NM (n=6) group were then compared using the two-tailed student's t-test software, for which $P < 0.05$ was considered to be significant. The results obtained in this work were from duplicate determinations and represent independent experiments performed by identical methods.

3.9 Mouse malaria studies-2

3.9.1 Role of RANTES in severity and mortality of murine malaria

The hypothesis for this study was that blocking RANTES expression will minimize or abrogate the severity of malaria infection. Therefore, to determine the functional role of RANTES during *P. yoelii* 17X infection, a group (I) of twenty two (22) female SW mice were injected with anti-RANTES polyclonal antibody (pAb) (200 μ l/mouse), while another group (II) of 22 mice received mock polyclonal antibody (200 μ l/mouse) kindly provided by Dr. James Lillard, Morehouse School of Medicine, Atlanta, GA, USA. At day 0, post inoculation, plasma samples were collected from 5 mice from each group and stored at -70 °C until used. The remaining seventeen (17) mice in each group were challenged intra-peritoneally with *P.yoelii* 17X (10^6 infected RBC) parasite while another group of seventeen (17) mice serving as controls received uninfected blood. Infected mice were given a boost of 200 μ l/mouse of antibodies at day 2, 4, and 6.

The description of the experimental design is shown below;

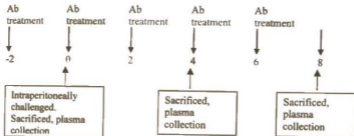
Mouse strain : SW female-6 weeks old

Parasite strain : *Plasmodium yoelii* 17X

Group I : Positive control (Infection + anti-RANTES pAbs)

Group II : Experimental (Infection + anti-mock pAbs)

Group III : Negative control



Parasitemia was monitored by making smears of blood obtained from the tail vein and counting 50 Giemsa-stained fields or at least 300 RBCs under oil immersion (1,200X). In addition, symptoms of *P.yoelii* 17X infection and mortality were determined to ascertain the severity of disease. Plasma was collected from both infected and uninfected mice at day 4 and 8 post infection. ELISA was performed on samples to determine RANTES expression using specific antibodies as described in 3.4.2.

CHAPTER FOUR

RESULTS

4.1 Mouse malaria studies-1

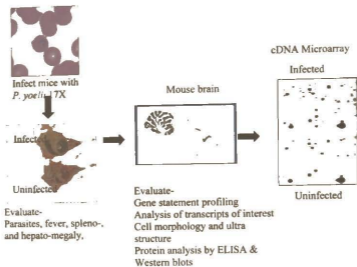


Figure 8: Murine malaria model: Mice were infected with *P.yoelii* 17X parasites and parasitemia monitored by evaluating the presence of parasites, fever, spleno-, and hepato-megaly at day 2, 4, 6 and 8 post-infection. Brains were evaluated for *P.yoelii* 17X induced gene statement profiling and transcripts of interest using cDNA microarray and RT-PCR. Ultrastructural changes in brain sections were analyzed by transmission electron microscopy. Western Blot and ELISA analyses were used to determine *P.yoelii* 17X induced protein expression of RANTES.

4.1.1 *P.yoelii* 17X murine malaria model

All mice infected with *P. yoelii* 17X developed malaria-related-symptoms, which included appearance of ruffled hair, shivering and ataxia by day 8 post infection. Percentage parasitemia in mice were approximately 12% and 32% for 300-500 RBCs count at day 6 and 8 post infection respectively. Examination of the viscera of dissected mice confirmed spleno- and hepato-megaly at peak parasitemia (Figure 9) concordant with reported *P. yoelii* 17X malaria infections (Kaul *et al.*, 1994). None of the control mice showed any of these signs.



Figure 9 *P.yoelii* 17X infection induces spleno-hepatomegaly in SW mice. Female Swiss Webster (SW) mice were injected intra-peritoneally with 10^6 ($100\mu\text{l}$) of *P. yoelii* 17X parasitized blood while uninfected control mice received $100\mu\text{l}$ of uninfected blood. *P. yoelii* 17X causes syndromes in SW mice characterized with spleno-hepatomegaly at day 8 post infection (peak parasitemia).

4.2 Transcriptional analysis of *P.yoelii* 17X induced immunomodulator mRNA expression

4.2.1 cDNA array gene statement and analyses of *P.yoelii* 17X induced immunomodulators

P. yoelii 17X-attributable alterations in approximately 7.5% (42/588) of genes encoding immuno-modulators, growth factors, stress factors, transcription factors, and neurotransmitters were observed on the micro-array analysis of brain samples. Expression of the altered genes at peak parasitemia in the infected mice varied when compared with that in the uninfected mice, showing anything from 2.0-fold down-regulation to 23.0-fold up-regulation (Table 4 and appendix viii). Marked alterations in expression of immunomodulator mRNA including adhesion molecules; PECAM-1, ICAM-1, and VCAM-1, cytokines; INF- γ , TNF- α , IL-12, and iNOS, C-C chemokine; MIP-2 α , MCP-1, and RANTES, C-C chemokine receptor; CCR1, CCR3, and CCR5, growth factors; growth differentiation factor 2 (GDF-2), and tumor growth factor beta (TGF)- β precursor, were observed to be 2.0 to 23.0-fold upregulated (Table 4, $P < 0.05$) at peak parasitemia whereas GAPDH levels remained unchanged. Semi-quantitative RT-PCR was performed to specifically examine the expression dynamics of selected immunomodulator gene expression during *P. yoelii* 17X malaria infection to validate the microarray data.

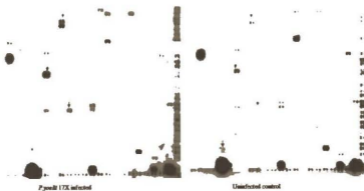


Figure 10: Autoradiograph of cDNA microarray analysis of mRNA expression in mouse brain (day 8 post-infection). Five hundred and eighty eight (588) reported genes were analyzed. ³²P-labelled cDNA were prepared from 5µg each of total RNA from infected and uninfected mouse brain. The probes were hybridized by autoradiography. Differentially expressed genes were reproducibly detected. Arrows indicate some differences in pattern of expression between infected and uninfected membrane.

Table 4: *Plasmodium yoelii* 17X infection alters immunomodulator gene expression in mouse brain at peak parasitemia (day 8 post-infection)

GENE NAME	FOLD CHANGE EXPRESSION	DESCRIPTION OF GENE
PECAM-1	23.0	Platelet Endothelia Cell Adhesion Molecule-1
MIP-2 α	18.0	Macrophage Inflammatory Protein-2 alpha
ICAM-1	13.0	Intercellular Adhesion Molecule-1
MCP-1	7.0	Monocyte Chemoattractant Protein-1
VCAM-1	6.0	Vascular Cell Adhesion Molecule-1
RANTES	6.0	Regulated upon Activation Normal T cell Expressed and Secreted
INF- γ	6.0	Interferon-gamma
TNF- α	5.0	Tumor Necrosis Factor-alpha
IL-12	4.0	Interleukin-12
CCR1	4.0	C-C chemokine receptor 1
CCR3	4.0	C-C chemokine receptor 3
CCR5	4.0	C-C chemokine receptor 5
INOS	4.0	Inducible Nitric Oxide Synthase
GDF-2	2.0	Growth Differentiation Factor 2
ZO-1	2.0	Zonula Occludin -1
GAPDH	0.0	Glyceraldehyde-3-Phosphate Dehydrogenase

cDNA microarray analysis of P.yoelii 17X infected and uninfected mouse brain. Gene listed were altered > 1.5 fold at peak parasitemia. Fold change in expression is defined as GAPDH normalized mRNA expression ratio of gene signals of infected to uninfected mouse brain.

4.2.2 Semi-quantitative RT-PCR validation and analysis of immunomodulator gene expression during *P.yoelii* 17X infection

4.2.2.1 Adhesion Molecule-PECAM-1, ICAM-1, VCAM-1 mRNA expression

Adhesion molecules, PECAM-1 (100-bp), ICAM-1 (106-bp) and VCAM-1(102-bp) mRNA expression were induced by *P.yoelii* 17X infection and were significantly upregulated in the brain at peak parasitemia. In general, induction of these markers began day 6 until day 8 post infection, 2-4 fold upregulation over control (Figure 11-13). Semi-quantitative analysis also indicated relatively high upregulation of mRNA of PECAM-1 and ICAM-1 than VCAM-1. PECAM-1, ICAM-1 and VCAM-1 expression by microarray data were markedly pronounced compared with semi-quantitative PCR data. Microarray experiment is based on hybridization of mRNA sequences; therefore less complementary sequence could bind to immobilized sequence on membranes and can provide results with significant upregulation of mRNA. PCR ensures that primers flank mRNA splicing regions and generate specific amplicons for gene of interest. Generation of non-specific amplicons is eliminated or minimized. It is therefore not surprise that microarray data for mRNA for PECAM-1, ICAM-1 and VCAM-1 are higher than semi-quantitative PCR data.

Histological analysis using antibodies against ICAM-1 and VCAM-1 has shown that there was greater expression of ICAM-1 in capillaries and small venules of *P.yoelii* 17X infected mouse brain than VCAM-1 (Shear *et al.*, 1998). Similar pattern in terms of mRNA expression was observed in this study. The level of expression of these adhesion molecules increased with time after infection, corresponding to the increase in parasitemia.

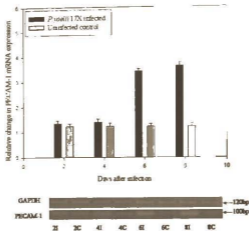


Figure 11: *P. yoelii* 17X upregulates PECAM-1 mRNA expression in mouse brain at day 6 and 8 post-infection. Semi-quantitative RT-PCR comparative analysis of adhesion molecule. PECAM-1 (100bp) mRNA expressions in brains of *P.yoelii* 17X infected (I, black bars) day 2, 4, 6 and 8 post-infections and control (C, grey bars) mice. Data presented are means and standard deviations of duplicate experiments and were normalized to GAPDH expression.

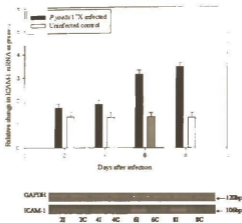


Figure 12: *P. yoelii* 17X upregulates ICAM-1 mRNA expression in mouse brain at day 6 and 8 post-infection. Semi-quantitative RT-PCR comparative analysis of adhesion molecule, ICAM-1 (106bp) mRNA expressions in brains of *P. yoelii* 17X infected (I, black bars) day 2, 4, 6 and 8 post-infections and control (C, grey bars) mice. Data presented are means and standard deviations of duplicate experiments and were normalized to GAPDH expression



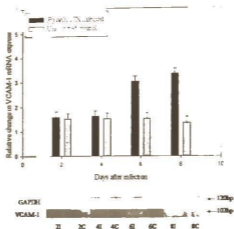


Figure 13: *P. yoelii* 17X upregulates VCAM-1 mRNA expression in mouse brain at day 6 and 8 post-infection. Semi-quantitative RT-PCR comparative analysis of adhesion molecule VCAM-1 (102bp) mRNA expressions in brains of *P.yoelii* 17X infected (I, black bars) day 2, 4, 6 and 8 post-infections and control (C, grey bars) mice. Data presented are means and standard deviations of duplicate experiments and were normalized to GAPDH expression

4.2.2.2 Cytokine- $\text{INF-}\gamma$, $\text{TNF-}\alpha$, IL-12 and iNOS mRNA expression

Upregulation of $\text{INF-}\gamma$ (98-bp) and $\text{TNF-}\alpha$ (100-bp) mRNA began early after day 2 post-*P. yoelii* 17X infection while IL-12 (102-bp) and iNOS (101-bp) started after day 4. $\text{INF-}\gamma$ (type II interferon) was significantly induced in infected mouse brain at day 6, approximately 5 fold over control and declined to about 2 fold increase at peak parasitemia (Figure 14). Type II interferon is important in clearance of pathogens in host. $\text{INF-}\gamma$ was highly induced at the initial phase of infection presumably to activate macrophages and natural killer (NK) cells to enhance their activity against the malaria parasite.

After day 4 post-infection, $\text{TNF-}\alpha$ and IL-12 mRNA expression were upregulated over 3 fold in infected mouse brain compared with controls (Figures 15 & 16). Meanwhile there was only a marginal increase (less than 2 fold) in iNOS mRNA expression in infected mouse brain relative to control (Figure 17).

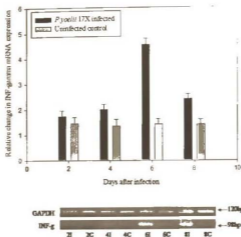


Figure 14: *P. yoelii* 17X upregulates INF-gamma mRNA expression in mouse brain day 6 and 8 post-infection. Semi-quantitative RT-PCR comparative analysis of murine INF-gamma, (98bp) mRNA expressions in brains of *P. yoelii* 17X (I, black bars) at 2, 4, 6 and 8 post-infections and control (C, grey bars) mice. Data presented were means and standard deviations of duplicate experiments and were normalized to GAPDH expression.

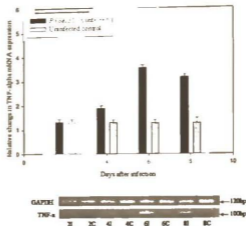


Figure 15: *P. yoelii* 17X upregulates TNF-alpha mRNA expression in mouse brain at day 6 and 8 post-infection. Semi-quantitative RT-PCR comparative analysis of cytokine TNF-alpha (100bp) mRNA expressions in brains of *P. yoelii* 17X infected (I, black bars) day 2, 4, 6 and 8 post-infections and control (C, grey bars) mice. Data presented were means and standard deviations of duplicate experiments and were normalized to GAPDH expression.

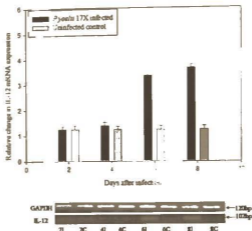


Figure 16. *P. yoelii* 17X upregulates IL-12 mRNA expression in mouse brain at day 6 and 8 post-infection. Semi-quantitative RT-PCR comparative analysis of cytokine IL-12 (102bp) mRNA expressions in brains of *P.yoelii* 17X infected (I, black bars) day 2, 4, 6 and 8 post-infections and control (C, grey bars) mice. Data presented were means and standard deviations of duplicate experiments and were normalized to GAPDH expression.

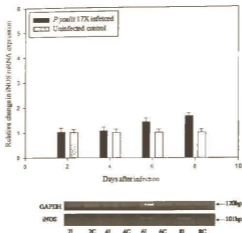


Figure 17: *P. yoellii* 17X induced iNOS mRNA expression in mouse brain at day 6 and 8 post-infection. Semi-quantitative RT-PCR comparative analysis of iNOS (101bp) mRNA expressions in brains of *P.yoellii* 17X infected (I, black bars) day 2, 4, 6 and 8 post-infections and control (C, grey bars) mice. Data presented were means and standard deviations of duplicate experiments and were normalized to GAPDH expression.

4.2.2.3 Chemokine- MIP-2alpha, MCP-1, RANTES mRNA expression

MIP-2alpha (94-bp) and MCP-1 (100-bp) mRNA expression were induced by *P.yoelii* 17X after day 4 post infection (Figure 18 & 19) while expression of RANTES (97-bp) mRNA began after day 2 (Figure 20). This indicates early mRNA expression of RANTES compared to MIP-2 alpha and MCP-1 during *P.yoelii* 17X infection. MIP-2alpha, MCP-1 and RANTES were upregulated 3-4 fold in infected mouse brain compared with controls at day 6 and 8 post infection (Figures 18, 19 & 20).

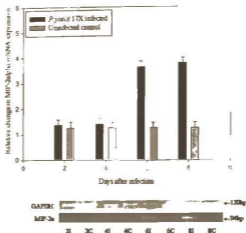


Figure 18 *P. yoelii* 17X upregulates MIP-2alpha mRNA expression in mouse brain at day 6 and 8 post-infection. Semi-quantitative RT-PCR comparative analysis of chemokine MIP-2alpha, (94bp) mRNA expressions in brains of *P. yoelii* 17X infected (I, black bars) day 2, 4, 6 and 8 post-infections and control (C, grey bars) mice. Data presented were means and standard deviations of duplicate experiments and were normalized to GAPDH expression

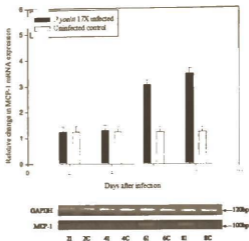


Figure 19: *P. yoelii* 17X upregulates MCP-1 mRNA expression in mouse brain at day 6 and 8 post-infection. Semi-quantitative RT-PCR comparative analysis of chemokine MCP-1 (100bp) mRNA expressions in brains of *P. yoelii* 17X infected (I, black bars) day 2, 4, 6 and 8 post-infections and control (C, grey bars) mice. Data presented were means and standard deviations of duplicate experiments and were normalized to GAPDH expression.

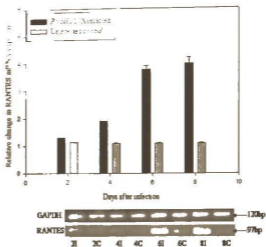


Figure 20: *P. yoelii* 17X upregulates RANTES mRNA expression in mouse brain at day 4, 6 and 8 post-infection. Semi-quantitative RT-PCR comparative analysis of chemokine RANTES (97bp) mRNA expressions in brains of *P. yoelii* 17X infected (I, black bars) day 2, 4, 6 and 8 post-infections and control (C, grey bars) mice. Data presented were means and standard deviations of duplicate experiments and were normalized to GAPDH expression.

4.2.2.4 Chemokine receptor-CCR1, CCR3 and CCR5 mRNA expression

All three C-C chemokine receptors, CCR1 (103-bp), CCR3 (96-bp) and CCR5 (100-bp) analyzed, were significantly upregulated at day 6 and 8 post-infection (Figures 21, 22 & 23). Messenger RNA expression levels of these receptors at day 6 and 8 post infection were 2-3 fold upregulated in infected mouse brain compared with controls. Messenger RNA expression of these receptors followed a similar pattern of their corresponding RANTES ligand.

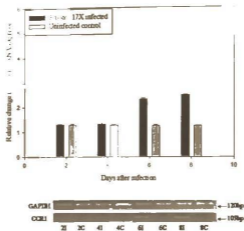


Figure 21: *P. yoelii* 17X upregulates CCRI mRNA expression in mouse brain at day 6 and 8 post-infection. Semi-quantitative RT-PCR comparative analysis of chemokine receptor CCRI (103bp) mRNA expressions in brains of *P. yoelii* 17X infected (I, black bars) day 2, 4, 6 and 8 post-infections and control (C, grey bars) mice. Data presented were means and standard deviations of duplicate experiments and were normalized to GAPDH expression.

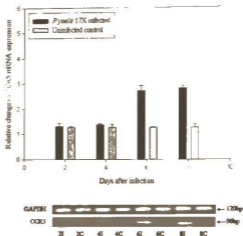


Figure 22: *P. yoelii* 17X upregulates CCR3 mRNA expression in mouse brain at day 6 and 8 post-infection. Semi-quantitative RT-PCR comparative analysis of chemokine receptor CCR3 (96bp) mRNA expressions in brains of *P. yoelii* 17X infected (I, black bars) day 2, 4, 6 and 8 post-infections and control (C, grey bars) mice. Data presented were means and standard deviations of duplicate experiments and were normalized to GAPDH expression.

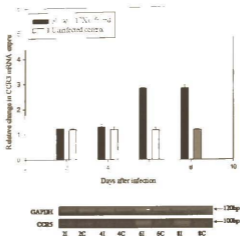


Figure 23: *P. yoelii* 17X upregulates CCR5 mRNA expression in mouse brain at day 6 and 8 post-infection. Semi-quantitative RT-PCR comparative analysis of chemokine receptor CCR5 (100bp) mRNA expressions in brains of *P. yoelii* 17X infected (I, black bars) day 2, 4, 6 and 8 post-infections and control (C, grey bars) mice. Data presented were means and standard deviations of duplicate experiments and were normalized to GAPDH expression.

4.3 Tissue and plasma protein expression of *P.yoelii* 17X induced RANTES

4.3.1 *P.yoelii* 17X induced RANTES protein expression

Results from the Western Blots analysis indicated the expression of RANTES (7.8kDa) protein in brain tissue samples from infected mice at day 4, 6 and 8 post-infection (Figure 24). Expression of α -tubulin ('housekeeping') gene was similar in both infected and uninfected control samples. Expression of tissue RANTES protein follows a similar profile to the transcript expression. This is an indication that tissue RANTES mRNA expressions in *P.yoelii* 17X infected mice are translated into protein. Brain tissue RANTES protein expression in infected mice was approximately 2-3 fold upregulated at day 4, 6 and 8 (Figure 24) compared with the expression in the uninfected control mice.

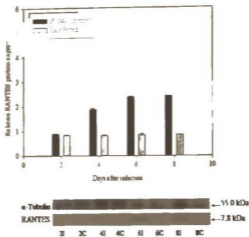


Figure 24: *P. yoelii* 17X infection upregulates RANTES protein expression in mouse brain at day 4, 6 and 8 post-infection. Comparative analysis of RANTES (7.8 kDa) protein expression in brain tissue samples from *P. yoelii* 17X infected mice day 2, 4, 6, & 8 post infection (black bars) versus uninfected controls (grey bars). Brain tissue protein samples from infected and uninfected mice were analyzed for RANTES expression by Western Blot. Data presented were means and standard deviations of duplicate experiments and were normalized to α -tubulin expression.

4.3.2 *P.yoelii* 17X infection induce RANTES expression in plasma

Levels of plasma RANTES expression was determined at different stages of *P. yoelii* 17X infection by ELISA. As shown in figure 25, expression of RANTES in plasma began at day 4 after infection, until day 8 post infection. RANTES levels in plasma were 3 times higher in *P. yoelii* 17X infected mice at day 8 than in controls. Systemic RANTES expression in plasma appeared to follow similar pattern as observed in the brain during the infection.

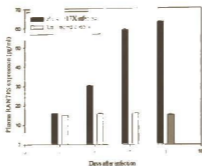


Figure 25. *P. yoelii* 17X infection upregulates RANTES protein expression in mouse plasma at day 4, 6 and 8 post-infection. *Comparative analysis of RANTES expression in plasma of *P. yoelii* 17X infected mice day 2, 4, 6, & 8 post infection (black bars) versus uninfected controls (grey bars). Plasma samples from infected and uninfected mice were analyzed for RANTES expression by ELISA. Data presented were means and standard deviations of duplicate experiments.*

4.4 Ultrastructural and immunohistological analysis of *P.yoelii* 17X infected brain samples

4.4.1 Ultrastructural analysis of *P.yoelii* 17X infected brain samples

Brains from parasitized mice were ultra structurally analyzed by transmission electron microscopy to evaluate effects of *P. yoelii* 17X infection on brain micro vessels at peak parasitemia (day 8 post infection). The result shows that uninfected mice (Mag. X15) have normal intact microvessel endothelia (ME) at blood brain barrier (BBB) while some infected mice (Mag. X15) show disintegrating ME and in certain parts of BBB (Figure 26). Although parasitized RBC's were observed in the distal microvasculature of infected mouse brain, evidence of extensive erythrocytic (RBC) adherence in micro vessels was not observed as expected for the 17X strain of *P. yoelii*.

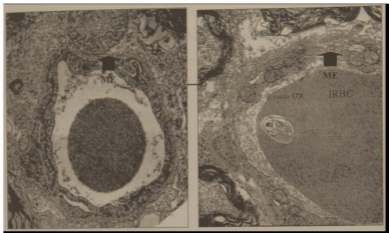


Figure 26. *P.yoelii* 17X induces ultra structural changes in mouse cerebellum at peak parasitemia (day 8 post-infection). Cerebellum from parasitized mice was ultra structurally analyzed by transmission electron microscopy to evaluate effects of *P. yoelii* 17X infection on brain micro vessels. Uninfected mice (Mag. X15) show normal intact micro vessel endothelia (ME) at blood brain barrier (BBB). Infected mice (Mag. X15) show disintegrating ME and BBB (arrow). There was no evidence of extensive erythrocytic (RBC) adherence in micro vessels of *P. yoelii* 17X strain.

4.4.2 Immunohistological analysis of GFAP expression in *P.yoelii* 17X infected mouse brain

The effect of *P.yoelii* 17X infection on astrocyte expressions in mouse brain was evaluated by immunohistology using antibody against GFAP, which is a specific marker for astrocytes. Results demonstrate that GFAP was upregulated in *P.yoelii* 17X infected mouse brain (Figure 27) compared with control. Upregulation of GFAP indicates activation of astrocytes during the infection.

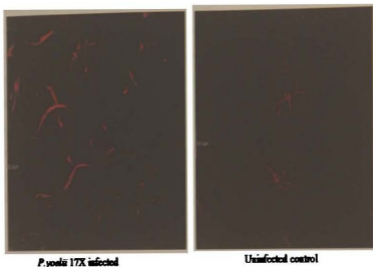


Figure 27: *P.yoelli* 17X upregulates GFAP expression in mouse brain at peak parasitemia (day 8 post-infection). Glial fibrillary acidic protein (GFAP) was analyzed in *P.yoelli* 17X infected and uninfected mouse brain using anti-GFAP antibodies. *P.yoelli* 17X infected brain samples shows high GFAP immunoreactivity compared with uninfected controls.

4.5 Human malaria studies

4.5.1 Post-mortem CM and NM brain samples

A Blantyre coma of 3 or less during severe malaria, in the absence of other causes of unconsciousness, such as hypoglycemia, meningitis or other encephalopathy, was used to define cerebral malaria (WHO 2000). The non-malaria cases, used as controls, had no history of neurological illness. Prior to deaths, the CM cases had been febrile and hyper-parasitaemic (38,213-87,570 *P.falciparum* parasites/ μ l). Examination of the brain samples revealed numerous ring-form-infected erythrocytes in the cerebral microvascular endothelia of the CM but no infected erythrocytes in the cerebral microvessels of the NM cases (Prof. Andrew Adjei personal communication).

4.5.2 Transcriptional analysis of RANTES, CCR1, CCR3 and CCR5 mRNA expression in cerebellum, cerebrum, brain stem and hippocampus of CM and NM samples

As expected, the level of GAPDH (226-bp) mRNA expression in the CM samples was the same as in the NM. Although the level of CCR1 (130-bp) mRNA expression was also similar in all of the brain samples, expression of RANTES (154-bp), CCR3 (193-bp) and CCR5 (101-bp) mRNA were significantly higher ($P < 0.0001$) in the cerebellum (Figure 28) and cerebrum (Figure 29) from the CM samples than in the corresponding samples from the NM controls. The expression of RANTES mRNA (but not that of CCR3 and CCR5 mRNA) was also slightly higher in the samples of brain stem ($P < 0.0027$, Figure 30) and hippocampus ($P = 0.0018$, Figure 31) from the victims of CM than in the corresponding samples from the NM controls.

In the samples of cerebellum and cerebrum from the CM cases, there was a direct relationship between the (up-regulated) expression of RANTES mRNA and that of each corresponding receptors (i.e. CCR3 and CCR5).

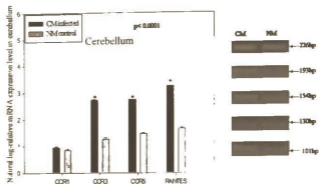


Figure 28: CM upregulates RANTES, CCR3 and CCR5 mRNA expression in cerebellum. Semi-quantitative RT-PCR comparative analysis of RANTES (154bp), CCR1 (130bp), CCR3 (193bp), and CCR5 (101bp), mRNA expression in cerebellum of human post-mortem CM-infected (black bars) and NM (grey bars) control brain tissue samples. Densitometric data presented were log-transformed (to adjust for small sample size) and represent the mean and \pm SEM of duplicates CM (n=12) and NM (n=6) cases, normalized to those for GAPDH (226bp). Asterisk(s) indicate statistically significant differences between CM and NM groups.

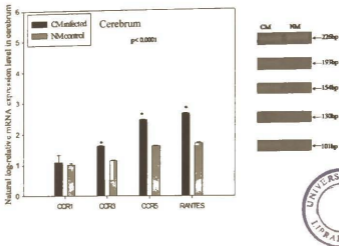


Figure 29: CM upregulates RANTES, CCR3 and CCR5 mRNA expression in cerebrum. Semi-quantitative RT-PCR comparative analysis of RANTES (154bp), CCR1 (226bp), CCR3 (193bp), and CCR5 (101bp), mRNA expression in cerebrum of human post-mortem CM-infected (black bars) and NM (grey bars) control brain tissue samples. Densitometric data presented were log-transformed (to adjust for small sample size) and represent the mean and \pm SEM of duplicates CM (n=12) and NM (n=6) cases, normalized to those for GAPDH (226bp). Asterisk(s) indicate statistically significant differences between CM and NM groups.

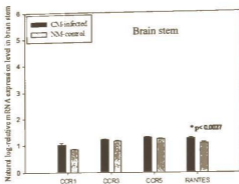


Figure 30: CM upregulates RANTES mRNA expression in brain stem. Semi-quantitative RT-PCR comparative analysis of RANTES (154bp), CCR1 (130bp), CCR3 (193bp), and CCR5 (101bp), mRNA expression in brain stem of human post-mortem CM-infected (black bars) and NM (grey bars) control brain tissue samples. Densitometric data presented were log-transformed (to adjust for small sample size) and represent the mean and \pm SEM of duplicates CM (n=12) and NM (n=6) cases, normalized to those for GAPDH (226bp). Asterisk(s) indicate statistically significant differences between CM and NM groups.

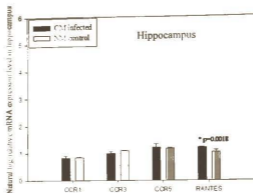


Figure 31: CM upregulates RANTES mRNA expression in hippocampus. Semi-quantitative RT-PCR comparative analysis of RANTES (154bp), CCR1 (130bp), CCR3 (193bp), and CCR5 (101bp), mRNA expression in hippocampus of human post-mortem CM-infected (black bars) and NM (grey bars) control brain tissue samples. Densitometric data presented were log-transformed (to adjust for small sample size) and represent the mean and \pm SEM of duplicates CM (n=12) and NM (n=6) cases, normalized to those for GAPDH (226bp). Asterisk(s) indicate statistically significant differences between CM and NM groups.

4.5.3 Western Blot and plasma analyses of RANTES, CCR1, CCR3 and CCR5

4.5.3.1 Western Blot analysis of RANTES, CCR1, CCR3 and CCR5 protein in cerebellum, cerebrum, brain stem and hippocampus of CM and NM samples

The Western blots analysis indicated that the expression of RANTES and CCR5 proteins in both cerebellum ($P < 0.0013$, Figure 32) and cerebrum ($P < 0.0001$, Figure 33) were also significantly higher for the CM samples than for the NM. Expression of α -tubulin ('housekeeping gene') was unchanged as expected in samples analyzed. Although the results of the transcriptional analysis indicated up-regulation of CCR3 in the samples of cerebellum and cerebrum from the CM cases, CCR3 protein could not be detected, by western blotting in the same samples.

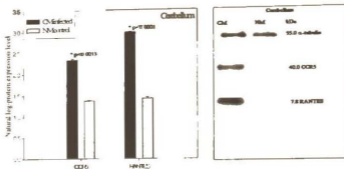


Figure 32: CM upregulates RANTES and CCR protein expression in cerebellum. SDS-PAGE/Western Blot demonstrating expression of RANTES (7.8 kDa) and CCR5 (40.0 kDa) in cerebellum of human post-mortem CM (black bars) and NM (grey bars) brain samples. Blots were probed with RANTES and CCR5 antibodies. Densitometric data presented were log-transformed (to adjust for small sample size) and represent the mean and \pm SEM of duplicates CM ($n=12$) and NM ($n=6$) cases, normalized to those for α -tubulin. Expression of α -tubulin (55.0 kDa) was unchanged in CM and NM.

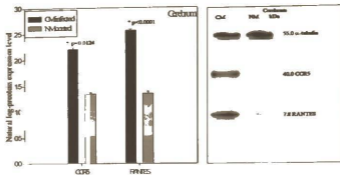


Figure 33: CM upregulates RANTES and CCR protein expression in cerebellum. SDS-PAGE/Western Blot demonstrating expression of RANTES (7.8 kDa) and CCR5 (40.0 kDa) in cerebellum of human post-mortem CM (black bars) and NM (grey bars) brain samples. Blots were probed with RANTES and CCR5 antibodies. Densitometric data presented were log-transformed (to adjust for small sample size) and represent the mean and \pm SEM of duplicates CM (n=12) and NM (n=6) cases, normalized to those for α -tubulin. Expression of α -tubulin (55.0 kDa) was unchanged in CM and NM.

4.5.4 *P.falciparum* induce RANTES expression in plasma

Examination of plasma RANTES expression by ELISA revealed that plasma from subjects with *P.falciparum* antigens had significantly higher ($P < 0.0001$) level of RANTES than control subjects (Figure 34).

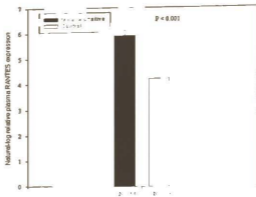


Figure 34: *P. falciparum* upregulates RANTES expression in plasma. Comparative analysis of RANTES expression in plasma of malaria positive ($n=64$) and control ($n=19$) subjects. Plasma samples from *P. falciparum* infected and control subjects were analyzed for RANTES expression by ELISA. Data presented were means and standard deviations of duplicate experiments.

4.5.5 Correlation of RANTES expression with malaria infection

There was a positive correlation between plasma RANTES expressions and malaria infection (Figure 35). Though the presence of other infections was not determined in this study, the correlation between plasma RANTES and malaria infection was mildly positive with $R^2 = 0.093$. Mathematically the correlation equation was determined as $y = 1.305 + 0.813X$. This is interpreted as an increased in malaria antigens results in an increased in RANTES expression.

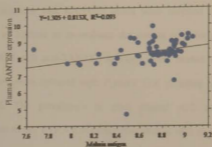


Figure 35: Plasma RANTES expression correlated positively with malaria antigens.

Regression analysis of log-transformed data of plasma RANTES (y-axis) and malaria antigens (x-axis) was determined using the Intercooled Stata 8.0 software. The results show a positive correlation represented by the equation $y = -1.305 + 0.813x$ with a coefficient of $R^2 = 0.093$.

4.6 Murine malaria studies-2

4.6.1 Role of RANTES in severity and survival during *P.yoelii* 17X malaria in mice

Since results demonstrate that RANTES levels were elevated during *P.yoelii* 17X infection, it was of interest to re-evaluate the course of infection when RANTES expression is blocked with anti-RANTES antibody. Mice treated with mock and anti-RANTES antibodies were infected with *P.yoelii* 17X parasites and parasitemia and mortality analyzed. The parasitemia in mice treated with mock antibody was comparatively higher at day 8 ($P < 0.06$) than mice treated with anti-RANTES antibody (Figure 36). At day 8 post-infection (peak parasitemia), parasitemia in mice treated with mock antibody was approximately 35% of *P.yoelii* 17X compared with 23% of *P.yoelii* 17X in mice treated with anti-RANTES antibody (Figure 36).

At peak parasitemia (day 8 post infection) when most mice died, the survival in mock antibody treated mice was 12% of seventeen mice compared with 42% of seventeen mice in the anti-RANTES antibody treated ones (Figure 37). Anti-RANTES antibody treated mice survived 6 days longer (day 14 post infection) than mock antibody treated mice indicating that blocking of RANTES extended the lives of infected mice by probably decreasing parasitemia.

There was 30% change in survival at day 8 post infection. Decrease (approximately 10%) in RANTES production effected 30% reduction in mortality by day 8 post *P.yoelii* 17X infection (Figure 38).

The level of RANTES provided in antibody treated mice that were subsequently infected with parasites was greater (2-3 fold increase) than uninfected control mice at day 8

(Figure 38). *P.yoelii* 17X parasite infection in mice induces RANTES expression above normal levels.

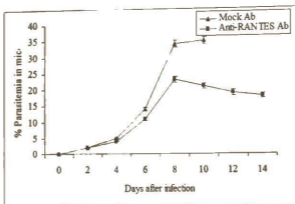


Figure 36: Course of *P.yoelii* 17X infection in mock and anti-RANTES antibody treated mice. Mice were challenged with parasite (day 0) after they were treated with mock and anti-RANTES antibodies. Level of parasitemia was monitored from the tail vein blood and counting at least 300 RBCs under immersion oil. Data represent mean \pm SEM of 5-10 counts per point. Parasitemia was comparatively higher ($p < 0.06$) in mock antibody (triangular points) treated than in anti-RANTES antibody (square points) treated mice.

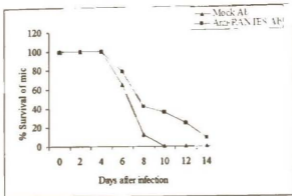


Figure 37: Survival of mock and anti-RANTES antibody treated mice, infected with *P.yoelii* 17X parasites. Mice were challenged with parasite (day 0) after they were treated with mock and anti-RANTES antibodies. Mortality and symptoms of infection were determined in each group. Twelve percent of seventeen mice treated with mock antibody were able to survive compared with 42% of seventeen mice treated with anti-RANTES antibody, at peak parasitemia. Anti-RANTES antibody treated mice were able to survive 6 days beyond peak parasitemia (day 8).

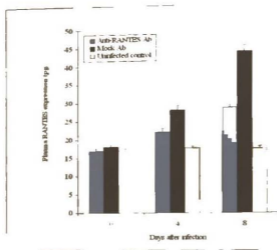


Figure 38: *P. yoelii* 17X infection upregulates RANTES expression in plasma of mock antibody treated mice, at day 4 and 8 post-infection. Comparative analysis of RANTES expression in plasma of *P. yoelii* 17X infected mice treated with mock (black bars) and anti-RANTES (blue bars) antibodies versus uninfected controls (white bars). Plasma samples from infected and uninfected mice were analyzed for RANTES expression by ELISA. Data presented were means and standard deviations of duplicate experiments.

CHAPTER FIVE

DISCUSSION

5.1 *P.yoelii* 17X murine malaria studies-1

Malaria-induced brain inflammation is mediated partly by complex cellular and immunomodulator interactions involving co-regulators such as cytokines and adhesion molecules. However, the role of chemokines and chemokine receptors in malaria brain immunopathogenesis has only been recently considered. The incomplete understanding of the role of the immune response during malaria infection has been partly responsible for the inability to develop a successful malaria vaccine.

The brain pathology associated with malaria remains a major cause of death with severe *P. falciparum* infection. Using experimental models has facilitated a better understanding of the pathogenesis of this syndrome and therefore better intervention strategies can now be developed to minimize or abrogate the severity of the disease. Some experimental models of cerebral malaria have been identified, showing similar pathological features with that of human CM. For instance, infection of Rhesus monkeys with *P. coomeyi* induced knobs on the surface of infected erythrocytes (Aikawa *et al.*, 1992). Grau *et al.*, (1987) have shown that lesions found in the brain of malaria-infected mice are characterized by endothelial damage. Though *P.yoelii* infected red blood cells do not display surface knobs, close adherence of infected RBCs to brain endothelium was observed by transmission microscopy. Mice infected with *P.yoelii* often develop hind

limb paralysis; an observation which is in parallel with the study of comatose Malawian children who exhibited signs of decortication (arms or legs extended) during cerebral malaria infection (Molyneux *et al.*, 1989). Also, like *P.falciparum*, *P.yoelii* can invade both mature and immature red blood cells (Shear *et al.*, 1998). Experimental cerebral malaria models may not exactly duplicate the brain pathological complications in human CM due to genetic variations, but the common features of this pathology which is shared by both human and murine models justify the use of these animal models in research to understand disease conditions in human.

In this study all the mice infected with *P. yoelii* 17X developed malaria-related-symptoms, which included appearance of ruffled hair, shivering with hind limb paralysis by day 8 post infection. Spleno-and hepato-megaly at peak parasitemia (Figure 9) was common and concordant with reported *P. yoelii* malaria infections (Kaul *et al.*, 1994). Spleno-and hepato-megaly (enlargement of spleen and liver), which have been observed to be important symptoms of human *falciparum* malaria, develop as a result of deposition of malaria pigments in infected liver during the exoerythrocytic schizogony, and increased phagocytocytic activity in the spleen.

The complementary DNA (cDNA) microarray results confirmed with semi-quantitative RT-PCR analysis from this study revealed changes in expression of a number of new immunomodulators that were previously unknown to be associated with malaria-induced brain dysfunction. This study is the first that may lead to the developing of a fingerprint for brain immunopathogenesis associated with CM. cDNA microarray analysis allows for

characterization of the mRNA levels for a large number of genes simultaneously, thus providing a useful tool for identifying broad-spectrum changes in gene expression in cells and tissues in response to a given stimulus. Recent studies with infectious agents such as *Salmonella*, *Chlamydia* and *Trypanosoma* using cDNA microarray technology have revealed unique gene-expression profiles (Dessus-Babus *et al.*, 2000; Rosenberg *et al.*, 2000; Stiles *et al.*, 2001) which may be of unique diagnostic value.

Among altered immunomodulator gene expression in the brain due to infection with *P.yoelii* 17X in the current study are adhesion molecules, PECAM-1 (23 fold), ICAM-1 (13 fold) and VCAM-1 (6 fold) at peak parasitemia. Temporal expression analysis by RT-PCR revealed that mRNA expression of these adhesion molecules began early during the infection, mostly by day 6 and plateaued by day 8 post infection (Figures 11, 10 & 13). It appears that increase parasitemia during *P.yoelii* 17X infection results in increased expression of these molecules.

PECAM-1 binds to platelets, and its expression has recently been reported to be upregulated in the post-mortem brain tissue samples of Malawian cerebral malaria patients (Wassmer *et al.*, 2003). Also, using antibodies against ICAM-1 and VCAM-1 in other studies have revealed an increased expression of these molecules in the microvessels of the brain during murine malaria infection (Shear *et al.*, 1998).

Elevated expression levels of PECAM-1, ICAM-1 and VCAM-1 may therefore be an important correlates of malaria brain immunopathology.

Gene expression analysis by cDNA microarray have also revealed significant upregulation of mRNA expression of cytokines INF- γ (6-fold), TNF- α , (5-fold) and IL-12 (4-fold) at peak parasitemia in this study. Temporal expression analysis by RT-PCR have shown that expression of these molecules started at day 6 and peaked at day 8 post infection (Figures, 14, 15, and 16).

INF- γ mRNA expression was significantly upregulated at day 6 but declined to a lower level at day 8 post infection. INF- γ belongs to type II interferons and is essential for parasite clearance during infection. There are other data which reinforce the importance of early production of INF- γ and TNF- α by T lymphocytes and natural killer (NK) cells in parasites clearance (Choudhury, *et al.*, 2000). Increased level of INF- γ expression in mouse brain at day 6 in this study could be partly due to the early immune response mounted by the host to the *P.yoelli* 17X parasite infection.

Report by Grau (1992) indicated that high TNF- α level is associated with the severity of malaria in humans. A decrease in TNF- α level reportedly resulted to a reduction in duration of coma in cerebral malaria in children (Di Perri *et al.*, 1995). More so, high expression of TNF- α receptor, tumor necrosis factor receptor-2 (TFR2) reportedly predisposed rodents to experimental cerebral malaria (Stoelcker *et al.*, 2002). Although the scope of this study did not involve analysis of TFR2, increased level of TNF- α which is a ligand for TFR2, in the brain in the current study could potentially increase the risk of malaria brain immunopathology in infected mice.

A role for IL-12 in early response against *Plasmodium* has been proposed. It may be involved in making mice resistant or susceptible; it may also possibly mediate pathology (Su *et al.*, 2002). Zhong & Stevenson (2002) demonstrated that IL-12 exhibited immunoregulatory role to antibody-mediated immunity against *Plasmodium* parasites. IL-12 expression during malaria infection appears to be linked or act through INF- γ production. IL-12 induces NK cells to produce INF- γ (Tripp *et al.*, 1993) which in turn activates macrophages to present antigens to antigen-specific T cells (Farra, *et al.*, 1993). This type of immune response is involved in the clearance of microbial pathogens. Expression of IL-12 together with INF- γ in *P.yoelii* 17X infected mice in this investigation demonstrate the involvement of antibody and T cells mediated immunity during murine malaria infection.

Cerebral malaria is characterized by coma in patients with *P.falciparum* infection that is also accompanied by metabolic acidosis, seizures and hypoglycemia (Miller *et al.*, 2002). Animal models have provided enough evidence implicating the role of inflammatory processes in the development of malaria brain pathology (Brian *et al.*, 2002). However not all proinflammatory cytokines are relevant for the development of the brain pathology associated with malaria. Expression of INF- γ , TNF- α and IL-12 have been identified as immunoregulatory cytokines in CM. Adhesion molecules and platelets induced immune-mediated damage of vascular endothelium of the brain has also been reported (Lou *et al.*, 2001). With the exception of INF- γ , which expression declined to a lower level after day 6 post infection, expression of all the other immunomodulators were observed to be elevated steadily after day 4 until day 8 post infection in this study.

CD⁺ T cells produce immune mediators and it comprises of at least two functionally different subsets, distinguished on the basis of lymphokine secretion in T helper 1 (Th1), (INF- γ producing cytokine), and Th2 (IL-4 cytokine) cells (Dong *et al.*, 2001). Th1 or Th2 cell types have regulatory functions in malaria. Recent report indicates that both Th1 and Th2 responses seem to be required to control malaria infection (Torre *et al.*, 2002, Kobayashi *et al.*, 2000). Increased expression of INF- γ and IL-12 in the current study also indicates Th1 immune response in *P.yoelii* 17X infection.

Inducible nitric oxide synthase (iNOS) mRNA was marginally expressed in mouse brain during *P.yoelii* 17X infection compared with the other immunomodulators. Though iNOS has been reported to play a role in human CM (Maneerat, 2000), its low expression in infected mouse brain in this investigation, suggests that it might not be one of the key molecules involved in the immunopathology of *P.yoelii* 17X infection.

This is the first report of the global profile as well as temporal expression studies of immunomodulator gene expression in the brain at peak parasitemia in murine malaria model which demonstrated that cytokines, INF- γ , TNF- α , and IL-12 mRNAs were significantly upregulated at day 6 and 8 post-infection, implicating these molecules in the immunoregulatory or immunopathogenesis during *P.yoelii* 17X infection.

This study has also demonstrated for the first time, that MIP-2 α (CCL), MCP-1 (CCL2) and RANTES (CCL5) chemokine and receptors CCR1, CCR3 and CCR5 mRNAs are important in *P.yoelii* 17X infection in mice. MIP-2 α , MCP-1 and RANTES are proinflammatory chemokines which are involved in chemotaxis of leukocytes during

infection. Chemokines are immunoregulatory factors that play an important role in the chemotaxis, activation and haematopoiesis of leukocytes (Keane *et al.*, 1998, Lillard *et al.*, 2001, 2003). Activation of chemokines involves initial binding to specific, seven-transmembrane-domain, G-(guanine-nucleotide-binding)-protein-coupled receptors on target cells. In response to a relatively higher concentration of chemokines at the site of injury or infection, leukocytes are activated to perform effector functions such as release of their granule contents and increase in cytokine production. Increase in mRNA expression of INF- γ , TNF- α and IL-12 during *P.yoelii* 17X infection in the current study, could be attributable to this phenomenon. Unique expressions of chemokines and their receptors involved in the immunopathogenesis of malaria brain pathology could serve as new markers for following the course and possibly predicting the outcome of the disease.

The cDNA microarray analysis has revealed significant upregulation of MIP-2 α (18-fold), MCP-1(7-fold) and RANTES (6-fold) at peak parasitemia. The results of RT-PCR analysis indicate that at day 6 and 8 post infection (Figures, 18, 19 & 20) mRNA expressions of these molecules are significantly upregulated in infected mouse brain compared with controls, indicating that these chemokines are involved in immunoregulatory or immunopathogenesis in *P.yoelii* 17X infected mouse.

Expression by cDNA analysis has shown that CCR1, CCR3 and CCR5, receptors for RANTES were also upregulated 4-fold, in infected mouse brain than in controls. RT-PCR analysis indicates approximately 3 fold increase in mRNA (Figures, 21, 22 & 23) expression of these receptors in mouse brain at day 6 and 8 post infection. In addition to

their RANTES ligand, these receptors could be playing an important role in migration of immune markers into the brain in *P.yoelii* 17X infected mice.

The cDNA microarray data showed a higher fold increase in mRNA expressions compared with the RT-PCR results. This discrepancy in cDNA array and RT-PCR data could be attributable to sequence-dependent hybridization characteristics or variations which are inherent in hybridization reactions.

MCP-1 and RANTES in addition to CCR1 and CCR5 are expressed by Th1 cells. Trafficking of inflammatory Th1 but not Th2 cells into the brain was reportedly mediated largely by RANTES interaction with CCR5 receptor (Zang *et al.*, 2001). Also the absence of CCR5 receptor in *Plasmodium berghei* ANKA infected mouse brain resulted in a reduced Th1 cytokine production (Belnoue *et al.*, 2003b). The observed expression of RANTES and CCR5 in addition to INF- γ mRNA in *P.yoelii* 17X infected mouse brain in this study demonstrated Th1 mediated immune response and that factors capable of inducing Th1 response could play an important role in managing malaria infections.

RANTES is an inflammatory chemokine. Activated T lymphocytes, platelets and endothelial cells release large amounts of RANTES during infection. RANTES plays an important role in the maintenance and prolongation of inflammatory response during infection. Macrophages and other leukocytes release proinflammatory cytokines including TNF- α and IL-1 which in turn promote the release of chemokines. A soluble gradient of these chemokines within the tissue recruits various cell types that express

receptors for different chemokines. Expressions of all the C-C chemokine receptors, CCR1, CCR3 and CCR5 for RANTES were upregulated in the brain of *P.yoelii* 17X infected mouse. RANTES expression possibly enhanced the expression of its receptors. RANTES also binds to endothelial cell surface, where it acts as a sign post for immune cells (Figure 7). Report by Sano *et al.*, (1998) demonstrated that ICAM-1 induce RANTES mRNA expression and also increase its protein synthesis and secretion by endothelial cells. *P. yoelii* 17X induced RANTES production, observed in the current study, possibly enhanced by ICAM-1, could activate leukocytes in the inflammatory sites to induce intense inflammation to exacerbate the immunopathology of the disease. Investigations conducted by Belnoue *et al.*, (2003b) showed that, brains of wild-type mice with murine cerebral malaria have significant levels of CCR5, a chemokine receptor for RANTES, implicating these molecules in the pathological conditions in the brain during the infection.

Ultrastructural analysis of mouse brain by transmission electron microscopy at peak parasitemia in this study revealed disintegrating microvessel endothelia layer at the blood brain barrier in the cerebellar region of infected mouse brain (Figure 26). Infected RBC's occluding the microvessels of the brain was also observed. This breach in microvessels endothelial layer could be associated with the action of RANTES. Perivascular oedema was also observed in this region of infected mouse brain as a result of endothelial cell damage which has allowed lymphatic and other tissue fluids to move across the blood brain barrier. Endothelia cells interacting with *P.yoelii* 17X parasitized RBCs can be induced to produce and present specific chemokines, such as RANTES, which can lure

CCR1, CCR3 and CCR5 cells into the brain (Pober *et al.*, 1991). CCR1 and CCR5 receptors are expressed by brain endothelial cells (Dzenko *et al.*, 2001, Andjelkovic *et al.*, 2000). Brain endothelial cells, microglia and astrocytes express CCR5 receptors (Berger *et al.*, 1999) and could be playing a role in the brain immunopathology during *P. yoelii* 17X infection. The binding of RANTES to its receptors on these cells can serve to further activate them and enhance the breakdown of the microvessel endothelia, as observed in infected mouse brain in the current investigation.

Immunohistological analysis revealed high reactivity to glial fibrillary acidic protein (GFAP) in *P. yoelii* 17X infected mouse brain. High GFAP expression is an indication of activation of astrocytes in infected mouse brain. Astrocytes are involved in the development of astrogliosis (increase in astrocytic proliferation and hypertrophy) which could lead to neurodegeneration (Wilhelmsson *et al.*, 2004). Also, astrocytes are significant source of RANTES in the brain (Kim *et al.*, 2004).

Based on this observation, this report suggests that, *P. yoelii* 17X-induced astrocytes which is a great source of RANTES will potentially induce astrogliosis, leading to brain immunopathological complications.

Chemokines have been shown to have a direct antiprotozoal activity for three protozoans: *Toxoplasma gondii*, *Leishmania donovani* and *Trypanosoma cruzi* (Mannheimer *et al.*, 1996, Villalta *et al.*, 1998). Chemokine production is important for host defense against infection. However, excessive production is deleterious to the host. It has been observed that CC chemokines such as MIP-1 α , MIP-1 β and RANTES are significantly upregulated

in brains of *Trypanosoma brucei brucei* infected rats (Sharafeldin *et al.*, 2000). This increase in expression of these chemokines occurs before brain lesions developed in infected rats (Sharafeldin *et al.*, 2000), implying that induction of these chemokines could be directly responsible for the observed brain lesions. Over expression of chemokines therefore appears to be detrimental to the host during African trypanosomiasis disease.

The hypothesis investigated in the present study was that upregulation of RANTES chemokine and receptor expressions are associated with the immunopathology of malaria infection and that blocking RANTES overexpression will minimize or abrogate the outcome of the disease. The results demonstrate that increase in production of RANTES follows the course of *P.yoelii* 17X malaria infection such that RANTES and receptors CCR1, CCR3 and CCR5 were detected at high levels at day 6 and 8 post infection, implicating these molecules in the immunopathology of *P.yoelii* 17 X infection.

The ELISA data from this study indicate significant upregulation of RANTES after day 4 until day 8 in *P.yoelii* 17X infected mouse plasma than in controls (Figure 25). Also, Western blot analysis revealed that brain tissue transcripts of RANTES were actually translated into protein and were significantly upregulated in infected mice (Figure 24). It was evident from the results obtained in this investigation that the expression pattern of RANTES was similar to the increase level of parasitemia. RANTES production was significantly elevated at day 6 and 8 post-infection (Figure 20 & 24). Parasitemia in mice were also observed to be high at day 6 and 8. Most of the pathological conditions were observed on those days, especially at day 8 (peak parasitemia). Increase in RANTES production correlated with increase in parasitemia and pathological conditions. RANTES

causes inflammation which opens up spaces between cells, allowing the escape of leukocytes into tissues and also the spread of infectious agents. With reduced leukocyte population in blood vessels, phagocytosis of infected RBCs is minimized and parasites could therefore increase in numbers. This could be a plausible correlation between RANTES production and the increase level of parasitemia in *P.yoelii* 17X infected mice in this investigation.

P.yoelii 17X infection upregulates RANTES and its corresponding receptors, CCR1, CCR3 and CCR5 in mouse brain and that ultrastructural change in microvascular endothelium layer occurred in the cerebellum of infected mice. This is the first temporal expression study of RANTES and receptors associated with murine malaria.

5.2 Murine malaria studies-2

This study shows that blocking RANTES causes a decline in the level of parasitemia in infected mice. This decline was associated with increased life expectancy for the infected mice. At day 8 post infection, the percentage of parasitemia was 23% in anti-RANTES treated mice compared with approximately 35% in mock antibody treated ones (Figure 36). Since the expression of RANTES causes inflammation which opens up the spaces between cells allowing the escape of leukocytes, blocking of RANTES during *P.yoelii* 17X infection in this study purportedly prevented the escape of these leukocytes, and with their accumulation in blood vessels together with platelets, phagocytosis of infected red blood cell is enhanced and parasites numbers is declined.

It is believed that over expression of RANTES does not only play a significant role in the immunopathology of malaria infection, but it also mediates increased parasitemia. This is evident from the survival plot in the current study (Figure 37) which demonstrated that comparatively higher percentage (42%) of mice, treated with anti-RANTES antibody were able to survive compared with mock antibody treated ones (12%) at peak parasitemia. RANTES therefore play an important role in mortality during malaria infection. Analysis by ELISA has shown that, RANTES was expressed more in mock antibody treated plasma than in anti-RANTES antibody treated and uninfected controls (Figure 38). The level of RANTES expression in plasma of *P.yoelii* 17X infected mock and anti-RANTES antibody treated were observed to be higher than uninfected controls. This is further evidence that RANTES expression is associated with *P.yoelii* 17X infection.

5.3 Human malaria studies

The mechanism by which chemokines mediate immunopathogenesis and neuropathology associated with human CM is not well understood. This lack of understanding is partly due to the fact that data from patients in which a clinical diagnosis of CM has been established prior to death are rare. Studies using rodent cerebral malaria models have previously been criticized as inadequately comparable with human CM. In particular, the *P. berghei* ANKA model suggests that sequestration of infected red blood cells, leukocytes and platelets mediate CM pathogenesis. Leukocyte sequestration in human brain microvasculature has not been previously considered as a diagnostic feature of CM. However, recent histopathological analysis of CM brain samples from Malawian patients



demonstrated a high degree of platelets and mononuclear cell accumulation in brain microvessels (Grau *et al.*, 2003; Wassmer *et al.*, 2003). This suggests a new overlap between human and rodent CM.

Since this investigation has revealed that RANTES and corresponding receptor expression occurs in the brain of murine malaria model, we tested the hypothesis that chemokine RANTES and receptors are associated with brain immunopathogenesis in humans due to CM, and also determined which regions of the brain these expressions occur.

This study shows that expression of RANTES (a C-C chemokine produced by endothelial and CD8⁺ T cells and macrophages), a potent chemoattractant for lymphocytes, eosinophils, NK cells and CD8⁺T cells (Kameyoshi *et al.*, 1992; Kuna *et al.*, 1998; Iijima *et al.*, 2003) and CCR5 (a C-C chemokine receptor), are significantly upregulated in cerebellum and cerebrum of post mortem human CM samples.

Although a much larger sample size would have been desirable for this study, the results obtained using log-transformed data were statistically significant between CM and NM groups. This survey has provided the opportunity to report for the first time that RANTES and CCR5 at the mRNA and protein levels are significantly upregulated in human post-mortem CM tissue samples.

Messenger RNA (mRNA) and protein expression analyses revealed differential expression patterns of RANTES and its receptors in different parts of the brain. RANTES, CCR3 and CCR5 but not CCR1 transcripts were significantly upregulated ($P < 0.001$) in the cerebellum and cerebrum in CM infected brain tissues than in NM controls (Figure 26 & 27). Also, expression of RANTES mRNA was upregulated in the brain stem ($P < 0.0027$) and hippocampus ($P = 0.0018$) of CM-infected samples than in controls (Figures 28 & 29).

Western blot analysis indicated that RANTES and CCR5 proteins were significantly upregulated in cerebellum ($P < 0.0001$ for RANTES, $P < 0.013$ for CCR5) and cerebrum ($P < 0.0001$ for RANTES, $P < 0.0124$ for CCR5) but not in brain stem and hippocampus during CM. However, CCR3 protein expression in all the CM samples examined could not be detected though its mRNA was expressed in cerebellum and cerebrum. This protein loss could be due to post-transcriptional modification or other downstream mechanisms that may have resulted in inhibition or degradation of the protein product.

In the current study RANTES, in association with its receptor CCR5 could be major immune modulators of brain immunopathology, particularly in the cerebellum and cerebrum during CM. It is proposed that CM infection may induce localized host immune responses mediated in part by RANTES, which in turn recruits CCR5⁺ leukocytes and possibly elevating the expression of CCR5 (Iijima *et al.*, 2003). The observation of an association of RANTES and CCR5 with CM in the brain is interesting and requires further examination in malaria endemic populations.

RANTES expression was also analyzed in plasma samples obtained from patients who have had malaria episode to determine if its expression is systemic or localized during human malaria infection. Results indicate that expression of RANTES in plasma of malaria positive subjects are significantly upregulated ($P < 0.0001$) compared with controls (Figure 32). Also, regression analysis indicates that plasma RANTES expression correlated positively with *P.falciparum* antigens. The regression equation shows that increase in malaria antigens resulted in increased plasma RANTES (Figure 33).

Studies by Burgmann *et al.*, (1995) showed that serum concentrations of MIP-1 α and IL-8 chemokine were upregulated even in cases where *P.falciparum* parasite was not detected in the smears. In this investigation, it was observed that there were elevated levels of RANTES in plasma of patients who were positive for malaria antigens indicating that the presence of malaria antigens can even induce RANTES expression.

Though, plasma samples from malaria positive subjects were not screened for other infectious agents to determine if the source of RANTES was due to other pathogens, expression of RANTES was observed to be significantly higher in malaria antigen positive plasma compared to the non-malaria controls. This demonstrates that RANTES expression, and levels in plasma could be calibrated and used as a diagnostic marker for human malaria infection.

Recently, it has been shown that malaria infection induces CCR3 and CCR5 expression in placenta of pregnant women (Tkachuk *et al.*, 2001) giving credence to the fact that

CCR3 and CCR5 expression is associated with malaria infection. Luo *et al.*, (2001) have indicated that CCR1 and CCR5 on human astrocytes function in the recruitment of leukocytes to specified brain regions. During CM in Vietnamese adults, Medana *et al.*, (2002) observed axonal injury in the cerebral cortices and cerebellum, the regions of the brain in which, during CM, RANTES, CCR3 and CCR5 transcript expressions were found to be significantly up-regulated in the present study. This observation was surprising since other brain compartments may equally be exposed to circulating soluble chemokines in plasma and probably the cerebrospinal fluid. In addition to malaria infected red blood cells adhering to cerebral micro-capillaries and obstructing microcirculation, RANTES may recruit CCR5⁺ leukocytes to these regions of the brain during CM infection and possibly causing localized necrosis. An incidence of CM during a critical period of brain development and organization will especially impact those brain systems most vulnerable to cerebrovascular crisis. These vulnerable regions support cognition, memory, and executive neurological functions (Riva & Giorgi, 2000; Schmahmann, 1992) and any neuropsychological sequelae for CM will involve these abilities to a varying degree. Interestingly, CM has been implicated in cognitive impairment in children in Kenya and Senegal, some of whom were survivors of CM and severe malaria (Holding *et al.*, 2001; Boivin 2002).

Increased circulation of CCR3 and CCR5 receptors mediate fusion and infection with HIV (Choe *et al.*, 1996). Thus, malaria infections increase the potential reservoir for HIV by increasing the number of target cells. Therefore the increased levels of circulating receptors in CM-infected individuals, which are also, utilized by HIV presents a grim

scenario for the developing world where disease burden is high and both infections are prevalent.

It is not clear at this stage which cell types over express RANTES and CCR5 in the cerebellum and cerebrum during CM. However, evidence from PCR and immunohistological studies have revealed that microglia express CCR3, and CCR5 receptors (He *et al.*, 1997).

Due to technical constraints, post-mortem CM tissue samples could not be obtained and processed for immuno-histological analysis to determine which cell types express these receptors. It will be of interest in the future to examine expression of these markers in malaria-infected blood samples as well.

5.4 Conclusions

This is the first temporal expression study of RANTES and corresponding receptors CCR1, CCR3 and CCR5 associated with murine malaria. This study has concluded that *P. yoelii* 17X murine malaria model is useful in characterizing differentially expressed genes associated with human clinical malaria. This study has also revealed that expression of RANTES and its corresponding receptors CCR1, CCR3 and CCR5 is associated with malaria-induced brain pathogenesis and ultrastructural alterations in cerebellum of infected mice. High expression of RANTES mediates increase in parasitemia and mortality of murine malaria models. Blocking of RANTES reduced parasitemia and mortality associated with *P. yoelii* 17X infection.

The cerebellum and cerebrum in humans have been observed to be the focal points for increased malaria-induced RANTES and CCR5 expression, which suggest that active sequestration of IRBCs and platelets in addition to leukocytes in these regions of the brain will exacerbate CM immunopathology. The interaction of RANTES and associated CCR5 receptor in the cerebellum and cerebrum could lead to localized hyperinflammation in these regions of the brain, which in turn could lead to coma and cognitive impairment.

Also, upregulation of CCR5 expression, a co-receptor for HIV-1 suggests a potential link between infectious disease burden and susceptibility to HIV/AIDS in malaria endemic regions.

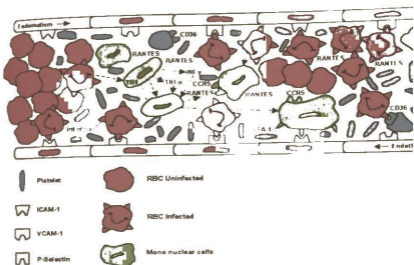


Figure 39: Proposed model for RANTES-mediated brain pathogenesis during CM. *Sequestered infected RBCs in addition to RANTES-mediated recruitment of leukocytes via the CCR5 receptor and platelets may be trapped in the distal microvessels of the brain. This may impede the smooth flow of nutrients and oxygen. The resulting ischemia and neurological conditions associated with cerebral malaria possibly could lead to degradation or mechanical breaching of the BBB which could lead to the neuropathology associated with CM.*

SUGGESTIONS FOR FUTURE STUDIES

1. Perform ultrastructural studies with human samples to examine role of BBB, glial cells and astrocytes in CM post treatment encephalopathy (PTE)
2. Perform FACS analysis to determine cells producing RANTES and CCR5
3. Use specific glial, astrocyte, endothelial and neuronal cell antibody probes in immunohistochemistry to localize and determine the role of these cell types in CM immunopathology.
4. Determine whether the cerebellar and cerebral regions recruit and sequester CCR5+ astrocytes, glia or T cells

REFERENCES

- Aikawa, M., Brown, A., Smith, C.D., Tegoshi, T., Howard, R.J., Hasler, T.H., Ito, Y., Perry, G., Collins, W.E. & Webster, K. (1992). A primate model for human cerebral malaria: *Plasmodium coatneyi*-infected rhesus monkeys. *Am J Trop Med Hyg.* **46**:391-397.
- Andjelkovic, A.V. & Pachter, J.S. (2000). Characterization of binding sites for chemokines MCP-1 and MIP-1 α , on human brain microvessels. *J. Neurochem.* **75**:1898-1906.
- Badolato, R., Sacks, D.L., Savoia, D. & Musso T. (1996). *Leishmania major*: infection of human monocytes induces expression of IL-8 and MCAF. *Exp. Parasitol.* **82**: 21-26.
- Baggiolini M. & Dahinden C.A. (1994). CC chemokines in allergic inflammation. *Immunol. Today.* **15**:127.
- Bajetto, A., Bonavia, R., Barbero, S., Florio, T. & Schettini G. (2001). Chemokines and their receptors in the central nervous system. *Front. Neuroendocrinol.* **22**:147-184.
- Barragan, A., Kremsner, P.G., Weiss, W., Wahlgren, M. & Carlson, J. (1998). Age-related buildup of humoral immunity against epitopes for rosette formation and agglutination in African areas of malaria endemicity. *Infect. Immun.* **66**:4783-4787.
- Baruch, D.I., Gormely, J.A., Ma, C., Howard, R.J. & Pasloske, B.L. (1996). *Plasmodium falciparum* erythrocyte membrane protein 1 is a parasitized erythrocyte receptor for adherence to CD36, thrombospondin, and intercellular adhesion molecule 1. *Proc. Natl. Acad. Sci.* **93**:3497-3502.

- Belnoue, E., Costa, F.T., Vigario, A.M., Voza, T., Gonnet, F., Landau, I., Van, Rooijen, N., Mack, M., Kuziel, W.A. & Renia, L. (2003a). Chemokine receptor CCR2 is not essential for the development of experimental cerebral malaria. *Infect. Immunol.* **71**:3648-3651.
- Belnoue, E., Kayabanda, M. & Deschemin, J.C. (2003b). CCR5 deficiency decreases susceptibility to experimental cerebral malaria. *Blood.* **101**:4253-4259.
- Belperio J.A., Keane, M.P., Arenberg, D.A., Addison, C.L., Ehlert, J.E., Burdick, M.D. & Strieter, R.M. (2000). CXC chemokines in angiogenesis. *J. Leukoc. Biol.* **68**: 1-8.
- Berger, O., Gan, X., Gujulova, Burns, A.R., Sulur, G., Stins, M., Way, D., Witte, M., Weinand, M., Said, J., Kim, K.S, Taub, D., Graves, M.C. & Fiala, M. (1999). CXC and CC chemokine receptors on coronary and brain endothelia. *Mol. Med.* **5**:795-805.
- Bifare, Y.D., Gianinazzi, C., Imboden, H., Leib, S.L. & Tauber, M.G. (2003). Bacterial meningitis causes two distinct forms of cellular damage in the hippocampal dentate gyrus in infant rats. *Hippocampus.* **13**:481-488.
- Boivin, M.J. (2002). Effects of early cerebral malaria on cognitive ability in Senegalese children. *J. Dev. Behav. Pediatr.* **23**:353-364.
- Brester, D.R., Kwiatkowski, D. & White, N.J. (1993). Neurological sequelae of cerebral malaria in children. *Lancet.* **336**:1039-1043.
- Brian, S. J. & Riley, E.M. (2002). Cerebral malaria: the contribution of studies in animal models to our understanding of immunopathogenesis. *Microbes Infect.* **4**:291-300.
- Brown, K.M. & Kreier, J.P. (1986). Effect of macrophage activation on phagocyte *Plasmodium* interaction. *Infect. Immun.* **51**: 744-749.
- Burgmann, H., Hollenstein, U., Wenisch, C., Thalhammer, F., Looareesuwan, S. & Graninger W. (1995). Serum concentrations of MIP-1alpha and IL-8 in patients

- suffering from acute *Plasmodium falciparum* malaria. *Clin.Immunol. & Immunopathol.* 76:32-36.
- Campbell, C.C. (1997). Malaria: an emerging and re-emerging global plague. *Immunol. Med. Microbiol.* 76:325-331.
- Choe, H., Farzan, M., Sun, Y., Sullivan, N., Rollins, B., Ponath, P.D., Wu, L., Mackay, C.R., LaRosa, G., Newman, W., Gerard, N., Gerard, C. & Sodroski J. (1996). The beta-chemokine receptors CCR3 and CCR5 facilitate infection by primary HIV-1 isolates. *Cell.* 85:1135-1148.
- Chogle, A.R. (1998). Hypoglycaemia in *falciparum* malaria. *J. Assoc. Phy. Ind.* 46:921-922.
- Choudhury, H R., Sheikh, N.A., Banchroft, G.J., Katz, D.R. & DeSouza, J.B. (2000). Early non-specific immune responses and immunity to blood-stage non-lethal *Plasmodium yoelii* malaria. *Infect. Immun.* 68: 6127-6132.
- Clark, I.A. & Cowden, W.B. (1992). Roles of TNF in malaria and other parasitic infections. *Immunol. Ser.* 56:365-407.
- Cohen, S., McGregor, I.A. & Carrington S. (1961). Gamma globulin and acquired immunity to human malaria. *Nature.* 4: 733-737.
- Cowman, A.F., Coppel, R.L., Saint, R.B., Favoloro, J., Crewther, P.E., Stahl, H.D., Bianco, A.E., Brown, G.V., Anders, R.F. & Kemp, D.J. (1984). The ring-infected erythrocyte surface antigen (RESA) polypeptide of *Plasmodium falciparum* contains two separate blocks of tandem repeats encoding antigenic epitopes that are naturally immunogenic in man. *Mol. Biol. Med.* 2: 207-221.
- Craig, A. & Scherf, A. (2001). Molecules on the surface of the *Plasmodium falciparum* infected erythrocyte and their role in malaria pathogenesis and immune evasion. *Mol. Biochem. Parasitol.* 115: 129-143.
- Curtis, C. (1997). Prevention of malaria with pyrethroid treated bednets. *Afr. Health.* 19:17-18.

- Day, K. & Marsh, K. (1991). Naturally acquired immunity to *Plasmodium falciparum*. *Parasitol. Today*. A: 68-71.
- Denney, C.F., Eckmann, L. & Reed, S.L. (1999). Chemokine secretion of human cells in response to *Toxoplasma gondii* infection. *Infect. Immun.* 67: 1547-1552.
- Dessus-Babus, S., Knight, S.T. & Wyrick, P.B. (2000). *Chlamydial* infection of polarized HeLa cells induces PMN chemotaxis but the cytokine profile varies between disseminating and non-disseminating strains. *Cell Microbiol.* 2:317-327.
- Di Perri, G., Guasparri, I., Monteiro, G.B., Bonora, S., Hennig, C., Cassatella, M., Micciolo, R., Vento, S., Dusi, S., Bassetti, D. & Conica, E. (1995). Pentoxifylline as a supportive agent in the treatment of cerebral malaria in children. *J.Infect. Dis.* 171: 1317-1322.
- Dodoo, D., Theander, T.G., Kurtzhals, J.A., Koram, K., Riley, E., Akanmori, B.D., Nkrumah, F. & Hviid, L. (1999). Levels of antibody to conserved parts of *Plasmodium falciparum* merozoite surface protein in Ghanaian children are not associated with protection from clinical malaria. *Inf. Immun.* 67: 2131-2137.
- Dong, C. & Flavell, R.A. (2001). Th1 and Th2 cells. *Curr. Opin. Hematol.* 8:47-51.
- Dzenko, K.A., Andjelkovic, A.V., Kuziel, W.A. & Packter, J.S. (2001). The chemokine receptor CCR2 mediates internalization of monocyte chemoattractant protein-1 along brain microvessels. *J. Neurosci.* 21: 9214-9223.
- Edozien, J.C., Gilles, H.M. & Udeozo, I.K. (1962). Adult and cord blood gammaglobulin and immunity to malaria in Nigerians. *Lancet.* 2: 951-955.
- English, M., Muambi, B., Mithwani, S. & Marsh, K. (1997). Lactic acidosis and oxygen debt in African children with severe anaemia. *Q.J. Med.* 9: 563-569.

- Farrar, M.A. & Schreiber, R.D. (1993). The molecular cell biology of interferon-gamma and its receptor. *Annu. Rev. Immunol.* 11:571.
- Felger, L., Marshal, V. M., Reeder, J. C., Hunt, J. A. Mgone C. S. & Beck, H.P. (1997). Sequence diversity and molecular evolution of the merozoite surface antigen 2 of *Plasmodium falciparum*. *J. Mol. Evol.* 45:154-160.
- Fernando, D., Wickremasinghe, R., Mendis, K.N. & Wickremasinghe, A.R. (2003). Cognitive performance at school entry of children living in malaria-endemic areas of Sri Lanka. *Trans. R. Soc. Trop. Med. Hyg.* 97:161-165.
- Fujioka, H., Millet, P., Maeno, Y., Nakazawa, S., Ito, Y., Howard, R.J., Collins, W.E., & Aikawa, M. (1994). A non-human primate model for human cerebral malaria: rhesus monkeys experimentally infected with *Plasmodium fragile*. *Exp. Parasitol.* 78: 371-376.
- Gallup, J.L. & Sachs, J.D. (2001). The economic burden of malaria. *Am. J. Trop. Med Hyg.* 64:85-96.
- Garnica, M.R., Silva, J.S. & de Andrade, H.F. (2003). Stromal cell-derived factor-1 production by spleen cells is affected by nitric oxide in protective immunity against blood-stage *Plasmodium chabaudi* CR in C57BL/6j mice. *Immunol. Lett.* 89:133-142.
- Grau, G.E. (1992). Essential role of tumor necrosis factor and other cytokines in the pathogenesis of cerebral malaria: experimental and clinical studies. *Verh. K. Acad. Geneesk. Belg.* 54:155-175.
- Grau, G.E., Fajardo, L.F., Piguat, J.F., Allet, B., Lambart, P.H. & Vassalli, P. (1987). Tumor necrosis factor (cachectin) as an essential mediator in murine cerebral malaria. *Science.* 237: 1210-1212.
- Grau, G.E., Mackenzie, C.D., Carr, R.A., Redard, M., Pizzolato, G., Allasia, C., Cataldo, C., Taylor, T.E. & Molyneux, M.E. (2003). Platelet accumulation in brain microvessels in fatal pediatric cerebral malaria. *J. Infect. Dis.* 187:461-466.

- Grau, G.E., Piguët, P.F., Engers, H.D., Louis, J.A., Vassalli, P. & Lambert, P.H. (1986) L3T4+ T lymphocytes play a major role in the pathogenesis of murine cerebral malaria. *J Immunol.* **137**:2348-2354.
- Greenwood, B. (1999). Malaria mortality and morbidity in Africa. *Bull. WHO.* **77**:617-618.
- Grote, C.L., Pierre-Louis, J.C. & Durward, W.F. (1997). Deficits in delayed memory following cerebral malaria. A case study. *Cortex.* **33**:385-388.
- Grun, J.L. & Weidanz, W.P. (1981). Immunity to *Plasmodium chabaudi adami* in the B-cell-deficient mouse. *Nature.* **290**: 143-145.
- Hanum, P.S., Hayano, M., & Kojima, S. (2003). Cytokine and chemokine responses in a cerebral malaria-susceptible or - resistant strain of mice to *Plasmodium berghei* ANKA infection: early chemokine expression. *Int. Immunol.* **15**:633-640.
- He, J., Chen, Y., Farzan, M., Choe, H., Ohagen, A., Gartner, S., Busciglio, J., Yang, X., Hofmann, W., Newman, W., Mackay, C.R., Sodroski, J. & Gabuzda, D. (1997). CCR3 and CCR5 are co-receptors for HIV-1 infection of microglia. *Nature.* **385**: 645-649.
- Hill, A.V.S., Allsopp, C.E.M., Kwiatkowski, D., Antey, N.M., Twumasi, P., Rowe, P., Bennett, S., Brewster, D., McMichael, A.J. & Greenwood, B.M. (1991). Common West African HLA antigens are associated with protection from severe malaria. *Nature.* **352**: 595-600.
- Holder, A.A. (1988). The precursor to major merozoite surface antigens: Structure and role in immunity. *Prog.Allergy.* **41** :72-97.
- Holden, P.A. & Snow, R.W. (2001). Impact of *Plasmodium falciparum* malaria on performance and learning: review of the evidence. *Am.J.Trop.Med.Hyg.* **64**:68-75.

- Holgate, S.T., Bodey, K.S., Janezic, A., Frew, A.J., Kaplan, A.P. & Teran, L.M. (1997). Release of RANTES, MIP-1alpha and MCP-1 into asthmatic airways following endobronchial allergin challenge. *Am. J. Resp. Crit. Care. Med.* 156: 1377.
- Hollingdale, M.R., Nardin, E.N., Tharavanij, S., Schwartz, A.L. & Nussenzweig, R.S. (1984). Inhibition of entry of *Plasmodium falciparum* and *Plasmodium vivax* sporozoites into cultured cells; an assay of protective antibodies. *J. Immunol.* 132: 909-913.
- Iijima, W., Ohtani, H., Nakayama, T., Sugawara, Y., Sato, E., Nagura, H., Yoshie, O. & Sasano T.(2003). Infiltrating CD8+ T cells in oral lichen planus predominantly express CCR5 and CXCR3 and carry respective chemokine ligands RANTES/CCCL5 and IP-10/CXCL10 in their cytolytic granules: a potential self-recruiting mechanism. *Am. J. Pathol.* 163:261-268.
- Jakobson, P.H., Bate, C.A., Tarverne, J. & Playfair, J.H. (1995). Malaria: toxins, cytokines and disease. *Parasite Immunol.* 17:223-231.
- Jennett, B., Teasdale, G., Braakman, R., Minderhoud, J. & Knill-Jones, R (1976). Predicting outcome in individual patients after severe head injury. *Lancet*, 7968:1031-1034.
- Jennett, B. & Teasdale G. (1978). Assessment of coma and severity of brain injury. *Anesthesiol.* 49: 225-226.
- Kameyoshi, Y., Dorschner A., Mallet, A.I., Christopher, E. & Schroeder, J.M. (1992). Cytokine RANTES released by thrombin-stimulated platelets is a potent attractant for human eosinophils. *J. Exp. Med.* 176:587.
- Kaul, D.K., Liu, X.D., Nagel, R.L., & Shear, H.L. (1998). Microvascular hemodynamics and *in vivo* evidence for the role of intercellular adhesion molecule-1 in the sequestration of infected red blood cells in a mouse model of lethal malaria. *Am. J. Trop. Med. Hyg.* 58:240-247.
- Kaul, D.K., Nagel, R.L., Llana, J.F. & Shear, H.L (1994). Cerebral malaria in mice: demonstration of cytoadherence of infected red blood cells and microtheologic correlates. *Am. J. Trop. Med. Hyg.* 50:512-521.

- Keane, M.P., Arenberg, D.A., Moore, B.B., Addison, C.L. & Strieter, R.M. (1998). CXCL chemokines and angiogenesis/angiostasis. *Proc.Assoc. Am. Physi.* 110: 288-296.
- Kim, M.O., Suh, H.S., Brosnan, C.F. & Lee, S.C (2004). Regulation of RANTES/CCL5 expression in human astrocytes by interleukin-1 and interferon-beta. *J.Neurochem.* 90:297-308.
- Kobayashi, F., Ishida, H., Matsui T. & Tsuji, M. (2000). Effects of *in vivo* administration of anti-IL-10 or INF- γ monoclonal antibody on the host defense mechanism against *Plasmodium yoelii yoelii* infection. *J. Vet. Med. Sci.* 62: 583-587.
- Kumar, S., Miller, L.H., Quakyi, I.A., Keister, D.B., Houghten, R.A., Maloy, W.L., Moss, B., Berzofsky, J.A. & Good, M.F. (1988). Induction of circumsporozoite protein-specific CTL by malaria sporozoites and epitope identification. *Nature.* 334: 258-260.
- Kuna, P., Alam, R., Ruta, U. & Gorski, P. (1998). RANTES induces nasal mucosal inflammation rich in eosinophils, basophils, and lymphocytes *in vivo*. *Am.J.Respir.Crit Care Med.* 157:873-879.
- Lillard, J.W., Boyaka, P.N., Singh, S. & McGhee, J.R. (2001). *Salmonella*-mediated mucosal cell-mediated immunity. *Cell Mol. Biol.* 47: 1115-1120.
- Lillard, J.W., Singh, U.P., Boyaka, P.N., Sing, S., Taub, D.D. & McGhee, J.R. (2003). MIP-1alpha and MIP-1beta differentially mediate mucosal and systemic adaptive immunity. *Blood.*101: 807-814.
- Liu, Y., Yu, Y.M. & Weng, E.Q. (1999). Upregulation of the chemokines RANTES, MCP-1, MIP-1 α , and MIP-2 in early infection with *trypanosoma brucei* and inhibition by sympathetic denervation of the spleen. *Trop. Med. Int. Health.* 4: 85-92.
- Logie, D.E., McGregor, I.A., Rowe, D.S & Billewicz, W.Z. (1973). Plasma immunoglobulin concentration in mothers and newborn children with special

- reference to placental malaria. Studies in The Gambia, Nigeria and Switzerland. *Bull. WHO.* 49:547-554.
- Lou, J., Lucas, R. & Grau, G.E. (2001). Pathogenesis of cerebral malaria: Recent experimental data and possible applications for humans. *Clin. Micro. Rev.* 14: 810-820.
- Macpherson, G., Warrel, M., White, N. (1985). Human cerebral malaria: a quantitative ultrastructure analysis of parasitized erythrocytes sequestration. *Am. J. Pathol.* 119: 385-401.
- Malik, A., Egan, J.E., Houghten, R.A., Sadoff, J.C. & Hoffman, S.L. (1991). Human cytotoxic T lymphocytes against the *Plasmodium falciparum* circumsporozoite protein. *Proc. Natl. Acad. Sci.* 88:3300-3304.
- Mannheimer, S.B., Hariprasad, J., Stoeckle, M.Y. & Murray, H.W. (1996). Induction of macrophage antiprotozoal activity by monocyte chemotactic and activating factor. *Immunol. Med. Microbiol.* 14:59-61.
- Maneerat, Y., Pongponratn, E., Viriyavejaku, P., Punpoowong, B. & Looa-reesuwan, S., Udomsangpetch. (1999). Cytokines associated with pathology in the brain tissue of fatal malaria. *Southeast Asian J. Trop. Med. Public Health.* 30:643-649.
- Maneerat, Y., Viriyavejakul, P., Punpoowong, B., Jones, M., Wilairatana, P., Pongponratn, E., Turner, G.D. & Udomsangpetch, R. (2000). Inducible nitric oxide synthase expression is increased in the brain in fatal cerebral malaria. *Histopathol.* 37:269-277.
- Mashaal, H.A. (1986). Splenomegaly in malaria. *Indian J. Malariol.* 1:1-18.
- McCutchan, T.F., de la Cruz, V.F., Good, M.F. & Wellems, T.E. (1988). Antigenic diversity in *Plasmodium falciparum*. *Prog. Allergy.* 41:173-192.

- McDermott, D.H., Beecroft, M.J., Kleeberger, C.A., Al-Sharif, F.M., Ollier, W.E., Zimmerman, P.A., Boatman, B.A., Leitman, S.F., Detels, R., Hajeer, A.H & Murphy, P.M. (2000). Chemokine RANTES promoter polymorphism affects risk of both HIV infection and disease progression in the Multicenter. *AIDS*. **17**:2671-2678.
- McGregor, I.A., Carrington, S.P. & Cohen, S. (1962). Treatment of East African *Plasmodium falciparum* malaria with West African human gammaglobulin. *Trans. R. Soc. Trop. Med. Hyg.* **56**:364-367.
- Medana, I., M., Day, N.P., Hien, T.T., Mai, N.T.H., Bethell, D., Phu, N.H., Farrar, J., Esiri, M.M., White, N.J. & Turner, G. D. (2002). Axonal injury in cerebral malaria. *Am. J. Pathol.* **160**:655-666.
- Mehta, K.S., Halankar, A.R., Makwana, P.D., Torane, P.P., Satija, P.S. & Shah, V.B. (2001) Severe acute renal failure in malaria. *J. Postgrad. Med.* **47**:24-26.
- Mogil, R.J., Patton, C.L. & Green, D.R. (1987). Cellular subsets involved in cell-mediated immunity to murine *Plasmodium yoelii* 17X malaria. *J. Immunol.* **138**: 1933-1938.
- Molyneux, M.E., Taylor, T.E., Wirima, J.J. & Borgstein, A. (1989). Clinical features and prognostic indicators in paediatric cerebral malaria: A study of 131 comatose Malawian children. *Q. J. Med.* **71**:441-459.
- Miller, L.H., Baruch, D. I., Marsh, K. & Doumbo, O. K. (2002). The pathogenic basis of malaria. *Nature*. **415**: 673-679.
- Mturi, N., Musumba, C.O., Warnola, B.M., Ogutu, B.R. & Newton, C.R. (2003). Cerebral malaria: optimising management. *C.N.S. Drugs*. **17**:153-65.
- Neil, A.L., Chanling, T. & Hunt, N.H. (1993). Comparison between microvascular changes in cerebral and non-cerebral malaria in mice, using the retinal whole-mount technique. *Parasitol.* **107**:477-487.

- Nicolas, P., Hovette, P., Merouze, F., Touze, J.E. & Martet, G. (1994). Cytokines and malaria. A study of TNF- α , IL-1 β , IL-6, IL-2R in 28 patients. *Bull. Soc. Pathol. Exot.* 87: 91-95.
- Nitcheu, J., Bonduelle, O., Combadiere, C., Tefit, M., Scilhean D., Mazier D. & Combadiere, B. (2003). Perforin-dependent brain-infiltrating cytotoxic CD8+ T lymphocytes mediate experimental cerebral malaria pathogenesis. *J. Immunol.* 170: 2221-2228.
- Nussler, A.K., Renia, L., Paschetto, V., Miltgen, F., Matile, H. & Mazier, D. (1993). *In vivo* induction of nitric oxide pathway in hepatocytes after injection with irradiated malaria sporozoites, malaria blood parasites or adjuvants. *Eur. J. Immunol.* 23:882-887.
- Ockenhouse, C.F., Magowan, C. & Chulay, J.D (1989). Activation of monocytes and platelets by monoclonal antibodies or malaria-infected erythrocytes binding to the CD36 surface receptor in vitro. *J.Clin Invest.* 84:468-475
- Pober, J.S., Cotran, R.S. (1991). Immunologic interactions of T lymphocytes with vascular endothelium. *Adv. Immunol.* 50:261-302.
- Porta, J., Carota, A., Pizzolato, G.P., Wildi, E., Widmer, M.C., Margairaz, C., Grau, G.E. (1993). Immunopathological changes in human cerebral malaria. *Clin. Neuropathol.* 12(3):142-146.
- Price, R.N., Brew, B., Sidtis, J., Rosenblum, U., Schneck, A.C. & Cleary, P. (1990). The brain in AIDS: central nervous system HIV-1 infection and AIDS dementia complex. *Science.* 939: 586-592.
- Rajakulasingham, K., Hamid Q. & O'Brien F. (1997). RANTES in human allergen-induced rhinitis: cellular source and relation to tissue eosinophilia. *Am. J. Resp. Crit. Care. Med.* 155: 696.
- Rest, J.R. (1983). Pathogenesis of cerebral malaria in golden hamsters and inbred mice. *Contrib. Microbiol. Immunol.* 7:139-147.

- Riley, E.M., Allen, S.J., Bennett, S., Thomas, P.J., O'Donnell, A., Lindsay, S.W., Good, M.F. & Greenwood, B.M. (1990). Recognition of dominant T cell stimulating epitopes from the circumsporozoite protein of *Plasmodium falciparum* and relationship to malaria morbidity in Gambian children. *Trans. R. Soc. Trop. Med. Hyg.* 84:648-657.
- Ringwald, P., Peyron, F. & Lepers, J. (1993). Parasite virulence factors during *P.falciparum* malaria: resetting, cytoadherence and modulation of cytoadherence by cytokines. *Infect. Immun.* 61: 5198-5204.
- Riva, D. & Giorgi C. (2000). The cerebellum contributes to higher functions during development: evidence from series of children surgically treated for posterior fossa tumours. *Brain.* 123:1051-1061.
- Rockett, K., Awburn, M., Rockett, E. & Clark, I. (1994). TNF and IL-1 synergy in the context of malaria pathology. *Am.J. Trop. Med. Hyg.* 50: 735-742.
- Rockett, K.A., Awburn, M.M., Aggarwal, B.B., Cowden, W.B. & Clark, I.A. (1992). *In vivo* induction of nitrite and nitrate by tumor necrosis factor, lymphotoxin and interleukin-1: possible roles in malaria. *Infect. Immun.* 60:3725-3730.
- Rogerson, S.J., Chaiyaroj, S.C., Ng K, Reeder, J.C. & Brown, G.V. (1995). Chondroitin sulfate A is a cell surface receptor for *Plasmodium falciparum*-infected erythrocytes. *J. Exp. Med.* 182:15-20.
- Roll Back Malaria. (2002). Press release, fact sheet no: 203
- Rosenberg, C. M., Scott, M. G., Gold, M. R., Hancock, R.E. & Finlay, B. B. (2000). *Salmonella typhimurium* infection and lipopolysaccharide stimulation induce similar changes in macrophage gene expression. *J. Immunol.* 164:5894-5904.
- Rossi, D. & Zlotnik A. (2000). The biology of chemokines and their receptors. *Annu. Rev. Immunol.* 18: 217-242.



- Rudin, W., Eugster, H.P., Bordmann, G., Bonato, J., Muller, M., Yamage, M. & Ryffel B. (1997). Resistance to cerebral malaria in TNF- α/β -deficient mice is associated with reduction on intercellular adhesion molecule-1 up regulation and T helper type 1 response. *Am. J. Pathol.* **150**: 257-266.
- Sachs, J. & Malaney, P. (2002). The economic and social burden of malaria. *Nature*. **415**: 680-685.
- Sano, H., Nakagawa, N., Chiba, R., Kurasawa, K., Saito, Y. & Iwamoto I. (1998). Cross-linking of intercellular adhesion molecule-1 induces interleukin-8 and RANTES production through the activation of MAP kinases in human vascular endothelial cells. *Biochem. Biophys. Res. Commun.* **29**:694-698.
- Saroj, K.M., Shradhanand, M., Sanjib, M., Patel, N.C. & Mohapatra, D.N. (2002). Acute renal failure in *falciparum* malaria. *J. Ind. Aca. Clin. Med.* **3**: 141-147.
- Schmahmann, J.D. (1992). An emerging concept. The cerebellar contribution to higher function. *Arch. Neurol.* **49**:1229-12230.
- Schuh, J.M., Blease, K. & Hogaboam, C.M. (2002). The role of CC chemokine receptor 5 (CCR5) and RANTES/CCL5 during chronic fungal asthma in mice. *Fed. American Soc. Exp. Biol. J.* **16**:228-2230.
- Sein, K.K., Maeno, Y., Thuc, H.V., Anh, T.K. & Aikawa, M. (1993). Differential sequestration of parasitized erythrocytes in the cerebrum and cerebellum in human cerebral malaria. *Am. J. Trop. Med. Hyg.* **48**: 504-511.
- Shiao, M.F., Lin, P.R., Liu, J.Y. & Yang, K.D. (1995). Generation of interleukin-8 from human monocytes in response to *Trichomonas vaginalis* stimulation. *Infect. Immun.* **63**: 2379-2382.
- Sharafeldin, A., Eltayeb, R., Pashenkov, M., Bakhiet, M. (2000). Chemokines are produced in the brain early during the course of experimental African trypanosomiasis. *J. Neuroimmunol.* **103**:167-170.
- Shear H.L., Marino, M.W., Wanidworanun, C., Berman, J.W. & Nagel, R.L. (1998).

- Correlation of increased expression of intercellular adhesion molecule-1, but not high levels of tumor necrosis factor-alpha, with lethality of *Plasmodium yoelii* 17X, a rodent model of cerebral malaria. *Am. J. Trop. Med. Hyg.* 59:852-858.
- Shrestha, B., Gottlieb, D. & Diamond, M.S. (2003). Infection and injury of neurons by West Nile encephalitis virus. *J. Virol.* 77:13203-13213.
- Silamat, K., Phu, N.H., Whitty, Turner, G.D., Louwrier, K., Mai, N.T., Simpson, J.A., Hien, T.T. & White, N.J. (1999) Quantitative analysis of the microvascular sequestration of malaria parasites in the human brain. *Am. J. Pathol.* 155:395-410.
- Smith, C.D., Brown, A.E., Nakazawa, S., Fujioka, H. & Aikawa, M. (1996) Multi-organ erythrocyte sequestration and ligand expression in rhesus monkeys infected with *Plasmodium coatneyi* malaria. *Am. J. Trop. Med. Hyg.* 55:379-383.
- Smythe, J.A., Peterson, G.M., Coppel, R., Saul, A.J., Kemp, D.J. & Anders, R. (1990) Structural diversity in the 45-kilodalton merozoite surface antigen of *Plasmodium falciparum*. *Mol. Biochem. Parasitol.* 39:227-234.
- Stiles, J.K., Meade, J.C., Kucerova, Z.D., Thompson, W., Zakeri Z. & Whittaker, J. (2001). *Trypanosoma brucei* infection induces apoptosis and up-regulates neuroleukin expression in the cerebellum. *Ann. Trop. Med. & Parasitol.* 95: 797-810.
- Stoelcker, B., Hehlgans, T., Weigl, K., Bluethmann, H., Grau, G.E. & Mannel, D.N. (2002). Requirement for tumor necrosis factor receptor 2 expression on vascular cells to induce experimental cerebral malaria. *Infect. Immun.* 70:5857-5859.
- Su, Z. & Stevenson, M.M. (2002). IL-12 is required for antibody-mediated protective immunity against blood-stage *Plasmodium chabaudi* AS malaria infection in mice. *J. Immunol.* 1:1348-1355.
- Suguitan, A.L., Leke, R.G., Fouda, G., Zhou, A., Thuita, L., Metenou, S., Fogako, J., Megnekou, R. & Taylor, D.W. (2003). Changes in the levels of chemokines and cytokines in the placentas of women with *Plasmodium falciparum* malaria. *J. Infect. Dis.* 188:1074-1082.

- Sun, G., Chang, W.L., Li, J., Berney, S.M., Kimpel, D. & VanDder, H.C. (2003). Inhibition of platelet adherence to brain microvasculature protects against severe *Plasmodium berghei* malaria. *Infect. Immun.* 71:6553-6561.
- Tatke, M. & Bazaz-Malik, G. (1989). Brain histomorphology in protein deprived rhesus monkeys with fatal malarial infection. *Indian J Med Res.* 89:404-410.
- Taverne, J., Bate, C.A., Kwiatkowski, D., Jakobsen, P.H. & Playfair, J.H. (1990). Two soluble antigens of *Plasmodium falciparum* induced tumor necrosis factor release from macrophages. *Infect. Immun.* 58:2923-2928.
- Tkachuk, A.N., Moormann, A.M., Poore, J.D., Rochford, R.A., Chensue, S.W., Mwapasa, V. & Meshnick, S.R. (2001). Malaria enhances expression of CC chemokine receptor 5 on placental macrophages. *J.Infect. Dis.* 183: 967-972.
- Tran, R.S., Kara, A.U., Feng, C., Asano, Y. & Sinniah, R. (2000). Differential IL-10 expression in interferon regulatory factor-1 deficient mice during *Plasmodium berghei* blood-stage infection. *Parasite Immunol.* 22: 425-435.
- Tripp, C.S., Wolf, S.F. & Unanue, U.R. (1993). Interleukin 12 and tumor necrosis factor alpha are costimulators of interferon gamma production by natural killer cells in severe combined immunodeficiency mice with listeriosis, and interleukin 10 is a physiologic antagonist. *Proc. Natl. Acad. Sci.* 90: 3725.
- Torre, D., Speranza, F., Giola, M., Matteelli, A., Tambini, R. & Biondi (2002). Role of Th1 and Th2 cytokines in immune response to uncomplicated *Plasmodium falciparum* malaria. *Clin. Diagn. Lab. Immunol.* 9:348-351.
- Turner, G. (1997) Cerebral Malaria. *Brain Pathol.* 7:569-582.
- Turner, G.D., Morrison, H., Jones, M., Davis, T.M., Looareesuwan, S., Buley, I.D., Gatter, K.C., Newbold, C.I., Pukritayakamee, S. & Nagachinta, B. (1994). An immunohistochemical study of the pathology of fatal malaria. Evidence for widespread endothelial activation and a potential role for intercellular adhesion molecule-1 in cerebral sequestration. *Am. J. Pathol.* 145: 1057-1069.

- Udomsangpetch, R., Reinhardt, P.H., Schollaardt, T., Elliott, J.F., Kubes, P. & Ho, M. (1997). Promiscuity of clinical *Plasmodium falciparum* isolates for multiple adhesion molecules under flow conditions. *J. Immunol.* **158**:4358-4364.
- Villalta, F., Zhang, Y., Bibb, K.E., Kappes, J.C., Lima, M.F. (1998). The cysteine-cysteine family of chemokines RANTES, MIP-1 α and MIP-1 β induce trypanocidal activity in human macrophages via nitric oxide. *Infect.Immun.* **66**: 4690-4695.
- Waki, S., Uehara, S., Kanbe, K., Ono, K., Suzuki, M. & Nariuchi, H (1992). The role of T cells in pathogenesis and protective immunity to murine malaria. *Immunol.* **75**:646-651.
- Wassmer, S.C, Coltel, N., Combes, V. & Grau, G.E. (2003). Pathogenesis of cerebral malaria: facts and hypotheses. *Med.Trop* **63**:254-257.
- Wilhelmsson, U., Li, L., Pekna, M., Berthold, C.H., Blom, S., Eliasson, C., Renner, O., Bushong, E., Ellisman, M., Morgan, T.E. & Pekny, M. (2004). Absence of glial fibrillary acidic protein and vimentin prevents hypertrophy of astrocytic processes and improves post-traumatic regeneration. *J.Neurosci.* **24**:5016-5021.
- World Health Organization. (1996). World Health Organization revised facts on malaria. International (global). *Vacc.Weekly*: 11-13.
- World Health Organization. (2000). Severe *falciparum* malaria. *Trans. Royal. Soc. Trop. Med. & Hyg.* **94**:S1-S90.
- www.dpd.cdc.gov/.../M-R/Malaria/body_Malaria_page1.htm
- www.expertreviews.org
- www.who.int/inf-fs/en/informatioSheet10.pdf

- Xiao, L., Owen, S.M., Rudolph, D.L., Lal, R.B. & Lal, A.A. (1998). *Plasmodium falciparum* antigen-induced human immunodeficiency virus type 1 replication is mediated through induction of tumor necrosis factor- α . *J. Infect. Dis.* 177:437-445.
- Yanez, D.M., Manning, D.D., Cooley, A.J., Weidanz, W.P. & Heyde, H.C. (1996). Participation of lymphocytes subpopulations in the pathogenesis of experimental murine cerebral malaria. *J. Immunol.* 157: 1620-1724.
- Yu, Y., & Chadee, K. (1997). *Entamoeba histolytica* stimulates interleukin 8 from human colonic epithelial cells without parasite-enterocyte contact. *Gastroenterol.* 112: 1536-1547.
- Zang, Y.C., Halder, J.B., Samanta, A.K., Hong, J., Rivera, V.M. & Zhang, J.Z. (2001). Regulation of chemokine receptor CCR5 and production of RANTES and MIP-1 α by interferon- β . *J. Neuroimmunol.* 112:174-180.
- Zhong, S. & Stevenson, M.M. (2002). IL-12 is required for antibody-mediated protective immunity against blood-stage *Plasmodium chabaudi* AS malaria infection in mice. *J. Immunol.* 168. 1348-1355.

APPENDICES

- I Publication **Sarfo BY**, Singh S, Lillard JW, Gyasi RK, Armah H, Adjei AA, Jolly P and Stiles JK (2005). *Plasmodium yoelii* upregulates RANTES, CCR1, CCR3 and CCR5 expression and induces ultrastructural changes in the cerebellum. *Malaria Journal*, 4:63.
- II Publication **Sarfo BY**, Singh S, Lillard JW, Quarshie A, Gyasi RK, Armah H, Adjei AA, Jolly P & Stiles JK (2004) The cerebral-malaria-associated expression of RANTES, CCR3 and CCR5 in post-mortem tissue samples. *Ann Trop Med Parasitol*. 98:297-303
- III Publication Stiles JK, Whittaker J, **Sarfo BY**, Thompson WE, Powell MD & Bond VC (2004) Trypanosome apoptotic factor mediates apoptosis in human brain vascular endothelial cells. *Mol Biochem Parasitol*. 133:229-240.
- IV Publication Stiles JK, Kucerova Z, **Sarfo B**, Meade CA, Thompson W, Shah P, Xue L & Meade JC (2003) Identification of surface-membrane P-type ATPases resembling fungal K (+)- and Na(+)-ATPases, in *Trypanosoma brucei*, *Trypanosoma cruzi* and *Leishmania donovani*. *Ann Trop Med Parasitol*. 97:351-366.
- V Publication Jacqueline M. Hibbert, Lewis L. Hsu, Sam Bhatena, Irune I, **Sarfo B**, Melissa Creary, Beatrice E. Gee, Ali I. Mohamed, Iris Buchanan and Jonathan K. Stiles, (2005). Metabolic stress and proinflammatory cytokines in children with sickle cell anemia. *Exp Biol Med* 230:68-74

VI Procedure for designing a primer

The following steps describe the design of primers

1. Enter www.ncbi.com website
2. Draw and enter nucleotide window
3. Enter the name of the gene
4. Select the CDS (coding sequence)
5. Highlight and copy the sequence
6. Minimise the window
7. Open the website www.genome.wi.mit.edu/cgi-bin/primer/primer3.cgi
8. Paste the copied sequence in the opened window
9. Select general primer picking conditions
10. Select product size
11. Click primers button
12. Copy and paste primer sequence
13. Open NCBI site and click BLAST
14. Select nucleotide-nucleotide BLAST
15. Paste copied primer sequence in the BLAST
16. Click BLAST
17. Compare E-values of results and select the best primer pair (The lower the E-value the better the primer).

VII **Table 3: Mouse and human primer sequence with corresponding annealing temperatures**

Mouse Gene	GenBank accession number	Sequence (forward)	Sequence (reverse)	Anne Temp (°C)
PECAM	L06039	TGCTCTCGAAGCCCAGTATT	ATGGGTGCAGTTCATTTTC	56
MIP-2 α	NM009140	GCCAAGGGTTGACTTCAAGA	GCCCTTGAGAGTGGCTATGA	54
ICAM-1	BE630415	AAACCAAGTCCAGTCCACAT	AAAGATCACATGGGTGAGG	58
VCAM	NM011693	TGGAGGAAATG GCATAAAG	ACCTAGCGAGGCAACAAGA	55
RANTES	AF252285	GGAAATCTTCGCACTCAAG	GAGCGTGCGAACTTCTGT	58
INF- γ	K00083	ACTGGCAAAAGGATGGTGAC	GCTGATGGCCTGATTGTCTT	59
TNF- α	NM013693	CCAGTGTGGGAAGCTGTCTT	AAGCAAAAGAGGAGGCAACA	55
IL-12	M86671	GCAACGTTGGAAAGGAAAGA	AAAGCCAACCAAGCAGAAGA	50
CCR1	NM009912	CCACTCCATGCCAAAAGACT	ATTAGGACATTGCCACCAC	53
CCR3	NM009914	TATCATTACCTGGGGCCTTG	CGAGGACTGCAGGAAAACCTC	52
CCR5	D83648	CGAAAACACATGGTCAAACG	GTTCTCTGTGGATCGGGTA	55
INOS	AF427516	AATCTTGGAGCGAGTTGTGG	GCAGCCTCTGTCTTTGACC	51
GAPDH	NM_008084	CACAATTTCCATCCCAGACC	GTGGGTGCAGGCAACTTTAT	55

Human Gene	GenBank accession number	Sequence (forward)	Sequence (reverse)	Anne Temp (°C)
RANTES	NM_002985	GAGGCTTCCCCTCACTATCC	TCAAGTGATCCACCCACCTT	59
CCR1	BC064991	GGCTGTGCACCTGGTAAAT	GTTGGCCTCCTATGGTCTGA	55
CCR3	NM_001837	TTTGGTGTATCACCAGCAT	GCAGAGGGAGAAACGAGACAG	54
CCR5	BC038398	GGCAAAGACAGAAGCCTCAC	CTAGCCTTGTCTTCTCTCCC	56
GAPDH	BC014085	GAGTCAACGGATTTGGTCGT	TTGATTTTGGAGGGATCTCG	57

VIII cDNA microarray table showing complete list of induced immunomodulator gene expression in the brain during *P.yoelii* 17X infection

GENE	FOLD CHANGE EXPRESSION	DESCRIPTION OF GENE
PECAM-1	23.0	Platelet Endothelia Cell Adhesion Molecule-1
MIP-2 α	18.0	Macrophage Inflammatory Protein-2 alpha
ICAM-1	13.0	Intercellular Adhesion Molecule-1
IRF2	12.0	Interferon regulatory factor-2
MCP-1	7.0	Monocyte Chemoattractant Protein-1
VCAM-1	6.0	Vascular Cell Adhesion Molecule-1
RANTES	6.0	Regulated upon Activation Normal T cell Expressed and Secreted
INF- γ	6.0	Interferon-gamma
TGF- β	6.0	Transforming growth factor beta
GLYCAM-1	6.0	Endothelial ligand for L-selectin
TNF- α	5.0	Tumor Necrosis Factor-alpha
IL-12	4.0	Interleukin-12
CCR1	4.0	C-C chemokine receptor 1
CCR3	4.0	C-C chemokine receptor 3
CCR5	4.0	C-C chemokine receptor 5
INOS	4.0	Inducible Nitric Oxide Synthase
IL-3R	3.0	Interleukin-3 receptor
Int-6	3.0	Integrin alpha 6
IL-1 β	2.0	Interleukin-1 beta precursor
ZO-1	2.0	Zonula Occludin -1
VEGF	2.0	Vascular endothelial growth factor precursor
IL-4	1.8	Interleukin-4
IL-11	1.5	Interlukin 11
IL-7	1.5	Interleukin 7 precursor
IL-6R	1.5	Interleukin 6 receptor
CD40L	1.5	Cluster of differentiation 40 ligand
PGP1	1.5	Phagocytic glycoprotein 1
IL-1R	1.5	Interleukin-1 receptor
INF- γ R	1.5	Interferon gamma receptor
IL-10	1.0	Interleukin 10
CD27LR	1.0	Cluster of differentiation 27 ligand receptor
CD30LR	1.0	Cluster of differentiation 30 ligand receptor
CDK5	1.0	Cyclin dependent kinase 5
GAPDH	0.0	GlycerAldehyde-3-Phosphate Dehydrogenase
IL-15	0.9	Interlukin 15
ICE	0.7	Interleukin converting enzyme
EGF	0.6	Epidermal growth factor

IGFRII	0.6	Insulin growth factor receptor II
IL-5R	0.5	Interleukin-5 receptor
GADD45	0.4	Growth arrest and DNA-damage-protein 45
VEGFTKR	0.1	Vascular endothelial growth factor tyrosine kinase receptor
IRF1	0.1	Interferon regulatory factor 1

Table 3: Plasmodium yoelii 17X infection alters immunomodulator gene expression in mouse brain at peak parasitemia (day 8 post-infection). cDNA microarray analysis of P.yoelii 17X infected and uninfected mouse brain. Gene listed were altered at peak parasitemia. Fold change in expression is defined as GAPDH normalized mRNA expression ratio of gene signals of infected to uninfected mouse brain.

IX Spectrophotometric analysis of total RNA samples

1. Add 5µl of RNA sample to 995µl of RNase-free water
2. Measure spectrophotometer absorbance at 260nm and 280nm
3. Absorbance in 260 multiply by 10 is the amount of RNA in µg/µl
4. Ratio of 260/280 absorbance gives the purity of the RNA sample
5. Pure RNA has a ratio of > 1.5

X Preparation, loading and running of 1% formaldehyde RNA agarose gel

1. Use RNaseZAP (Ambion Inc. TX) to remove any contaminating RNase from gel tank/comb and conical flask
2. Add 1g of agarose powder into 10ml of MOPS (3-[N-Morpholino] PropaneSulfonic acid) (Ambion Inc. Tx,) in 90 ml of RNase-free water
3. Microwave the agarose solution
4. Cool agarose solution to 50 °C
5. Cast 50ml of agarose solution in a hood and allow gel to solidify at room temperature
6. Prepare 1X running buffer with 50ml of MOPS in 450ml of RNase-free water
7. After removing comb, pour running buffer to a depth of 0.5-10cm
8. Prepare 5µg/µl of RNA sample in 15µl formaldehyde dye containing 2µl of 10mg/ml ethidium bromide stain
9. Electrophorese at 100volts until the formaldehyde dye has migrated to within 2 mm of the anode
10. Remove the gel from the electrophoresis unit and observe bands under UV-transilluminator

XI Preparation, loading and running of 2% DNA agarose gel

1. Weigh 2g of agarose powder and place it in a 100ml of 1X Tris-Acetate EDTA (TAE) buffer
2. Swirl to mix the solution
3. Heat the flask in a microwave until the solution is completely clear (2-3 minutes). Do not allow the agarose to boil over
4. Cool the solution to 55°C
5. Add 5 μ l of 10mg/ml ethidium bromide stain
6. Place a plastic comb in the slots on the side of the casting tray
7. Pour the agarose solution into the gel tray until the comb teeth are immersed about $\frac{1}{4}$ into the agarose
8. Allow the agarose gel to cool until solidified
9. Remove the comb from the wells
10. Pour 1X TAE buffer to cover the gel
11. Add 2 μ l of 10X loading dye (7.58 Ficoll 400 + 0.125 Bromophenol blue in 50ml deionized water) to 10 μ l of PCR sample and load into separate wells
12. Load 10 μ l of DNA size marker
13. Electrophorese at 100volts until the bromophenol blue has migrated to within 2 mm of the anode
14. Remove the gel from the electrophoresis unit and observe bands under UV-transilluminator

This Provisional PDF corresponds to the article as it appeared upon acceptance. The fully-formatted version will become available shortly after the date of publication, from the URL listed below.

Plasmodium yoelii 17XL infection up-regulates RANTES, CCR1, CCR3 and CCR5 expression, and induces ultrastructural changes in the cerebellum

Malaria Journal 2005, 4:63 doi:10.1186/1475-2875-4-63

Brismark Y Sarfo (BSarfo@noguchi.mimcom.net)

Henry B Armah (harmah@msm.edu)

Ikowwaiza Irune (irune@msm.edu)

Andrew A Adjei (andrewadjei50@hotmail.com)

Christine S Olver (christine_olver@colostate.edu)

Shailesh Singh (ssingh@msm.edu)

James W Lillard Jr (lillard@msm.edu)

Jonathan K Stiles (jstiles@msm.edu)

ISSN 1475-2875

Article type Research

Submission date 23 Aug 2005

Acceptance date 16 Dec 2005

Publication date 16 Dec 2005

Article URL <http://www.malariajournal.com/content/4/1/63>

This peer-reviewed article was published immediately upon acceptance. It can be downloaded, printed and distributed freely for any purposes (see copyright notice below).

Articles in *Malaria Journal* are listed in PubMed and archived at PubMed Central.

For information about publishing your research in *Malaria Journal* or any BioMed Central journal, go to

<http://www.malariajournal.com/info/instructions/>

For information about other BioMed Central publications go to

***Plasmodium yoelii* 17XL infection up-regulates RANTES, CCRI, CCR3 and CCR5
expression, and induces ultrastructural changes in the cerebellum**

Bismark Y. Sarfo¹, Henry B. Armah^{2,3}, Ikovwaiza Irune², Andrew A. Adjei¹,

Christine S. Olver⁴, Shailesh Singh², James W. Lillard, Jr², Jonathan K. Stiles^{2*}

¹Parasitology Unit, Noguchi Memorial Institute for Medical Research, University of Ghana, P.O. Box LG581, Legon, Accra, Ghana.

²Department of Microbiology, Biochemistry and Immunology, Morehouse School of Medicine, 720 Westview Drive S. W., Atlanta, GA, 30310-1495, USA.

³Department of Pathology, University of Ghana Medical School & Korle-Bu Teaching Hospital, P.O. Box 4236, Accra, Ghana.

⁴Department of Pathology, Colorado State University, Fort Collins, CO, 80523, USA.

*Corresponding author

Email addresses:

BYS: bsarfo@noguchi.mimcom.net

HA: harmah@msm.edu

II: ikovwa6@yahoo.com

AAA: andrewadjei50@hotmail.com

CSO: christine.olver@colostate.edu

SS: ssingh@msm.edu

JWL: jjillard@msm.edu

JKS: jstiles@msm.edu

Abstract

Background

Malaria afflicts 300-500 million people causing over 1 million deaths globally per year. The immunopathogenesis of malaria is mediated partly by complex cellular and immunomodulator interactions involving co-regulators such as cytokines and adhesion molecules. However, the role of chemokines and their receptors in malaria immunopathology remains unclear. RANTES (Regulated on Activation Normal T-Cell Expressed and Secreted) is a chemokine involved in the generation of inflammatory infiltrates. Recent studies indicate that the degradation of cell-cell junctions, blood-brain barrier dysfunction, recruitment of leukocytes and *Plasmodium*-infected erythrocytes into and occlusion of microvessels relevant to malaria pathogenesis are associated with RANTES expression. Additionally, activated lymphocytes, platelets and endothelial cells release large quantities of RANTES, thus suggesting a unique role for RANTES in the generation and maintenance of the malaria-induced inflammatory response. The hypothesis of this study is that RANTES and its corresponding receptors (CCR1, CCR3 and CCR5) modulate malaria immunopathogenesis. A murine malaria model was utilized to evaluate the role of this chemokine and its receptors in malaria.

Methods

The alterations in immunomodulator gene expression in brains of *Plasmodium yoelii* 17XL-infected mice was analysed using cDNA microarray screening, followed by a temporal comparison of mRNA and protein expression of RANTES and its corresponding receptors by qRT-PCR and Western blot analysis, respectively. Plasma RANTES levels was determined by ELISA and ultrastructural studies of brain sections from infected and uninfected mice was

conducted

Results

RANTES ($p < 0.002$), CCR1 ($p < 0.036$), CCR3 ($p < 0.033$), and CCR5 ($p < 0.026$) mRNA were significantly upregulated at peak parasitaemia and remained high thereafter in the experimental mouse model. RANTES protein in the brain of infected mice was upregulated ($p < 0.034$) compared with controls. RANTES plasma levels were significantly upregulated; two to three fold in infected mice compared with controls ($p < 0.026$). Some distal microvascular endothelium in infected cerebellum appeared degraded, but remained intact in controls.

Conclusions

The upregulation of RANTES, CCR1, CCR3, and CCR5 mRNA, and RANTES protein mediate inflammation and cellular degradation in the cerebellum during *P. yoelii* 17XL malaria.



Background

Malaria afflicts between 300-500 million people causing up to 2 million deaths globally per year [1]. Cerebral malaria (CM), characterized by seizures and loss of consciousness, is the most severe complication of *Plasmodium falciparum* infection with mortality rates ranging from 15 to 20% [2, 3]. Malaria-induced brain inflammation is known to be mediated partly by complex cellular and immunomodulator interactions, involving co-regulators such as cytokines and adhesion molecules, resulting in the sequestration of parasite-infected erythrocytes in the brain in human CM. Apart from the sequestration of *P. falciparum*-infected erythrocytes, recent studies [4-7] have revealed significant accumulation of platelets and leukocytes in the distal microvasculature of the brains of human cases of CM, suggesting a role for platelet and leukocyte sequestration in human CM pathology. However, the role of chemokines and chemokine receptors in malaria brain immunopathogenesis still remain unclear. Recently, the up-regulated expression of RANTES and its receptors (CCR3 and CCR5) in the cerebellar and cerebral regions of post-mortem human CM brains has been reported [8]. Additionally, others [9, 10] have reported increased migration of CCR5⁺ leukocytes into the brain in experimental murine CM models. These studies support the hypothesis that leukocyte recruitment by chemokines may play a role in the pathogenesis of human CM. Indeed, malaria has become one of the many inflammatory diseases in which RANTES and its receptors appear to play a role. RANTES, a chemokine involved in the generation of inflammatory infiltrates, plays a special role in the maintenance and prolongation of the inflammatory response. The trafficking of inflammatory Th1 cells into the brain is mediated partly by RANTES interactions with CCR5. RANTES binds to a variety of receptors including CCR1, CCR3 and CCR5, expressed by monocytes/macrophages, memory T-cells, eosinophils, endothelial cells, basophils and mast cells [11]. A comparative study using *Plasmodium berghei* ANKA infected C57BL/6 and BALB/c

mice indicated that at both strains of mice expressed CXCL10 (interferon-induced protein 10, IP-10) and CCL2 (monocyte chemoattractant protein-1, MCP-1) chemokine genes as early as 24 hours post-infection [12]. Moreover, the expression of IP-10 and MCP-1 genes in KT5, an astrocyte cell line, was induced *in vitro* upon stimulation with a crude antigen of malaria parasites [12]. Other more recent studies, using malaria animal models, showed that experimental cerebral malaria (ECM) was induced in perforin-deficient mice (PF⁰) after adoptive transfer of cytotoxic CD8⁺ T cells from infected C57BL/6 mice, which were directed to the brains of PF⁰ mice. This specific recruitment involved chemokines and their receptors, and indicated that lymphocyte cytotoxicity and trafficking are key players in ECM [10]. While CCR2 was not observed to be essential for the development of ECM [13], CCR5 deficiency in mice reportedly decreased susceptibility to ECM [9]. These studies, together, support the hypothesis that leukocyte recruitment by chemokine and chemokine receptor interactions play a role in the pathogenesis of malaria in these animal models. It seems that plasmodial infection has a significant impact on brain endothelial and parenchymal cells and, thus, provides a new dimension to our understanding of the role of systemic and localized (brain) chemokine expression in CM immunopathogenesis. The cytoadherence of infected red blood cells (IRBCs) to the postcapillary venules is the major cause of IRBC sequestration and vessel blockage in the cerebral form of human malaria. In both human cerebral malaria caused by *P. falciparum* and the *Plasmodium yoelii* 17XL-infected rodent model of malaria, the sequestration of IRBCs in the brain vessels is secondary to the cytoadherence of IRBCs to the postcapillary venules [14]. In this study, we analysed the alterations in immunomodulator gene expression in brain samples of *P. yoelii* 17XL-infected mice using cDNA microarray screening, coupled with analysis of temporal expression patterns of RANTES and its corresponding receptors, CCR1, CCR3 and CCR5, in brain samples and plasma of *P. yoelii* 17XL-infected mice to identify and characterize the role of these immunomodulators during rodent malaria.

Methods

Murine model of *P. yoelii* 17XL malaria and preparation of brain samples

All animal-related experiments were conducted according to the principles set forth in the *National Institutes of Health Guide for the Care and Use of Laboratory Animals* and approved by the Institutional Animal Care and Use Committee (IACUC) of Morehouse School of Medicine. Female Swiss Webster (SW) mice (6-8 weeks) obtained from Jackson Laboratory (Bar Harbour, Maine, USA) were maintained on a 12hr light/dark cycle with access to food and water *ad libitum*, in accordance with IACUC regulations of the Association for Assessment and Accreditation of Laboratory Animal Care (AAALAC). Humane methods were used to sedate mice prior to intra-peritoneal injection and tail-snipping. Briefly, the inhaled anesthetic (0.1-0.2 ml isoflurane or halothane per liter of induction chamber volume to give a gas concentration of 2-4%, required to induce anesthesia) were administered to the female SW mice. The induction process was visualized through the anesthetic chamber and the abolition of the toe-pinch pain reflex assessed by applying pressure to indicate the successful induction of anesthesia. Mice were injected intraperitoneally with *P. yoelii* 17XL parasitized blood, kindly provided by Dr. Christine Oliver (Department of Pathology, Colorado State University, USA). This rodent malaria strain causes a syndrome that resembles human malaria, characterized by fever, spleno- and hepatomegaly by day eight post-infection [14, 15]. Parasitaemia was determined in a total count of 300 to 500 red blood cells (RBCs) on Wright-Giemsa-stained (Sigma Diagnostics, USA) thin blood smears. Euthanasia was conducted by the inhalation of CO₂ or cervical dislocation, and groups of fifteen infected and uninfected mice were sacrificed after day two, four, six and eight post-infection. For each time point, five brains from infected mice were stored in RNA later (Ambion™ Inc. USA) at -80 °C for RNA isolation, five brains were stored in Lysis Buffer at

80 °C for protein analysis, and 5 were cryoprotected in 4% paraformaldehyde at 4 °C for light and transmission electron microscopy. Similarly, brains from uninfected mice were stored for RNA isolation, protein analysis, and light and transmission electron microscopy.

RNA isolation

Messenger RNA (mRNA) was isolated from brain samples using TRIzol Reagent (Life Technologies Inc., Rockville, MD., USA) according to the manufacturer's protocol. Genomic DNA contamination was removed from these samples by treatment with RNase-free DNase (Invitrogen, San Diego, CA, USA) for 15 minutes at 37 °C. RNA was then precipitated and re-suspended in diethylpyrocarbonated (DEPC)-treated water.

cDNA microarray screening

Five micrograms (5µg) of DNA-free RNA from day 8 post-infected (peak parasitaemia) mouse brain was reverse transcribed, in the presence of 100 µCi of [α -³²P] dATP, for microarray analysis. The commercial system used to investigate cDNA microarray gene expression (AtlasTM 1.0; CLONTECH, Palo Alto, CA., USA) consists of two identical nylon membranes, spotted with 588 different mouse genes grouped in functional blocks, including immunomodulators, neurotrophins, neurotransmitters and pro- and anti-apoptosis genes. A complete list of the cDNA samples and controls on each array, as well as their corresponding GenBank accession numbers, may be found at CLONTECH's Atlas web site (www.atlas.clontech.com). Briefly, [α -³²P] dATP-labelled cDNA synthesized from the 5µg DNA-free RNA by reverse transcription was column purified and hybridized, at high stringency, to a mouse cDNA array overnight at 70°C. Membranes were washed at high stringency and exposed to X-ray film at -80°C overnight, as recommended by the manufacturers. Message expression was analysed using the AtlasTM Image 1.0 software (CLONTECH, Palo Alto, CA., USA) and the data expressed as the ratios of the relative

changes in the mRNA levels in the infected brain samples and uninfected controls. Expression of mRNA populations (from infected and uninfected mice) at day 8 post-infection were compared and analysed by autoradiography and quantified by CLONTECH gene analysis software. An approximate estimate of the abundance level of a target cDNA in an RNA population can be made by comparing its signal to the signals obtained with housekeeping genes of known abundance (e.g. GAPDH).

RT-PCR validation of immunomodulator mRNA expression

Genes encoding induced RANTES, CCR1, CCR3 and CCR5 were selectively confirmed by semi-quantitative RT-PCR. Mouse mRNA sequences of RANTES, CCR1, CCR3, CCR5 and glyceraldehyde-3-phosphate dehydrogenase (GAPDH) were obtained from the National Institute of Health -National Center for Biotechnology Information (NIH-NCBI) GeneBank database accession numbers [AF_252285], [NM_009912], [NM_009914], [D_83648] and [NM_008084] respectively. These sequences were then used to design primers for RT-PCR analysis, which generated amplicons of 97, 103, 96, 100, and 95 base pairs in sizes for RANTES, CCR1, CCR3, CCR5 and GAPDH mRNA respectively. Primers were designed using the primer 3 software program from the Whitehead Institute at the Massachusetts Institute of Technology (MIT; Boston, MA., USA). Thermodynamic analysis of the primers was conducted using computer programs: Primer Premier TM (Integrated DNA Technologies, Coralville, Iowa, USA), and M11 Primer III (Boston, MA., USA). The resulting primer sets were compared against the entire mouse genome using NCBI to confirm specificity and ensure that the primers flanked mRNA splicing regions. Complementary DNA (cDNA) was generated (Maxim Biotech Inc., CA., USA), and amplified with specific primers using *Taq* polymerase and polymerase chain reaction (PCR) reagents (Qiagen Inc. Valencia, CA., USA). The levels of band intensities of mRNA of these targets relative to GAPDH were evaluated by PCR analysis using thermocycler (Perkin-Elmer,

Norwalk, Conn., USA). Conditions for DNA amplifications were set as follows: heating at 94°C for five minutes, followed by 25 cycles of DNA denaturation at 94°C for one minute, an annealing step at X°C (see Table 1 for respective temperature values for each primer) for one minute, strand extension at 72°C for one minute and a final extension step at 72°C for 10 minutes. The number of cycles required to attain products in the linear range of the PCR was determined before the final assay was run. Working within this range, it was possible to determine expression differences after 25-30 cycles. PCR products were analysed on 2% agarose/ethidium-bromide gels and quantified using Gelexpert software (NucleoTech, San Mateo, CA, USA). Band intensities in each experiment were normalized to the mean intensity of GAPDH. Data were expressed as the relative change in mRNA level in infected and uninfected controls.

Western blot analysis of RANTES

Western blot analysis was used to confirm RANTES protein expression in mouse brain during *P. yoelii* 17XL infection. Infected and uninfected mice brains were lysed and their total protein determined by standard methods using a commercial kit (BioRad, Hercules, CA, USA). Twenty five micrograms (25µg) of total protein from mouse brain was subjected to 15% SDS-PAGE, and blotted onto nitrocellulose membranes. Membranes were then probed with 1:1000 biotinylated anti-mouse recombinant RANTES (R&D Systems, Inc. MN, USA) and 1:2000 anti-mouse alpha-tubulin (Sigma-Aldrich, MO, USA) antibody. Membranes probed with biotinylated anti-mouse recombinant RANTES were incubated with streptavidin-horseradish peroxidase (HRP) secondary antibody while those probed with alpha-tubulin were incubated with anti-mouse IgG secondary antibody at the same conditions. The methods used for pre-incubation, incubation and detection by chemiluminescence have already been described [16]. Bands of protein corresponding to RANTES (7.8 kDa) and alpha-tubulin (55kDa) were quantified using Versa Doc Imaging

System (BioRad, CA, USA). RANTES protein expression was normalized to that of albumin

ELISA determination of plasma RANTES levels

To determine whether RANTES and its receptor interactions were localized (brain) or systemic (peripheral blood), plasma RANTES levels were determined in *P. yoelii* 17XL-infected and control mice, using RANTES specific ELISA (Biosource International, Camarillo, CA, USA) according to the manufacturer's specifications. Since RANTES may be released by platelets during venum collection, heparinized blood was collected, centrifuged at 13,000rpm for 10 minutes to obtain plasma samples, and subsequently stored at -20°C until used. Briefly, duplicates of standard controls, and samples were aliquoted into RANTES-coated microtiter wells. Biotin-conjugated antibody was added to the wells and incubated at room temperature for 2 hours. Streptavidin-horseradish peroxidase (Streptavidin-HRP) was then added to each well and incubated at room temperature for 30 min. The plates were developed with stabilized chromogen in the dark at room temperature. The reaction was stopped and optical densities of samples were read at 450nm.

Histopathologic analysis of *P. yoelii* 17XL infected mouse brain

Whole brains of infected and uninfected mice at peak parasitaemia were examined by light microscopy to evaluate erythrocytic and leucocytic sequestration in brain microvasculature.

Whole mouse brains fixed in 4% paraformaldehyde were processed for routine histology, with haematoxylin and eosin staining. Sections of these paraformaldehyde-fixed samples (20 randomly selected sections of microvessels) from each brain were scored positive or negative for erythrocyte and leukocyte sequestration. The percentages of microvessels from each brain that showed erythrocytic and leucocytic sequestration were noted

Ultrastructural analysis of *P. yoelii* 17XL infected mouse brain

Whole brains of infected and uninfected mice at peak parasitaemia were examined by electron microscopy to evaluate parasite induced morphological changes in brain microvasculature. Brains were dissected, cut into smaller cubes (2 mm³), washed twice with phosphate buffered saline (PBS) and fixed for 60 minutes in 100 mM potassium phosphate buffer pH 7.2, containing 0.1 % glutaraldehyde and 2% freshly prepared formaldehyde. After fixation the brains were dehydrated in methanol and embedded in Lowicryl K4M at -20 °C. Thin sections were collected on 300-mesh nickel grids and examined by transmission electron microscopy at 60eV as described previously [17].

Statistical analysis

The results obtained in this work were from triplicate experiments performed independently by identical methods. ELISA data and densitometric measurements from agarose gel electrophoresis, as well as Western blot analyses, were log-transformed to normalize the distribution for infected (n=15) and control (n=15) samples, and also to correct for small sample size. Data were expressed as the mean \pm standard error of mean (SEM). Data from the *P. yoelii* 17XL infected and control groups were then compared, and the p values were determined by using nonparametric Mann-Whitney U-test. A value of $p < 0.05$ was considered statistically significant.

Results

Plasmodium yoelii 17XL murine malaria

All the mice infected with *P. yoelii* 17XL parasites developed malaria-related symptoms, which included the appearance of ruffled fur and shivering at peak parasitaemia by day eight post-

infection (Figure 1). Examination of the viscera of dissected mice confirmed spleno- and hepatomegaly at peak parasitaemia, concordant with reported *P. yoelii* 17XL malaria infections [14, 15]. None of the control or uninfected mice showed any of these signs. The mice infected with *P. yoelii* 17XL did not develop the classic signs of cerebral pathology (such as hemiplegia, paraplegia, ataxia with hind limb paralysis, convulsions and coma associated with murine CM previously described in the *Plasmodium berghei* ANKA murine CM model [18, 19]). Additionally, histopathologic analysis of brains of the *P. yoelii* 17XL-infected mice revealed plugging of brain microvessels with parasitized erythrocytes, but did not reveal evidence of disseminated petechial haemorrhages and extensive leukocyte accumulation in the microcirculation. However, there was ultrastructural evidence of oedema and disintegrating macrovascular endothelia in the cerebellum, which reflect local perturbations induced by the *P. yoelii* 17XL infection.

cDNA microarray screening

P. yoelii 17XL-attributable alterations in approximately 7.5% (44/588) of genes encoding immunomodulators, growth factors, stress factors, transcription factors and neurotransmitters were observed in infected mouse brain during the microarray analysis. Expression of the altered genes at peak parasitaemia in the infected mice varied when compared with that in the uninfected mice (Figure 2). Marked alterations in expression of immunomodulator mRNA, including C-C chemokine RANTES, C-C chemokine receptors CCR1, CCR3 and CCR5, adhesion molecules PECAM-1, ICAM-1, and VCAM-1, cytokines IFN-gamma, TNF-alpha, IL-12, IL-4, and iNOS were observed to be up-regulated, while growth factors, GDF-2 and TGF-beta precursor, were down-regulated (Table 2, $P < 0.05$) at peak parasitaemia.

RT-PCR validation of immunomodulator mRNA expression

The expression of RANTES and its corresponding receptors, CCR1, CCR3 and CCR5, were altered by *P. yoelii* 17XL infection and were significantly up-regulated ($p < 0.002$ for RANTES, $p < 0.036$ for CCR1, $p < 0.033$ for CCR3 and $p < 0.026$ for CCR5) in the brain during malaria infection. Up-regulation of RANTES mRNA began four days after infection, until eight days post-infection, approximately three-fold increase in infected mouse brain at day six and day eight post-infection compared with controls [Figure 3A]. Messenger RNA expression levels of CCR1, CCR3 and CCR5 were approximately two to three fold higher in infected mice than in controls [Figures 3B, 3C & 3D]. CCR3 and CCR5 expression profiles were similar to the expression profile of their corresponding RANTES ligand. The degree of variation of GAPDH mRNA from sample to sample was within 5% of the mean expression level in both infected and uninfected control samples throughout the course of the infection.

Western blot analysis

Results from the Western blots analysis indicated that the expression of RANTES (7.8 kDa) protein in brain tissue samples from infected mice at day four, six and eight post-infection, was significantly up-regulated ($p = 0.049$ at day four and $p < 0.036$ at day six and day eight) [Figure 4A]. Expression of RANTES protein in brain tissues followed a similar profile consistent with mRNA expression indicating that RANTES mRNA expression in brains of *P. yoelii* 17XL infected mice were translated into protein. Expression of alpha-tubulin protein from sample to sample was within 5% of the mean expression level in both infected and uninfected samples throughout the course of the infection.

Plasma RANTES protein level during *P. yoelii* 17XL infection

Plasma samples from infected mice at each time point as well as uninfected controls were assayed for RANTES protein expression. Systemic increase in RANTES protein expression

began four days after *P. yoelii* 17XL infection, until peak parasitaemia at day eight with about three-fold upregulation in infected plasma compared with control [Figure 4B].

Histopathologic analysis of mouse brain

Sequestered parasitized erythrocytes were observed in brain microvessels of all the *P. yoelii* 17XL-infected mice studied at peak parasitaemia, but none of the uninfected mice. There was no histopathologic evidence of sequestered or accumulated mononuclear leukocytes (monocytes/macrophages and lymphocytes) or extensive petechial haemorrhages in the brains of both the infected and uninfected mice. In the brain of the infected mice, the erythrocyte sequestration observed in the white and grey matter regions was identical.

Ultrastructural analysis of mouse brain

Brains from parasitized mice were ultrastructurally analysed by transmission electron microscopy to evaluate effects of *P. yoelii* 17XL infection on brain microvessel endothelium. Uninfected mouse cerebellar tissues (Mag. X15000) showed normal intact microvessel endothelia (ME) at blood brain barrier (BBB). Infected mouse cerebellar tissues (Mag. X15000) showed perivascular clearing concomitant with oedema as well as some disintegrating ME and BBB (Figure 5). This endothelial cell damage (lesions) was observed in 6 out of 10 mice examined at day eight post-infection. Erythrocytic (RBC) adherence in the microvessels, but not leukocytic (WBC) adherence, was observed in the infected mouse brains examined.

Discussion

The brain pathology associated with malaria remains a major cause of death during severe *P. falciparum* infection. Cerebral malaria, characterized by coma and seizures in patients with *P. falciparum* infection, is a major cause of malaria-associated mortality, and may be accompanied

by metabolic acidosis and hypoglycaemia in African children [20]. Using experimental models will facilitate a better understanding of the pathogenesis of this syndrome and therefore ensuring that better intervention strategies can be developed to minimize or abrogate the severity of the disease. The cytoadherence of infected red blood cells (IRBCs) to the postcapillary venules is the major cause of IRBC sequestration and vessel blockage in the cerebral form of human malaria. In both human cerebral malaria caused by *P. falciparum* and the *P. yoelii* 17XL-infected rodent model of malaria, the sequestration of IRBCs in the brain vessels is secondary to the cytoadherence of IRBCs to the postcapillary venules [14, 15]. This observation has resulted in the general suggestion that the *P. yoelii* 17XL mouse model resembles human *P. falciparum* infection more closely than the *P. berghei* ANKA mouse model, since it shows little accumulation of monocytes/macrophages in the brain microvessels [14, 15]. However, recent human CM studies [4-7], indicating significant accumulation of platelets and leukocytes in the distal cerebral microvasculature in CM, suggest some other similarities between human CM and the *P. berghei* ANKA mouse CM model, in addition to the similarities in symptomatology [18, 19]. These recent reports [4-7] of significant leukocyte accumulations in the brain microvasculature in human CM draws a similarity with the *P. berghei* ANKA-infected rodent model of malaria, in which the major histopathologic finding is extensive accumulation of monocytes or macrophages, rather than sequestered erythrocytes, in the brain [18, 19]. In this study, all the mice infected with *P. yoelii* 17XL developed malaria-related symptoms, which included the appearance of ruffled fur and shivering by peak parasitaemia at day eight post-infection. Spleno- and hepato-megaly at peak parasitaemia was common, and concordant with reported *P. yoelii* 17XL malaria infections [14, 15]. The observation of the absence of the classic signs of cerebral pathology in the *P. yoelii* 17XL-infected mice at peak parasitaemia and the histopathologic findings of IRBC sequestration and vessel plugging with the absence of leukocyte accumulation in brains of *P. yoelii* 17XL-infected mice, confirms previously reported



observations [14, 15]. The classic signs of cerebral pathology, namely hemiplegia, paraplegia, ataxia with hand-limb paralysis, convulsions and coma, have been previously described in the *P. berghei* ANKA mouse model [18, 19]. These observations provide a justification for the complementary use of both murine malaria models to study human CM. The *P. berghei* ANKA model shows similarity with human CM in terms of symptomatology, whilst the *P. yoelii* 17XL model exhibits similarity to human CM in terms of histopathology. This study focused mainly on malaria induced chemokine and chemokine receptor expression in the *P. yoelii* 17XL murine model. Animal models have provided compelling evidence implicating the role of inflammatory processes in the development of malaria brain pathology [21]. Adhesion molecules and platelet-induced immune-mediated damage of vascular endothelium of the brain have also been reported [21]. Tkachuk and colleagues observed that malaria infection induced the expression of CCR3 and CCR5 on placental macrophages in pregnant women [22]. Sarfo and colleagues indicated that RANTES and its receptors CCR3 and CCR5 were upregulated in the cerebellum and cerebrum of post-mortem human CM tissue samples [8]. Furthermore, activated T-lymphocytes, platelets and endothelial cells release large amount of RANTES 3-5 days after activation, giving this chemokine a unique role in the generation, maintenance and prolongation of immune and inflammatory response [23]. By understanding the role of RANTES and its receptors during malaria immunopathogenesis, a new strategy for preventing or minimizing the outcome of CM and other severe forms of malaria can be developed. The microarray results (Table 2) confirmed with semi-quantitative RT-PCR analysis from this study revealed changes in the expression of a number of immunomodulators that had previously been associated with malaria-induced brain dysfunction [12]. In this study, the expressions of RANTES and its corresponding receptors CCR1, CCR3 and CCR 5 were up-regulated in the brain during *P. yoelii* 17XL infection, further implicating these molecules in the pathogenesis of rodent cerebral malaria. This study is a first towards the development of a molecular fingerprint (diagnostic) for brain immunopathogenesis

associated with malaria. In this regard, recent studies with infectious agents such as *Salmonella*, *Chlamydia* and *Trypanosoma* using cDNA microarray technology have revealed unique gene-expression profiles [24-26] which may be of diagnostic value.

This study demonstrates that chemokine RANTES (CCL5) and its receptors (CCR1, CCR3 and CCR5) may play an important role in *P. yoelii* 17XL infection in mice. Chemokines are immunoregulatory factors that play an important role in the chemotaxis, activation and haematopoiesis of leukocytes [27-29]. Chemokine action involves initial binding to specific, seven-transmembrane-domain, G-(guanine-nucleotide-binding)-protein-coupled receptors on target cells. In response to a relatively higher concentration of chemokines at the site of injury or infection, leukocytes are activated to perform effector functions such as release of their granule contents and increased production of cytokines. The temporal expression profile of chemokines and their receptors as early immunomodulators in the immunopathogenesis of malaria could serve as important new bio-markers for monitoring the course and predicting the outcome of the disease. The cDNA microarray analysis has revealed significant up-regulation of RANTES (6-fold) at peak parasitaemia. The results of RT-PCR analysis indicate that by days 6 through 8 post-infection, mRNA expression of RANTES is significantly up-regulated ($p < 0.002$) in infected mice compared with controls, indicating that it is involved in the immunopathogenesis in *P. yoelii* 17XL-infected mouse. RANTES in addition to CCR1 and CCR5 are expressed by Th1 cells [30]. Indeed, trafficking of inflammatory Th1 cells into the brain was reportedly mediated largely by RANTES interaction with CCR5 receptor [30]. Also the absence of CCR5 receptor in *Plasmodium berghei* ANKA-infected mouse brain resulted in a reduced Th1 cytokine production [9]. The expression of RANTES and CCR5 mRNA in *P. yoelii* 17XL-infected mouse brain in this study suggests a Th1-mediated immune response, and that factors capable of inducing Th1 response could play an important role in modulating malaria infections. Macrophages and other leukocytes release proinflammatory cytokines, including TNF- α , IFN- γ and IL-1- β ,

which in turn will promote the release of chemokines [30]. The expression of chemokine, IP-10 and MCP-1, genes in KT-5, an astrocyte cell line, have been shown to be upregulated in vitro upon stimulation with a crude antigen of malaria parasites [12]. A soluble gradient of these chemokines within the tissue recruits various cell types that express receptors for the different chemokines. The expressions of all the C-C chemokine receptors for RANTES, CCR1, CCR3 and CCR5, were upregulated in the brains of *P. yoelii* 17XL-infected mice. The expression of RANTES probably enhanced the expression of its receptors. Sano and colleagues demonstrated that ICAM-1 induced RANTES mRNA expression and also increased its protein synthesis and secretion by endothelial cells [31]. It is likely that the *P. yoelii* 17XL-induced RANTES production observed in the current study would attract and activate leukocytes towards inflammatory sites to mediate localized hyper-inflammatory responses that could exacerbate the disease pathology in the cerebellum. Belnoue and colleagues showed that the brains of wild-type mice with CM have significantly higher levels of CCR5 than the knockout-type, implicating these molecules in the pathological changes produced in the brain during the infection [9]. The results of this study demonstrate that the increase in production of RANTES follows the course of *P. yoelii* 17XL malaria infection, thus RANTES and its receptors CCR1, CCR3 and CCR5 were detected at their highest levels at day six and day eight post-infection. This observed temporal association of the progression of *P. yoelii* 17XL infection with the increasing production of RANTES and its receptors suggests that the two events might be linked. Western blot analysis revealed that brain tissue transcripts of RANTES were actually translated into protein, and were significantly up-regulated ($p = 0.046$ for day 4 and $p < 0.034$ for day six and day eight post-infection) in infected mice (Figure 3A). The ELISA data from this study indicate significant upregulation ($p = 0.049$ for day 4 and $p < 0.026$ for day six and day eight post-infection) of RANTES in *P. yoelii* 17XL-infected mouse plasma than in controls (Figure 3B). Most of the ultrastructural pathological changes, observed as endothelial cell damage (lesions) in six out of

the 10 infected mice examined, occurred especially at day eight post-infection (peak parasitaemia) (Figure 5). Thus, the increase in RANTES production correlated with the increase in parasitaemia and pathological changes observed in the *P. yoelii* 17XL-infected mice in this investigation. Chemokines have been shown to have a direct antiprotozoal activity for three protozoans: *Toxoplasma gondii*, *Leishmania donovani* and *Trypanosoma cruzi* [32, 33]. Chemokine production is important for defending the host against infection. However, excessive production is also deleterious to the host [12]. It has been observed that C-C chemokines, such as MIP-1-alpha and RANTES, are significantly upregulated in brains of *Trypanosoma brucei brucei* infected rats [34]. This increase in expression of these chemokines occurs before brain lesions developed in these rats, implying that the induction of these chemokines could be directly responsible for the observed rat brain lesions [34]. Ultrastructural analysis of mouse brain by electron microscopy at peak parasitaemia in this study, revealed disintegrating microvascular endothelial layer at the blood brain barrier in the cerebellar region of infected mouse brain. This endothelial cell damage (lesions), in six out of 10 mice examined, occurred especially at day eight post-infection (peak parasitaemia) and was similar to the observations of Thumwood and colleagues in *B. berghei* ANKA-infected A/J and CBA/H mice [35]. The infected erythrocytes adhering and occluding brain microvessels observed in the sections examined, suggest that the breach in the cerebellar microvascular endothelial layer could be associated with parasite-induced inflammation or apoptosis. Perivascular oedema was also observed in this region of infected mouse brain probably as a result of the endothelial cell damage allowing excess fluid to move across the blood brain barrier. Endothelial cells interacting with *P. yoelii* 17XL-parasitized erythrocytes have been shown to be induced to produce and present specific chemokines, such as RANTES, which can lure CCR1, CCR3 and CCR5 expressing cells into the brain [36]. CCR1 and CCR5 are expressed by brain endothelial cells [37, 38]. Brain endothelial cells, microglia and astrocytes, which are the 3 major cellular components of the BBB, express CCR5 receptor

[39], and hence the binding of RANTES to its receptors on these cells can serve to further activate them and enhance a localized breakdown of the microvessel endothelial layer observed in the infected mouse brain in the current investigation.

Conclusions

In conclusion, *P. yoelii* 17XL infection upregulates RANTES and its corresponding receptors, CCR1, CCR3 and CCR5, in mouse brain, and that ultrastructural changes in the microvascular endothelial layer occurred in the cerebellum of infected mice. This is the first temporal expression study of RANTES and its receptors associated with murine malaria. Further studies are underway to examine the expression of these chemokines and chemokine receptors in a human CM symptomatology-like model such as *P. berghei* ANKA, to ascertain differences and similarities. As it is not clear which cell types in the mouse CM brain samples over-express RANTES, CCR1, CCR3 and CCR5, further comparative immunolocalization and antibody ablation studies are currently underway to examine the physiological relevance, source and expression patterns of these important biomarkers in both murine and human CM brain samples.

List of abbreviations used

BBB, Blood-Brain Barrier;

CM, cerebral malaria;

ECM, experimental cerebral malaria;

ME, microvascular endothelium;

NCM, non-cerebral malaria;

P., *Plasmodium*;